IEEE Access
Multidisciplinary | Rapid Review | Open Access Journal

Received June 25, 2020, accepted July 28, 2020, date of publication August 7, 2020, date of current version August 18, 2020.

Digital Object Identifier 10.1109/ACCESS.2020.3014977

Stability and Control Aspects of Microgrid Architectures–A Comprehensive Review

MOUDUD AHMED, (Member, IEEE), LASANTHA MEEGAHAPOLA, (Senior Member, IEEE), ARASH VAHIDNIA, (Senior Member, IEEE), AND MANOJ DATTA, (Senior Member, IEEE)
School of Engineering, RMIT University, Melbourne, VIC 3000, Australia
Corresponding author: Moudud Ahmed (s3636503@student.rmit.edu.au)

ABSTRACT Self-governing small regions of power systems, known as ''microgrids'', are enabling the integration of small-scale renewable energy sources (RESs) while improving the reliability and energy efficiency of the electricity network. Microgrids can be primarily classified into three types based on their voltage characteristics and system architecture; 1) AC microgrids, 2) DC microgrids, and 3) Hybrid AC/DC microgrids. This paper presents a comprehensive review of stability, control, power management and fault ride-through (FRT) strategies for the AC, DC, and hybrid AC/DC microgrids. This paper also classifies microgrids in terms of their intended application and summarises the operation requirements stipulated in standards (e.g., IEEE Std. 1547-2018). The control strategies for each microgrid architecture are reviewed in terms of their operating principle and performance. In terms of the hybrid AC/DC microgrids, specific control aspects, such as mode transition and coordinated control between multiple interlinking converters (ILCs) and energy storage system (ESS) are analysed. A case study is also presented on the dynamic performance of a hybrid AC/DC microgrid under different control strategies and dynamic loads. Hybrid AC/DC microgrids shown to have more advantages in terms of economy and efficiency compared with the other microgrid architectures. This review shows that hierarchical control schemes, such as primary, secondary, and tertiary control are very popular among all three microgrid types. It is shown that the hybrid AC/DC microgrids require more complex control strategies for power management and control compared to AC or DC microgrids due to their dependency on the ILC controls and the operation mode of the hybrid AC/DC microgrid. Case study illustrated the significant effects of microgrid feeder characteristics on the dynamic performance of the hybrid AC/DC microgrid. It is also revealed that any transient conditions either in the AC or DC microgrids could propagate through the ILC affecting the entire microgrid dynamic performance. Additionally, the critical control issues and the future research challenges of microgrids are also discussed in this paper.

INDEX TERMS Energy storage system (ESS), hybrid AC/DC microgrid, IEEE Std. 1547-2018, interlinking converter (ILC), microgrid stability, power management, renewable energy sources (RESs).

NOMENCLATURE

ACRONYMS:

CC:	Central control
CCVSI:	Current-controlled voltage source inverter
CPL:	Constant power load
DBS:	Data bus signaling
DCL:	Digital communication link
DER:	Distributed energy resources
DFIG:	Doubly-fed induction generator
DSTATCOM:	Distribution static-synchronous compensator
EMS:	Energy management system
ESS:	Energy storage system
ILC:	Inter-linking converter
IM:	Induction motor
LC:	Local control
LFO:	Low-frequency oscillation
LVRT:	Low voltage ride-through
MGCC:	Microgrid central controller
MPPT:	Maximum power point tracking
PCC:	Point of common coupling
PEC:	Power electronic converter
PF:	Power factor
PI:	Proportional-integral
PLL:	Phase-locked loop

The associate editor coordinating the review of this manuscript and approving it for publication was Canbing Li.

PLS: Power line signaling
PMSG: Permanent magnet synchronous generator
PV: Photovoltaic
RES: Renewable energy sources
SoC: State of charge
VCVSI: Voltage-controlled voltage source inverter
VI: Virtual impedance
VPD: Voltage active power
VQD: Frequency reactive power
VR: Virtual resistor
VSC: Voltage source converter

I. INTRODUCTION

Power electronic converter (PEC) interfaced distributed energy resources (DERs), such as solar photovoltaics (PVs), wind generators, micro-turbines and energy storage systems (ESSs) have paved the way for self-sustainable entity called microgrids [1]–[4]. AC microgrid was the main microgrid architecture for powering the remote-area power supply systems and distribution networks [4], [5]. Subsequently, the DC microgrid concept was emerged due to the fact that majority of the DERs generate DC power and increased utilisation of modern DC loads in recent years. The major advantages of the DC microgrid are efficiency, no reactive power requirement, and elimination of the need for AC-DC or DC-AC conversion stages [6]–[9]. However, since the existing distribution networks are operated at AC, and AC based DERs and loads are still prominent in power networks, the AC microgrid are still dominant. Also AC microgrid can be directly connected to the existing distribution networks without or with minimum modifications. Consequently, by merging a DC microgrid with an AC microgrid through a bidirectional interlinking converter (ILC), it has enabled to extract the benefits of both microgrids, and this architecture has been popular in the recent decade [10]–[12]. The concept of merging DC and AC microgrids through a bi-directional single or multiple parallel operating ILCs is known as the hybrid AC/DC microgrid, where both AC or DC type DERs, loads can easily be integrated into microgrids and ensures smooth power transfer between two sub-grids.

The hybrid AC/DC microgrid can be operated either in grid connected mode or in autonomous mode while the power transfer between them is controlled by the ILC. The hybrid AC/DC microgrid autonomous operation mode is far more critical compared to the grid-connected operation mode. The key challenge in autonomous operation mode is generation-demand management [13]. Furthermore, the intermittent behavior of DERs make this issue more severe. The ILC in grid-connected mode are responsible for DC microgrid voltage support and power transfer between the hybrid AC/DC microgrid and the distribution network. Extensive research studies have been carried out in the last decade on hybrid AC/DC microgrid power-sharing. In AC microgrid power-sharing realization, active power-frequency and reactive power-frequency droop characteristics are commonly employed while in DC microgrid current-voltage and active power-voltage droop characteristics are commonly employed. Therefore, in hybrid AC/DC microgrids, control strategies of AC and DC sub-grids should be coordinated with the ILC, which ensure power quality and economic benefit to its users.

The microgrid control techniques can be primarily classified into three types, 1) primary control, 2) secondary control, and 3) tertiary control. The primary control maintains stable voltage/frequency and it does not require communication links as it is operating locally. The primary control is also known as local control (LC). The voltage and frequency deviation after the LC actions are compensated by the secondary controller. The secondary control is responsible for power quality and energy management of microgrids. Centralized control and decentralized control are the two sub-division of secondary control. In the decentralized type of secondary control, all DERs are working in parallel to balance energy management using the locally obtained information from the neighboring DERs. In centralized control, there is a central controller, where optimal control decision is achieved by obtaining relevant information from the microgrid network and loads. The tertiary control operates after the secondary control and it helps to improve the power quality by energy management between multiple microgrids and the power grid. The tertiary control is implemented by coordination between microgrids and the power grids which ensures technical and economic benefits to its users. These control aspects are imperative for any type of microgrid architecture, hence it is important to shed lights on these control schemes in the context of microgrid architectures.

This paper presents a critical review of power management and control studies in AC, DC, and hybrid AC/DC microgrids, with special emphasis on primary control, secondary control, hierarchical control, and coordination control between ILC and ESS. This paper is structured as follows: Section II presents the definition and classification of microgrids, Section III discusses IEEE standards for interconnection of DERs, Section IV delineates the microgrid research focus areas, Section V presents the control and stability aspects of AC microgrids, control techniques and stability studies of DC microgrids are discussed in Section VI, control and stability aspects of hybrid AC/DC microgrids are presented in Section VII, in Section VIII fault ride-through of microgrids are reviewed, in Section IX hybrid AC/DC microgrid dynamic performance under different control strategies are analysed, and finally, conclusions of the review are summarized in Section X.

II. MICROGRID DEFINITION AND CLASSIFICATION

Various definitions have been proposed for microgrids over the past decade by researchers and various institutions considering the characteristics associated with different microgrid applications [14]–[17]. For example, in [14] microgrid is defined as ‘‘the concept of roaming DERs and various loads in the existing power system, such as solar-PV, wind turbines,

micro-turbines, and storage devices which can be operated either in grid-connected mode or in stand-alone mode''. Researchers in [15] defined the microgrid as '' a small-scale power system that consists of DERs, controllers, and load''. The department of energy of the United States defined the microgrid as ''a group of interconnected DERs and loads with precisely described electrical boundary that acts as a single controllable body w.r.t. the power grid and it can be operated either in grid connected mode or islanded mode'' [16], [17]. Essentially, all these definitions have recognised the pivotal role of DERs in microgrids and microgrid's capability to operate as a self-sustained entity independent from the main grid.

A. MICROGRID CLASSIFICATION

Microgrids can be primarily classified into three categories based on the system architecture and voltage characteristics, 1) AC microgrid, 2) DC microgrid, and 3) Hybrid AC/DC microgrid [18]–[20]. In addition, microgrids can be classified based on the application area, such as, 1) Utility microgrids, 2) Institutional microgrids (e.g., consortium for electric reliability technology solutions (CERTS) microgrid), 3) Commercial and industrial microgrids, 4) Transportation microgrids, and 5) Remote-area microgrids (e.g., King Island Microgrid) [21], [22]. The microgrid classification is illustrated in Fig. 1.

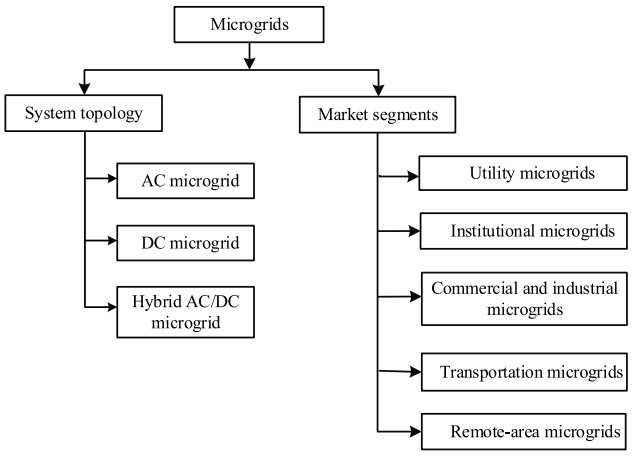

FIGURE 1. Classification of microgrids.

1) AC MICROGRIDS

The AC microgrid is the most conventional microgrid type. Different forms of DERs such as wind-turbine generators, micro-turbines, solar-PV, and fuel cells are integrated into the power networks via PECs [23]. As the conventional power networks are operating on AC, AC microgrid offers minimum modifications to integrate to the existing utility grid. AC microgrids are connected to the medium voltage and low voltage distribution networks which could enhance power flow in distribution networks and decrease transmission line power losses. But, they introduce new issues, such as system stability, power quality, synchronization of DERs and reactive power shortage, these issues could be resolved by applying the advanced control techniques [24], [25].

2) DC MICROGRIDS

Owing to technological developments in PECs, a large number of DC loads and power converters have been used for different types of applications [26]. Moreover, DC-based DERs and different kinds of ESSs create a new opportunity for DC microgrids. On average, around 30% of the generated AC power passes through a PEC before it is utilized [27]. Limited number of power conversion stages and no reactive current circulation are the main advantages of DC microgrids [28], [29].

3) HYBRID AC/DC MICROGRIDS

The AC and DC microgrids are combined to form the AC/DC hybrid microgrids; hence, they will offer the benefits of both microgrids such as increased reliability, efficiency and economic operation. The hybrid AC/DC microgrid is facilitating direct integration of AC and DC-based DERs, ESSs, and loads with the existing distribution system [30], [31]. DC appliances are being used in a wide range of domestic and commercial applications, and they require AC to DC conversion. Hybrid AC/DC microgrids reduce the number of required power converters and therefore lower the power losses. Moreover, the amount of power losses in the inverter is small compared to the rectifier [32], [33]. However, the network structure of hybrid AC/DC microgrids is complex. Therefore, the coordinated control of individual AC and DC microgrids, effect of intermittent nature of DERs, reactive power compensation, and ILC control strategies must be thoroughly investigated.

III. IEEE STANDARDS FOR INTERCONNECTION OF DERs

Microgrids are mostly covered by the distribution network and DER standards. High penetration of DERs in the low voltage or medium voltage distribution networks reduce the dependency and control capability of centralized synchronous generators, which drastically change the operating characteristics of the power network. Smaller capacity DER systems (known as microgrids) connected to the utility grid pose no special concern to the conventional power system engineers. This small capacity microgrids are treated as negative loads in the conventional power system while the system voltage and frequency are regulated by the synchronous generator [34]. However, integration of large number of microgrids to the utility grid is a matter of concern for power system operators to maintain system stability and reliability [35]. IEEE published IEEE Std. 1547-2018 (revision of IEEE Std 1547-2003) for DERs interconnection and interoperability with existing power systems [36]–[38]. IEEE Std.1547-2018 defines two main categories of DERs (e.g., Category A and Category B) based on performance requirements, such as voltage and frequency regulation, three sub-categories of DERs (e.g., Category I, Category II and Category III) based on disturbance ride-through

(low-voltage ride-through). Since a microgrid can be considered as a group of DERs, the requirements stipulated in the IEEE Std. 1547-2018 also applicable to microgrids.

Also, this standard helps to effectively integrate DERs into the existing electric power system and discussed seven different operation aspects, such as 1) reactive power capability, 2) voltage and reactive power control, 3) abnormal operating performance, 4) voltage disturbance ride-through requirements, 5) frequency tripping requirements, 6) islanding and protection aspects, and 7) power quality aspects. Fig. 2 shows a DER interconnected to the existing electric power system which describes the scope of the standard. Except the power quality and protection requirements, other aspects are succinctly discussed in the subsequent sub-sections [37].

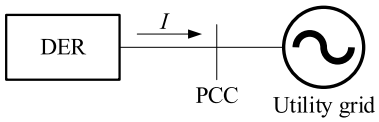

FIGURE 2. Illustration of a DER connected to the utility grid as per IEEE Std. 1547-2018.

A. REACTIVE POWER CAPABILITY OF THE DER

The DER should have the capability of either injecting or absorbing reactive power for its output active power levels equal to or higher than the steady-state active power capability. Fig. 3 illustrates the reactive power injection and absorption capability of both the category A and B DERs respectively. When the DER active power output (P_r) operating range is greater than 5% and less than 20% of the rated value, it can dispatch reactive power (S_r) up to the minimum value as shown in Fig. 3. Similarly, for the DER with the active power output operating range greater than 20% of the rated value, it can absorb or inject reactive power up to the maximum capability as specified in Fig. 3. The DERs should be capable of injecting/absorbing reactive power while it is dispatching active power up to the maximum capability limit [37].

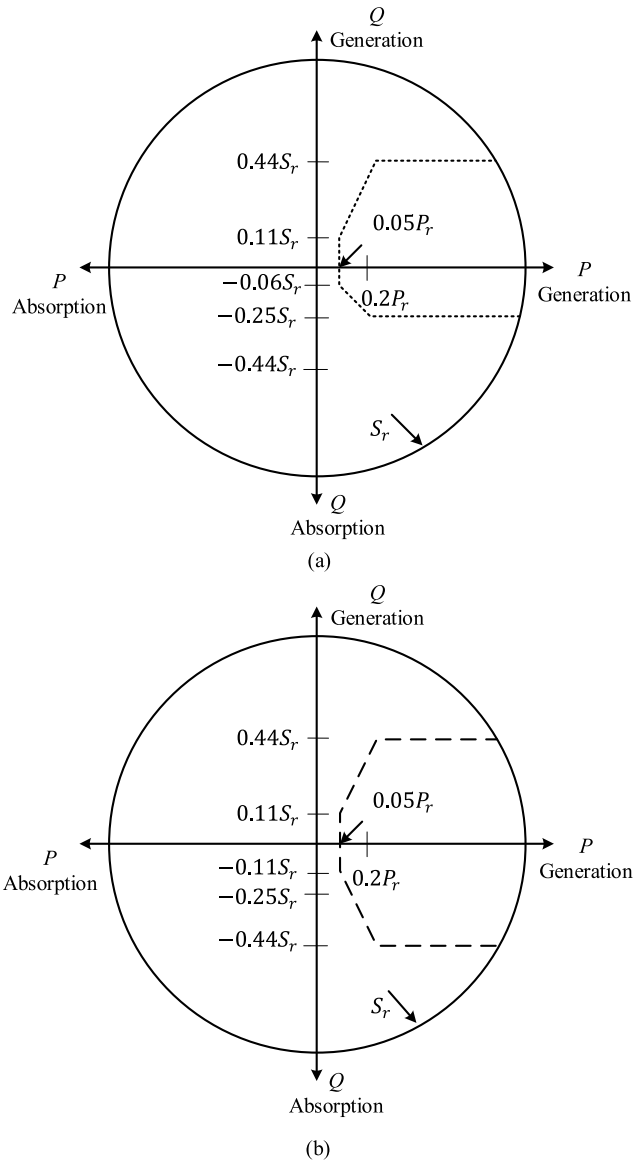

FIGURE 3. Reactive power capability curve of the DER, (a) Category A, (b) Category B [37].

B. VOLTAGE AND REACTIVE POWER CONTROL

The DER shall participate in voltage regulation by changing the reactive power dispatch. Despite the DER's participation in voltage regulation, it should not exceed the minimum reactive power capability limits specified in the previous subsection. The DER's voltage and reactive power control functions are classified into four modes, 1) constant power factor (PF), 2) voltage-reactive power, 3) active power-reactive power, and 4) constant reactive power [37]. These modes are described into the following sub-subsections.

1) CONSTANT POWER FACTOR MODE

In this mode, the DER is operating at a constant PF where the power system operator has specified the PF requirements, and it should not exceed the reactive power capability limits specified in the previous subsection. The power system operator can adjust PF settings either remotely or locally and the DER is allowed to maintain constant PF for up to 10 s.

2) VOLTAGE-REACTIVE POWER MODE

In this mode, the DER controls the reactive power dispatch as a function of voltage (a piece-wise linear function of voltage-reactive power characteristics). This mode voltage-reactive power characteristic is illustrated in Fig. 4, and the voltage-reactive power parameters are configured by the default values given in Table 1 if not specified by the power system. The power system operator can adjust voltage-reactive power characteristics either locally or remotely and the voltage reference (V_{ref}) is autonomously adjusted by the DER. Therefore, the voltage-reactive power

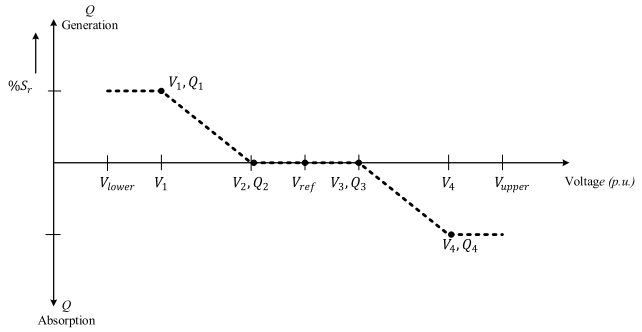

FIGURE 4. Voltage-reactive power characteristics of category A and B DERs [37].

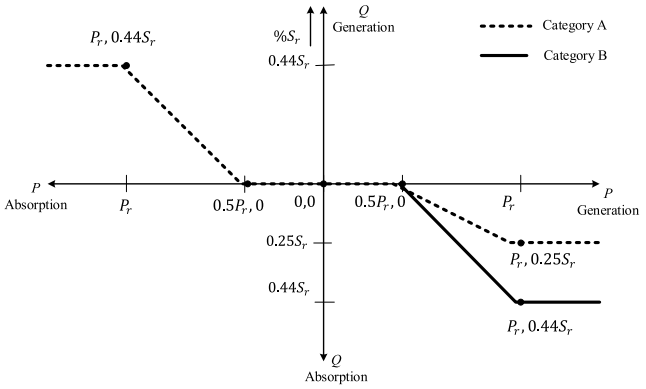

FIGURE 5. Active-reactive power characteristics of category A and B DERs.

TABLE 1. Voltage-reactive power parameters [37].

Parameters	Category A	Category B
V_{ref}	Nominal value (V_N)	V_N
V_1	0.9 V_N	V_{ref} - 0.08 V_N
V_2	V_N	V_{ref}-0.02 V_N
V_3	V_N	V_{ref} + 0.02 V_N
V_4	1.1 V_N	V_{ref} + 0.08 V_N
Q_1	0.25 S_r	0.44 S_r
Q_2	0	0
Q_3	0	0
Q_4	0.25 S_r	0.44 S_r

characteristics need to be changed based on the V_{ref}. The DER can autonomously adjust its reactive power capability to a lower value. Moreover, the DER can reduce its active power dispatch to meet this requirement; however, improper settings of those parameters may cause instability.

3) ACTIVE POWER-REACTIVE POWER MODE

In this mode, the DER controls the reactive power dispatch as a function of active power output (a piece-wise linear function of active-reactive power characteristics). This mode active-reactive power characteristic is illustrated in Fig. 5, and active-reactive power parameters are configured by the default values. The left-hand side of this characteristic curve corresponding to DER absorbing active power, whereas right-hand side corresponding to DER injecting active power. The power system operator can adjust active-reactive power characteristics either locally or remotely and the response time of the DER should not exceed 10 s [37].

4) CONSTANT REACTIVE POWER MODE

In this mode, the DER dispatches a fixed amount of reactive power, where the power system operator has specified the required reactive power requirements. It should not exceed the minimum capability limits specified in the previous subsection. The power system operator can adjust reactive power settings either locally or remotely and the DER is allowed to maintain constant reactive power for up to 10 s.

C. PERFORMANCE UNDER ABNORMAL OPERATING CONDITIONS

Many abnormal operating conditions may arise on the power system, where the DER is connected, and it is mandatory to respond appropriately. The DER's response contributes to the stability of the power system and can avoid possible damages to the DER itself. When the DER's actual output voltage is greater than the over-voltage threshold or less than the under-voltage threshold, it should terminate to energize the power system and must trip within the predefined clearing time. The under-voltage and under-voltage tripping thresholds and the clearing times must be specified over a range of allowable settings given in Table 2 for category I, II, and III DERs respectively. The power system operator can adjust voltage and clearing time set-points either locally or remotely. The power system operator specifies the maximum clearing times and the over-voltage/under-voltage thresholds within a range of allowable settings [37].

TABLE 2. Abnormal operating performance of the DER [37].

Trip	Voltage ($p.u.$)	Clearing time (s)	Allowable range settings	
			Voltage	Time
Category I				
Over voltage-2	1.20	0.16	1.2	0.16
Over voltage-1	1.10	2.0	1.1 to 1.2	1.0 to 13
Under voltage-1	0.7	2.0	0 to 0.88	2.0 to 21
Under voltage-2	0.45	0.16	0 to 0.5	0.16 to 2.0
Category II				
Over voltage-2	1.20	0.16	1.2	0.16
Over voltage-1	1.10	2.0	1.1 to 1.2	1.0 to 13
Under voltage-1	0.7	10.0	0 to 0.88	2.0 to 21
Under voltage-2	0.45	0.16	0 to 0.5	0.16 to 2.0
Category III				
Over voltage-2	1.20	0.16	1.2	0.16
Over voltage-1	1.10	13.0	1.1 to 1.2	1.0 to 13
Under voltage-1	0.88	21.0	0 to 0.88	21 to 50.0
Under voltage-2	0.5	2.0	0 to 0.50	2.0 to 21

TABLE 3. LVRT capability requirements [37].

Voltage range (p.u.)	Operating mode	Minimum ride-through time (s)	Maximum response time (s)
	Category I		
$V > 1.20$	Cease to energize	-	0.16
$1.175 < V \leq 1.20$	Permissive operation	0.2	-
$1.15 < V \leq 1.175$	Permissive operation	0.5 -	
$1.10 < V \leq 1.15$	Permissive operation	1	-
$0.88 \leq V \leq 1.10$	Continuous operation	infinite	-
$0.70 \leq V < 0.88$	Mandatory operation	$4s/1p.u.$ voltage	-
$0.50 \leq V < 0.70$	Permissive operation	0.16	-
$V < 0.50$	Cease to energize	-	0.16
	Category II		
$V > 1.20$	Cease to energize	-	0.16
$1.175 < V \leq 1.20$	Permissive operation	0.2	-
$1.15 < V \leq 1.175$	Permissive operation	0.5	-
$1.10 < V \leq 1.15$	Permissive operation	1	-
$0.88 \leq V \leq 1.10$	Continuous operation	infinite	-
$0.65 \leq V < 0.88$	Mandatory operation	$8.7s/1p.u.$ voltage	-
$0.45 \leq V < 0.65$	Permissive operation	0.32	-
$0.3 \leq V < 0.45$	Permissive operation	0.16	-
$V < 0.30$	Cease to energize	-	0.16
	Category III		
$V > 1.20$	Cease to energize	-	0.16
$1.1 < V \leq 1.20$	Momentary cessation	12	0.083
$0.88 \leq V \leq 1.10$	Continuous operation	infinite	-
$0.70 \leq V < 0.88$	Mandatory operation	20	-
$0.50 \leq V \leq 0.70$	Mandatory operation	10	-
$V < 0.50$	Momentary cessation	1	0.083

D. VOLTAGE DISTURBANCE RIDE-THROUGH REQUIREMENTS

This subsection describes the DER performance during voltage disturbance. The voltage disturbance ride-through requirements are not applicable if the frequency is outside the specified ride-through range. The DER should have the capability to provide specified voltage disturbance ride-through while the DER is within the capability limits. The voltage disturbance ride-through thresholds and the clearing times must be specified over a range of allowable settings given in Table 3 for category I, II, and III DERs respectively. The DER current exchange cessation with power system is not more than the maximum specified time and with no delay. It does not necessarily imply DERs disconnection, isolation, or a trip but may include momentary cessation or trip. When the voltage disturbance is within the mandatory operation region, the DER functionalities are to, 1) maintain synchronism with power system, 2) continue to exchange current with the power system, and 3) neither trip nor cease to energize. In the permissive operation region, the DER maintains synchronism with the power system and it will not trip. Moreover, when the voltage disturbance is within the continuous operation region of any duration, it will not cause the DER to cease to energize or trip from the power system and the DER will continue to deliver power and remain in operation [37].

E. FREQUENCY TRIPPING REQUIREMENTS

This subsection exemplifies the DER frequency tripping requirements during disturbance. The frequency ride-through requirements such as under frequency thresholds, over frequency thresholds and critical clearing time during abnormal conditions for category I, II, and III DERs are illustrated in Table 4. It is considered that the nominal system frequency is 60 Hz. The power system operator specifies the maximum clearing times and the over frequency/under frequency thresholds within a range of allowable settings. For the two under frequency trip functions (under frequency-1 and under frequency-2), under frequency-2 is used as the limiting requirement. Similarly, for the two over frequency trip functions (over frequency-1 and over frequency-2), over frequency-2 is used as the limiting requirement. Therefore, there are three distinct operating regions in the frequency tripping requirements.

- $f > 62.0$; No ride-through requirements
- $61.2 < f \leq 61.8$; Mandatory operation
- $58.8 \leq f \leq 61.2$; Continuous operation
- $57.0 \leq f \leq 58.8$; Mandatory operation
- $f < 57.0$; No ride-through requirements

F. ISLANDING REQUIREMENTS

A portion of an area power system is solely energized by one or more power systems through the PCC, while a portion

TABLE 4. Frequency tripping requirements [37].

Trip	f (Hz)	Clearing time (s)	Allowable range settings	
			Voltage	Time
Over frequency-2	62.0	0.16	61.8 to 66	0.16 to 1000.0
Over frequency-1	61.2	300	61 to 66	180 to 1000 s
Under frequency-1	58.5	300	50 to 59	180 to 1000 s
Under frequency-2	56.5	0.16	50 to 57	0.16 to 1000

of the area power system is electrically separated from the rest of the power system and DER is connected. When the DERs solely energize a portion of the power system, and it is electrically separated from the rest of the power system, the DER energizing the island is called ''islanding''. Islanding is categorized into two types, (1) unintentional islanding, (2) intentional islanding. Since microgrids are designed to operate either in grid-connected or islanding modes, the requirements set in the IEEE Std. 1547-2018 are also valid for microgrids.

1) UNINTENTIONAL ISLANDING

For unintentional islanding, the DER energizes a portion of the power system through the PCC, the DER detects the island (cease to energize the power system), and subsequently DER shall trip within 2.0 s. The power system operator and the DER operator may mutually be extended the clearing time from 2.0 s to up to 5.0 s. DER ride-through requirements may be terminated by the unintentional islanding specifications detection.

2) INTENTIONAL ISLANDING

An intentional island may include any portion of the area power system is known as intentional power system island. For intentional islanding, the DER must be designed and operated in coordination with the power system operator. Intentional islanding is categorized into two types, (1) scheduled islanding, (2) unscheduled islanding.

a: SCHEDULED INTENTIONAL ISLAND

Scheduled intentional island is formed through the power system operator or the DER operator dispatch means (such as automatic generation control action or energy management system) or mutual action. Scheduled intentional island ensures enhanced reliability, economic output power dispatch decisions, and preemptive power system operator action to island ahead of abnormal weather conditions.

b: UNSCHEDULED INTENTIONAL ISLAND

Unscheduled intentional island is autonomously formed following detection of abnormal conditions at the power system, and the relay will initiate the control action to isolate the intentional island from the power system. Unscheduled intentional island may switch to intentional island and disconnected from the power system if any of the following conditions are satisfied:

- Violation of any of the voltage disturbance ride-through and frequency disturbance ride-through requirements.
- If unintentional islanding conditions are met.
- Violation of any of the trip conditions for category I, II, and III DERs are met.

IV. MICROGRID RESEARCH - FOCUS AREAS

Microgrids consist of various intermittent renewable resources and the weather conditions determine their output power; the key challenge is to ensure stable operating conditions. To cope up with the output power fluctuations of renewable resources, ESS is implemented in the microgrid, and it needs to be adjusted instantly [39], [40]. The control systems should be designed considering all these issues to make sure that the microgrids are operating in stable condition. The key research areas are exemplified in the subsequent sub-sections.

A. VOLTAGE AND FREQUENCY STABILITY

A microgrid is considered as an inverter dominated small-scale power grid, where DERs and ESSs are connected by PECs called inverters and controlled via hierarchical schemes, with the ability to operate either in autonomous mode or grid-connected mode. The voltage and frequency deviations in microgrids arise due to the mismatch between the generation and the load demand. The grid forming inverters should maintain voltage and frequency within permissible limits. To maintain stable voltage and frequency in autonomous mode is more challenging than in grid-connected mode due to the absence of inertia and reactive power support.

B. DISTRIBUTED ENERGY STORAGE

The intermittent behavior of DERs results in variable output power which leads to voltage instability and potential costs in microgrid which can be solved by deploying an ESS. The major challenge for the ESS is to obtain a dynamic balance between generation and load demand while maintaining voltage and frequency within acceptable range. The ESS controller manages the power balance based on the dispatchable energy of each storage system [41]–[44]. The effective operation of microgrid depends on the optimum management of ESS, which remains as a key challenge for microgrids [45], [46].

C. REACTIVE POWER COMPENSATION

One of the most important issues for AC microgrids is reactive power compensation, which is directly related to the voltage instability and power quality problems [47]. The reactive power demand is mainly originating from the induction machine loads connected to the microgrid. The power quality in a microgrid can be improved by maintaining

generation and load balance, while keeping microgrid voltage within acceptable limits. If the reactive power flow through the microgrid is effectively controlled and compensated, power quality problems can be solved. Moreover, the reactive power issue in microgrid during grid forming mode is even more critical due to the absence of the power grid [48]–[50].

D. DISTRIBUTED COORDINATED CONTROL

Aforementioned, concept of hybrid AC/DC microgrid is gaining enormous popularity in the power industry for integrating various AC and DC based DERs, ESSs and loads with higher energy efficiency and better compatibility [51]–[53]. The ILC is an effective means to connect both the AC and the DC microgrids to form hybrid AC/DC microgrids. The ILC facilitates the transfer of real power into DC sub-grid from AC sub-grids and regulates DC bus voltage, while ILC transfers real and reactive power into AC sub-grid from DC sub-grid and regulates voltage and frequency. Voltage source converter (VSC) based DERs operate as a static generator [54]. Moreover, to transfer a large amount of power and to avoid overstressing a single ILC, researchers proposed multiple ILCs between the AC and the DC sub-grids. Furthermore, both the AC and the DC sub-grids are equipped with storage systems due to the intermittent behavior of renewable sources. Therefore, a coordinated control strategy is required for the safe and stable operation of the entire microgrid. The control can be centralized or distributed with or without communication links [52], [55], [56].

E. HARMONICS MITIGATION

Renewable sources such as solar-PV, wind, micro-turbines, or even fuel-cell are connected to the microgrid via VSC. The high frequency switching ripple introduces harmonics, which affects the power quality as well as dynamic stability margin of the microgrid [57], [58]. The LCL filter is used to interconnect an inverter to the microgrid to eliminate harmonics and improve power quality. The high performance and low cost are the main reasons for widespread use of LCL filters in the microgrid. The LCL filter performance is influenced by line impedance which may lead to resonance and instability issues [59]–[61].

F. PROTECTION ISSUES IN MICROGRIDS

A sophisticated protection system is required for a microgrid because of the bi-directional power flow between microgrid and main power grid. In addition, the microgrid protection system should resolve grid forming faults and grid following faults [62], [63]. The former protection scheme should isolate the smallest part of microgrid and the latter isolate microgrid from the utility grid. Moreover, mode of operation and nature of fault determine the amount of fault current and direction of flow of fault current [64]. The following features make the microgrid protection schemes distinct from the conventional protection systems [65], [66]

- Fault detection failure in the grid forming mode
- Tripping of adjacent feeders due to fault current contribution of DER
- False operation of sectionalizers due to the presence of voltage from the distribution lines from the DERs
- Overrating of equipment due to higher fault current level, and
- Auto reclosing failure (when a fault occurs, the breaker/isolator should operate to isolate the faulty parts, and finally, the recloser should operate to reconnect the healthy parts of the microgrid networks.)

V. CONTROL AND STABILITY OF AC MICROGRIDS

Robust control techniques are required for a stable and economic operation of the AC microgrid. This section discusses the following control techniques and stability issues of AC microgrids:

- Voltage and frequency control
- Coordination between DERs and power sharing aspects
- Microgrid synchronization
- Power flow control between multiple microgrids
- Smooth mode switching
- Loss reduction
- Economic efficiency
- Blackout mitigation

A. HIERARCHICAL CONTROL SCHEMES

To fulfill the above mentioned control aspects, three different levels of control strategies, namely (1) primary, (2) secondary, and (3) tertiary controls are applied in AC microgrids, and is known as the hierarchical control. The AC microgrid hierarchical control structure is shown in Fig. 6. Objectives of this three-level hierarchical control scheme are described in brief in subsequent sections.

1) PRIMARY CONTROL

The prime functions of the primary control are: (1) to maintain the voltage and the frequency within acceptable limits, (2) active and reactive power sharing between DERs operating in parallel, and 3) to ensure plug and play operations. The primary control should be faster compared to secondary and tertiary control schemes. During the mode transition from the grid-connected to islanded mode, primary control should maintain stable voltage and frequency. Otherwise, power generation and load demand mismatch could cause voltage and frequency fluctuations, which could lead to microgrid instability. The primary control scheme is consisted of voltage and current control loops of DERs, where VSC based DERs can be operated either as a voltage controlled voltage source inverter (VCVSI) or a current controlled voltage source inverter (CCVSI) [67]–[70]. Most commonly, the droop control and virtual impedance based methods are used as primary control strategies for power sharing among DERs in AC microgrids.

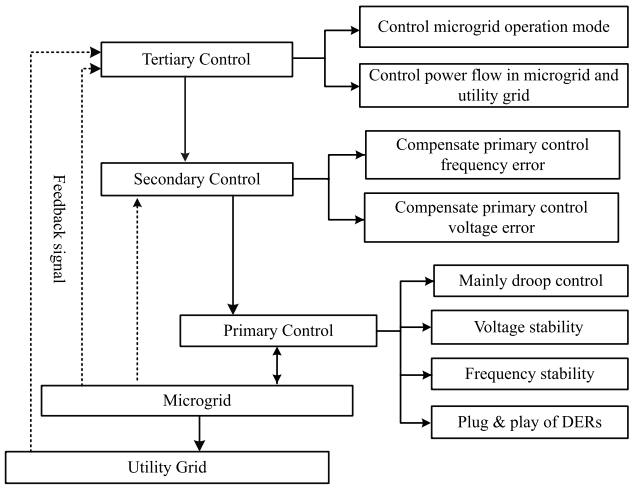

FIGURE 6. The conceptual framework of the hierarchical control schemes.

2) SECONDARY CONTROL

Although primary control maintains stable voltage and frequency, still there is a steady-state voltage and frequency deviations in AC microgrids. Secondary control is a controller which regulates the steady-state voltage and frequency deviations. Secondary control is usually slower than the primary control [71], [72]. As optimization strategies are used in secondary control it requires bi-directional communication links. Secondary control schemes can be divided into centralized and decentralized control schemes. Usually, centralized control is used in small AC microgrids while decentralised schemes are used in large microgrids.

3) TERTIARY CONTROL

The steady-state voltage and frequency deviations caused by the primary control are regulated by the secondary control, whereas the power flow between the utility grid and the microgrid are managed by the tertiary control, and it facilitates economic operation of the microgrid. When the microgrid is connected to the main grid, tertiary control manages the power flow between the utility grid and the microgrid by adjusting the power reference of DERs. As the last control level, it is slow compared to primary and secondary control schemes [69]. Different optimization algorithms, e.g., grossing algorithm, game theory, particle swarm optimisation, are employed to ensure economic operation. When all DERs are operating at the same marginal cost, then the condition for optimal economic operation can be achieved [73], [74].

B. COMMUNICATION BASED CONTROL SCHEMES

Renewable energy resources and energy storage systems within the microgrid should be coordinated properly to supply various loads. Therefore, the parallel operating DERs and battery storage systems are connected via the communication links [75] to coordinate their operation. Besides, the high capital investment of communication links, communication based control schemes can maintain proper voltage regulation and power sharing. The subsequent subsections will critically review the communication based control strategies of the AC microgrid.

1) CENTRALISED CONTROL SCHEMES

In centralised control schemes a central controller is employed in microgrids to determine the control actions of the DERs. An in-depth analysis of the microgrid central controller (MGCC) is given in [76], [77]. The MGCC initiates mode switching action (grid-connected to islanded mode or islanded to grid-connected mode) by observing the PCC voltage and the frequency. Besides, it monitors the power generated by individual DERs and optimizes the DERs power generation. Furthermore, the MGCC forecast the load and the generation plan within the microgrid based on the available previous load profile data and the system conditions [78]. The MGCC strategy needs the same synchronization signals and current sharing modules. The PEC interfaced DER has a phase locked loop (PLL) which maintains consistent phase among the synchronization signal, the frequency, and the output voltage. The current sharing module measures the load current at the PCC, which generates reference current of each DER by dividing total load current by the number of parallel operating DERs, where the reference load current is proportional to the capacity of individual DER. As the DERs are connected in parallel and controlled by the synchronization signal, there is a negligible frequency and phase difference. Central limit control is proposed in [79], [80], where all the DERs have the same configuration and tracks the same reference current to achieve equal current sharing. Also, multistage centralised control strategy in the presence of high penetration of electric vehicle is proposed in [81], [82]. As the microgrid is controlled centrally, it can achieve proper current sharing in both the steady-state and transient conditions. Due to centralized control, it is difficult to expand the microgrid and it cannot tolerate a single point of failure.

2) DISTRIBUTED CONTROL SCHEMES

This method has no central controller and each converter has individual control unit [83]–[86]. The point of common coupling (PCC) or common bus is used as the current sharing bus to generate and share reference current among parallel operating DERs. Same like the centralized control, an additional current loop is required to generate reference current for the current sharing. In [84], a distributed AC microgrid control is proposed to restore voltage, frequency, and reactive power sharing, whereas in [85], a two-layer distributed control of AC microgrid is proposed. In [87], a robust decentralized controller for active and reactive power sharing for an islanded AC microgrid is presented where robustness of the system is ensured by a feedback linearization approach. In decentralized control, adjacent DERs exchange information among them rather than all the DERs available in the microgrid. Therefore, it requires a

lower communication bandwidth. It can tolerate a single point of failure. As the adjacent DERs exchange information between them, it degrades the microgrids extenderbility and redundancy.

3) AC MASTER SLAVE CONTROL

In this method of control, several DERs act as master DERs and regulates bus voltage and determines the current reference for the slave DERs [88]–[90]. Slave DERs are continuously tracking current references defined by the master DERs for current sharing. Since the slave DERs communicate with the master DERs, there is no need of the PLL unit for synchronization. The major drawback of this control is in case of a failure of the master; the entire microgrid system will fail [88], [89]. Many approaches have been proposed to solve this problem. Random selection of master by the rotating priority window is proposed in [91], whereas auto master-slave control is developed in [89], where the highest capacity DER unit acts as a master unit and is driving the power to the bus and generates a reference for the other DERs. In [88], utility interface at PCC is being used as a master DER. In summary, this control method offers excellent power sharing capability. In case of a failure of the master DER, it switches to am improved control strategy, i.e., a normal DER acts as a master DER. Like other communication based control, it adds expandability and redundancy of the system. A comparative analysis of these three control methods are summarized in Table 5.

TABLE 5. Comparison of communication based control methods in AC microgrids.

Approach	Prospects	Problems
Centralized control	Improved power sharing in transient and steady-state conditions. Excellent voltage and frequency regulation.	High bandwidth is required. Higher implementation cost. Redundant communication required. Can not tolerate single point of communication failure.
Distributed control.	Constant voltage and power sharing. Can tolerate single point of failure. Medium bandwidth communication.	Reduce the modularity of the system.
Master/slave control.	Improved power sharing in the steady-state condition.	High current overshoot and high bandwidth communication.

4) DROOP BASED CONTROL TECHNIQUES

This section critically reviews control aspects, problems, and prospects of droop control. The droop control method, which is independent of inter-unit communication, is most commonly used between parallel operating converters (also know as LC). It can be implemented easily and it enables plug and play operation. A DER with voltage phasor ($E\angle\delta$) (shown in Fig. 7) is connected to the AC bus with voltage ($V_o\angle o$). The feeder impedance is $R_1 + jX_1 = Z\angle\theta$. The output power

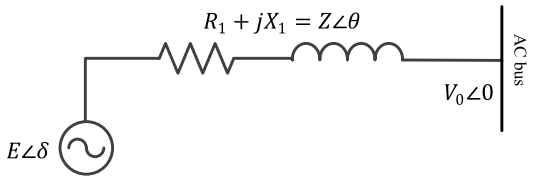

FIGURE 7. A DER connected to the microgrid.

of the DER injected to the AC bus is calculated as [92];

$$S = P + jQ = V_o * I^* = \frac{V_o * E\angle(\theta - \delta)}{Z} - \frac{V_o^2\angle\theta}{Z} \quad (1)$$

where, S, P, and Q are the complex power, real, and reactive power respectively. If the line is inductive i.e. $\theta = 90^0$, the real and reactive power can be calculated as [93];

$$P = \frac{V_o * E}{Z}cos(\theta - \delta) - \frac{V_o^2}{Z}cos\theta$$
$$Q = \frac{V_o * E}{Z}sin(\theta - \delta) - \frac{V_o^2}{Z}sin\theta \quad (2)$$

a: CONVENTIONAL DROOP CONTROL

Droop control enables DERs (static generators) to behave similar to the synchronous generator's droop used in a conventional power system. Most commonly used conventional droop are active power-frequency droop ($P-f$) and reactive power-voltage droop ($Q-v$). The simplified circuit of a VSC based DER with $P-f$ and $Q-v$ droop connected to AC bus is shown in Fig. 8. The VSC consists of power sharing control loop, voltage control loop and inner current control loop. Power angle is related to active power, while voltage is related to reactive power. Therefore, the P/Q droop control can be expressed as [94];

$$\omega = \omega_{ref} - m_p * P$$
$$E = E_{ref} - n_Q * Q \quad (3)$$

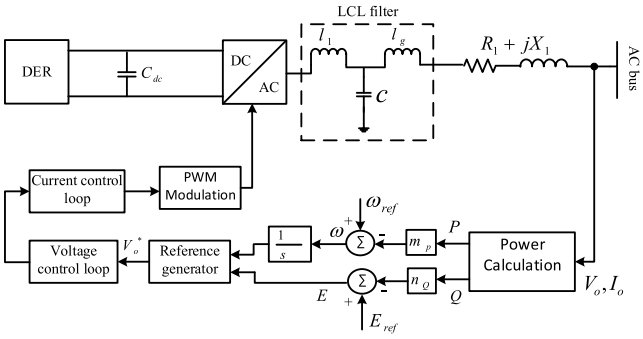

FIGURE 8. A DER with $P-f$ and $Q-v$ droop control.

where m_P and n_Q are active and reactive droop slope. ω_{ref} and E_{ref} are rated angular speed and rated voltage respectively. The droop coefficients have great influence on system

stability and may be adjusted heuristically or by tuning algorithms [95], [96]. The m_P and n_Q can be formulated as;

$$m_P = \frac{\omega_{max} - \omega_{min}}{P_{max} - P_{min}}$$
$$n_Q = \frac{E_{max} - E_{min}}{Q_{max} - Q_{min}} \tag{4}$$

Here, subscripts *max* and *min* represent the maximum and minimum quantity of the respective variables. The conventional droop control slopes with inductive feeder-based microgrid are illustrated in Fig. 9. The major disadvantages of conventional droop are:

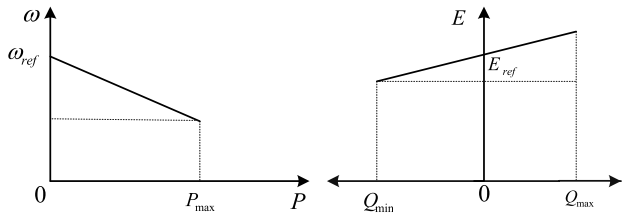

FIGURE 9. $P-f$ and $Q-v$ droop characteristics.

- It assumes that feeder is highly inductive. But low or medium voltage feeders are mostly resistive [97].
- As voltage is not a global variable, reactive power control is a challenge which results in circulating reactive current [98].
- For non-linear loads, only fundamental components of the voltage and current are considered. The droop control needs to be modified to reduce total harmonic distortion (THD) [99], [100].

b: VOLTAGE ACTIVE POWER (VPD) AND FREQUENCY REACTIVE POWER (FQD) DROOP CONTROL

Low voltage distribution feeders are mainly resistive. Therefore, conventional droop control does not work under these circumstances. For a purely resistive feeder, phase angle (θ) is small and $\cos(\theta) \approx 1$. Based on these assumptions (Eqn. 2) real and reactive power can be rewritten as [93];

$$P = \frac{V_o * E - V_o^2}{Z}$$
$$Q = -\frac{V_o * E}{Z}\delta \tag{5}$$

Therefore, modified voltage-real power ($P - v$) and frequency-reactive power ($Q - f$) droop schemes are characterized by [101];

$$E = E_{ref} - m * P$$
$$\omega = \omega_{ref} + n * Q \tag{6}$$

where, m and n are active and reactive droop coefficients respectively. Graphical representation of VPD/FQD droop slopes are shown in Fig. 10. It provides improved performance in low-voltage resistive line based AC microgrid. However, its performance depends on microgrid parameters.

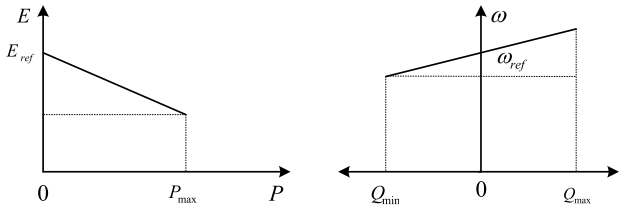

FIGURE 10. $P-v$ and $Q-f$ droop characteristics.

c: ANGLE DROOP CONTROL

Angle droop control is proposed in [102]–[104]. Similar to the conventional $P-f$ droop and $Q-v$ droop control, for the angle droop, the voltage angle (δ) is related to active power (P) instead of frequency (f). The δ of a DER can be calculated from (9);

$$\delta = \int \omega dt \tag{7}$$

The angle droop control is utilized to balance the power requirements between DER's. The equations of voltage magnitude and phase angle are;

$$\delta = \delta_{ref} - m_P(P - P_{ref})$$
$$E = E_{ref} - n_Q(Q - Q_{ref}) \tag{8}$$

Here, δ_{ref} is reference phase-angle of the DER. Angle droop method ensures proper load sharing between DERs. Therefore, frequency deviation is small. However, if the power converters are not properly synchronized, the processing delays of the digital processor clock makes a slight frequency difference among the synchronising converters which may cause phase synchronization problems and ultimately microgrid becomes unstable [105].

d: IMPROVED DROOP CONTROL

In [106], it is reported that the virtual impedance method is similar to the angle droop control and the frequency droop control with an additional power derivative feedback is similar to the virtual impedance method. The large droop co-efficient introduced by the improved droop control, ensures improved active and reactive power sharing which means large virtual impedance mitigates the effect of feeder impedance mismatch. By simultaneously adopting frequency droop and virtual impedance droop, the modified droop can be formed. The $Q-v$ and $P-f$ droop control can be expresses as follows;

$$E_{ref} = E^* - D_Q Q$$
$$\omega_{ref} = \omega^* - D_P P \tag{9}$$

where, D_Q and D_p are $Q-v$ and $P-f$ droop gain respectively. E_{ref}, and ω_{ref} are reference voltage and angular frequency, ω^* and E^* are no load angular frequency and voltage respectively. Angle droop control can be formulated as;

$$\delta_o = \delta_{ref} - m_p p$$
$$E_o = E_{ref} - n_Q Q \tag{10}$$

Here, n_Q and m_p are $Q-v$ and $P-\delta$ droop co-efficient respectively. After differentiating the above equation, it can be written as follows;

$$\omega_o = \omega_{ref} - m_p \frac{dP}{dt} \tag{11}$$

Therefore, frequency droop and virtual impedance droop are combined to form the modified droop as;

$$\begin{aligned} \omega_o &= \omega_* - D_P * P - m_p \frac{dP}{dt} \\ E_o &= E^* - (D_Q + n_Q)Q \end{aligned} \tag{12}$$

This improved droop control method can achieve improved transient response and is more robust for a wide range of system parameter variations. The only drawback is it requires a high bandwidth for the controller.

e: VIRTUAL FRAME TRANSFORMATION METHOD

A new reference frame (orthogonal linear transformation) is used to transform real-reactive power to a new reference frame [107]–[109], which can decouple the active and reactive power. In this approach, the real/reactive power is independent of feeder impedance. The expression of real and reactive power is given by;

$$\begin{bmatrix} P^* \\ Q^* \end{bmatrix} = \begin{bmatrix} sin\theta & -cos\theta \\ cos\theta & sin\theta \end{bmatrix} \begin{bmatrix} P \\ Q \end{bmatrix} \tag{13}$$

This transformed real and reactive power (P^* and Q^*) are used in the basic droop characteristics equations. Similarly, the expression of voltage and frequency in this reference frame are [110];

$$\begin{bmatrix} \omega^* \\ Q^* \end{bmatrix} = \begin{bmatrix} sin\theta & cos\theta \\ -cos\theta & sin\theta \end{bmatrix} \begin{bmatrix} \omega \\ E \end{bmatrix} \tag{14}$$

Conventional droop equation is used to calculate E and ω. This approach decouples real and reactive power, which improves system stability. However, this approach does not consider non-linear load's negative impedance impact. Moreover, the frame transformation angles should be same, otherwise transformed voltage and frequency will be inaccurate.

f: VIRTUAL IMPEDANCE SCHEME

The virtual impedance control strategy is proposed in [111]–[113]. In order to decouple real and reactive power, a supplementary control loop based on virtual output impedance is incorporated to adjust the output impedance of the VCVSI. The control architecture is illustrated in Fig. 11. The reference voltage equation can be expressed as;

$$V_{ref} = V_0^* - Z_v(s) * I_o \tag{15}$$

Here, $Z_v(s)$ denotes the virtual output impedance. Output impedance, in general, is considered as purely inductive. Therefore, $Z_v(s) = s * L_v$ can be obtained by drooping the output voltage proportional to the derivative of the output current. The non-linear loads result in high harmonics.

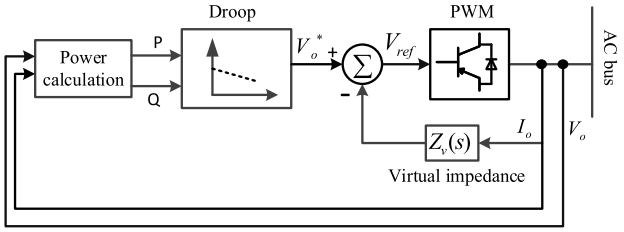

FIGURE 11. Virtual output impedance based control scheme.

These harmonic effects can be eliminated by using a high-pass filter instead of $s * Lv$ as follows [114];

$$V_{ref} = V_o^* - L_v I_o \frac{s}{s + \omega_c} \tag{16}$$

where, ω_c is the high-pass filter cutoff frequency. Properly adjusted time varying virtual output impedance can eliminate the current spike when the DER is connected to the microgrid. The time variant virtual output impedance can be formulated as [115];

$$Z_v(t) = Z_f - (Z_f - Z_i)e^{-t/T} \tag{17}$$

where, subscripts i and f represent initial and final values, whereas T denotes the start-up process time constant. This method can handle non-linear loads. However, poor voltage regulation, undesirable voltage, and frequency deviations may occur in the DER due to inaccurate selection of the time constant.

g: ADAPTIVE DROOP CONTROL METHOD

Compensation based adaptive droop control method for parallel operating DERs in AC microgrid is proposed in [97]. This approach adds two additional terms with the reactive power droop. Voltage is dropped across the feeder when DERs supply power to critical loads. One additional term compensates feeder voltage drop while other term improves reactive power sharing and hence improves the stability. A simple microgrid with two DERs supplying a load is shown in Fig. 12. The voltage equation for DER i can be written as;

$$V_i = E_i^* - n_{Qi}Q_i - \frac{r_i P_i}{E_i} - \frac{x_i Q_i}{E_i} \tag{18}$$

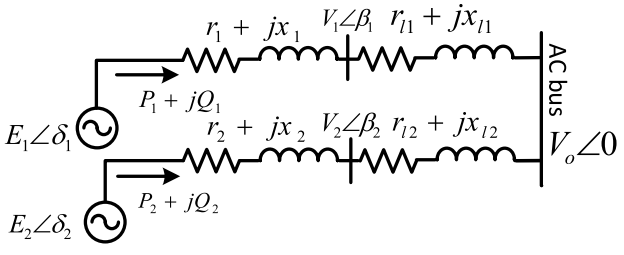

FIGURE 12. Two DERs supplying a load.

Here, r_1, n_{Q1} and x_1 are the feeder resistance, reactive droop co-efficient and reactance of the DER-1, whereas r_2, and x_2 are feeder resistance and reactance of DER-2 respectively.

TABLE 6. Review of droop control based control methods.

Approach	Advantages	Disadvantages
Conventional droop	Can be easily implemented without communication infrastructure; High expandability.	Poor voltage regulation; Poor power sharing; Poor power quality; Incapable of handling non-linear loads.
VPD/FQD droop	Easy to implement without communication infrastructure; Suitable for low voltage resistive microgrids.	Cannot manage nonlinear loads; Poor voltage regulation in inductive microgrids; System parameters affect controller performance.
Angle droop	Same frequency regulation performance as the conventional droop.	Require GPS signals for information exchange and synchronization; Poor power sharing.
Virtual frame transformation	Easy to implement; Easily decouples both the active and reactive power.	Cannot manage non-linear loads; Same transformation angle is required for all DERs; System parameters should be known in advance; Incapable of handling non-linear loads; Voltage regulation is not guaranteed.
Virtual output impedance	Easy to implement; Improves power sharing and system stability; Can manage both linear and non-linear loads; performance is not affected by the system parameters.	Voltage regulation is not guaranteed; Requires high bandwidth controllers.
Adaptive voltage droop control	Improved voltage regulation; Negligible impacts on performance by the system parameters.	Cannot manage non-linear loads; System parameters should be known in advance.

Here, the last two terms represent the voltage drop for feeder resistance and reactance respectively. By incorporating this two terms in the conventional $Q-v$ droop equation of (3), the reactive power droop can be modified as;

$$E_i = E^*_{i,ref} - n_{Qi}Q_i + \frac{r_iP_i}{E^*_i} + \frac{x_iQ_i}{E^*_i} \tag{19}$$

This method improves voltage regulation by considering voltage drop in reactive power droop control loop. However, voltage droop still depends on the active power control. In [97], this problem was solved by considering voltage droop as a non-linear function of both the active and reactive power as follows;

$$E_i = E^*_{i,ref} - n_i(P_i, Q_i) * Q_i + \frac{r_iP_i}{E^*_i} + \frac{x_iQ_i}{E^*_i}$$
$$n_i(P_i, Q_i) = n_{Qi} + m_{Qi}Q_i^2 + m_{Pi}P_i^2 \tag{20}$$

Here, m_{Qi}, m_{Pi}, and D_{Qi} are droop coefficients. The adaptive droop control method can improve reactive power sharing and stability margin. This method modifies the droop by considering feeder resistance and reactance. Therefore, small errors may cause instability of the entire microgrid. A concise overview of these droop control based strategies are summarized in Table 6.

C. STABILITY STUDIES OF AC MICROGRID

Small-signal stability analysis is an important technique to identify the dynamics of the AC microgrid. AC microgrids are usually comprised of VSC based DERs with active/reactive power controllers for parallel operation, dynamic loads (motor loads), passive loads, and resistive or inductive lines [130]–[132]. Extensive research studies have been carried out on small-signal analysis, voltage, and transient stability of AC microgrid to identify the dynamics of each parameter, such as controller dynamics, load dynamics, and system dynamics. In [133], performance of a microgrid controlled by a distributed controller was evaluated by small-signal stability analysis which synthesizes primary control loop, secondary control loop, and communication latency. It is reported that a microgrid with low latency communication link can eliminate some of the non-crucial communication edges to improve the rate of convergence. An AC microgrid with synchronized control under multiple parallel operating circumstances is evaluated in [134] by small-signal stability analysis. This research demonstrated that a doubly-fed induction generator (DFIG) with synchronized control strategy may enhance microgrid frequency support and provide power reserve capability. In [128], small-signal analysis of inverter dominated hybrid AC/DC microgrid is developed where the induction motor (IM) is used as a dynamic load. It was found that the droop gain of the VSC with dynamic load is small compared to the droop gain with static loads. Table 7 summarizes the small-signal analysis methods used for AC microgrid.

VI. CONTROL AND STABILITY OF DC MICROGRIDS

For stable operation of DC microgrids, different control strategies such as centralized, decentralized, and distributed control strategies are used. The following control aspects are listed below based on literature:

- Power sharing
- Load sharing
- Stable voltage
- Power flow control between the adjacent DC microgrids
- Smooth mode switching
- Power loss reduction
- Economic operation
- Reducing blackouts

TABLE 7. Microgrid modelling methods.

Approach	Analysis method and study Outcome
State-space model of inverter dominated AC microgrid is developed. Impedance (static) load model is considered.	AC microgrid network parameters and load sharing controller are responsible for low-frequency modes. However, inverter inner loop controller and load dynamics influence high frequency mode [95].
State-space model of inverter dominated AC microgrid with droop control is developed. Impedance (static) load model is considered.	Eigenvalue analysis is used to determine the stability limits of key controller parameters. Genetic algorithm is introduced to identify key controller parameters [116], [117].
State-space model of autonomous AC microgrid is developed. CPL load model is considered.	Eigenvalue analysis is used to determine the stability of key controller parameters. It is identified that the VSC droop gain, feeder impedance, and CPL loads determine the stability limits of the microgrid [118].
State-space model of autonomous AC microgrid is developed. Impedance (static) load model is considered.	Particle swarm optimization algorithm is used to tune parameters of the controller for better power sharing [119], [120].
State-space model of inverter dominated AC microgrid with modified droop control is developed. Impedance (static) load model is considered.	Converter dynamics do not allow higher droop gain which results poor power sharing performance. This study proposed a modified droop control to improve stability margin and transient response [121].
VSC based microgrid modelling is developed. Impedance (static) load model is considered.	An auxiliary loop, similar to the power system stabilizer, is proposed in addition to the frequency droop, which improves the damping and reduces frequency deviation [122].
Dynamic phasor model of AC microgrids is developed to identify the plug and play operation under various network conditions.	The phasor model is employed along with impedance matching approach to identify the stability criteria. The stability criteria obtained from the analytical analysis is validated using time-domain simulations [123], [124].
Small-signal analysis of inverter dominated AC microgrid is developed. IM (dynamic load) load model is considered.	Eigenvalue participation factors reveal that microgrid dominant eigenvalues are highly sensitive to motor dynamics and droop gain. A damping controller was proposed to improve power sharing [125], [126].
Small-signal analysis of inverter dominated hybrid AC/DC microgrid is developed with dynamic load.	IM loads affect the stability margin of the hybrid AC/DC microgrid. The droop gain of the VSC with dynamic load is small compared to the droop gain with the static loads [127]–[129].

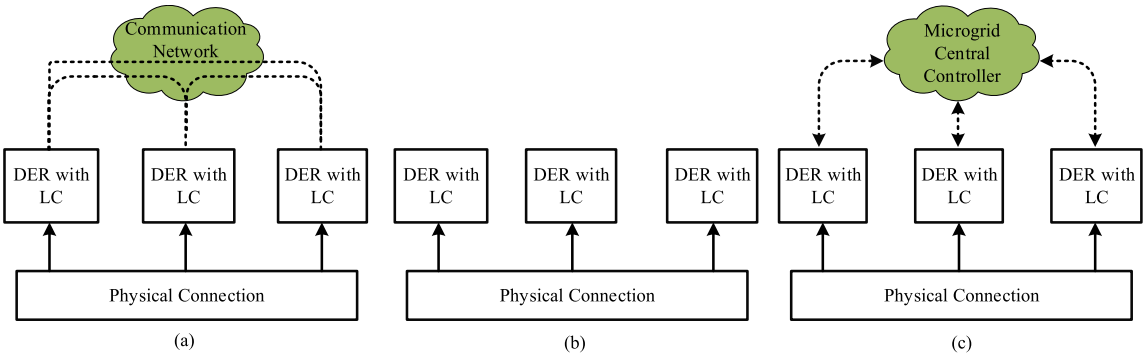

FIGURE 13. Basic control structures of a DC microgrid; (a) Distributed control, (b) Decentralized control, (c) Centralized control.

A. VARIOUS CONTROL STRUCTURES

DC microgrid consists of converter based parallel DERs and battery storage systems. Each converter has voltage, current, and droop control as a local controller. Solar-PV operates on maximum power point tracking (MPPT) as a source dependant controller, and state of charge controller for energy storage devices. These local controllers are coordinated centrally for proper energy management via communication links, which are called centralized control. From the communication point of view, DC microgrid control strategy can be divided into three categories, 1) decentralized, 2) centralized, and 3) distributed control. Fig. 13 illustrates three basic control structures of the DC microgrid.

1) DECENTRALIZED CONTROL

The decentralized control method is based on LC. Data bus signaling (DBS), adaptive control of droop coefficient, and power line signaling (PLS) are commonly used in decentralized control. In DBS based decentralized control, DC bus voltage variation is taken as input for coordination among

multiple DERs, ESS, and the utility grid. The utility dominating mode, storage dominating mode, and generation dominating mode are three basic operating modes of the DC microgrid and the DC bus voltage determines the operating mode. Therefore, the reliability and effectiveness of the decentralized control depend on the voltage measurement of the common DC bus [135], [136]. The principle of the DBS is the coordinated operation among solar-PV, wind, and ESS, which are achieved by the current-voltage (I-V) droop characteristics [137]. The grid interfacing inverters and ESS are controlled by poly-line droop curves with multiple segments [138]. The state of charge (SoC) controller of the ESS controls the output power of the solar-PV, wind, and utility grid. Virtual resistor (VR) with frequency shape is proposed in [139], where a super capacitor is used in ESS to cope with high-frequency power ripples and low-frequency response. As DBS relies on the local DC bus voltage and does not need communication infrastructure, it can be implemented easily. Therefore, the reliability and effectiveness of the decentralized control depend on the voltage measurement of the common DC bus.

The adjustment of droop coefficient adaptively without considering the change of operating mode is an extension of the conventional droop control method. It can adjust SoC among multiple ESSs to maintain accurate charging and discharging of ESSs. In [140]–[142] droop coefficient adjustment are used to balance SoC of multiple ESSs in both charging and discharging processes. Droop coefficient adjustment based on fuzzy logic is used in [143] to balance SoC of the ESS, whereas fuzzy logic based VR is employed to balance SoC of multiple ESSs in [144]. Adaptive droop adjustment needs expertise, and improper setting of droop curve may lead to the unstable operation of DC microgrid [145], [146]. PLS is also used in the decentralized method, which is a communication based method, and it is complex to implement than other two methods [147], [148].

2) CENTRALIZED CONTROL

The centralized control of a DC microgrid has a central control (CC) system with digital communication networks which connects sources and loads. Distributed sources in small DC microgrids are controlled by CC with a high bandwidth communication using master/slave control [149], [150], while in large DC microgrids hierarchical control is used [69]. The hierarchical control method comprises LC of inverters and digital communication links (DCLs) based coordinated control. A campus microgrid system with hierarchical control is proposed in [151], while in [152] a hierarchical control of a stand-alone DC microgrid is employed for stable and economic operation. The ESS charging and discharging control with a different SoC is investigated for DC bus voltage stabilization, while DC microgrid is critically loaded. The researchers in [141] proposed an adaptive droop control as a primary controller for SoC balancing, while supervisory control is employed for mode transition and coordinated control of SoC of multiple ESSs as a higher level control. Since considerable independence between different control levels are introduced by the hierarchical control, DC microgrid continues its operation even after the failure of centralized controller. The CC provides the best performance, but it cannot tolerate a single point of communication failure and requires a costly redundant communication link [153], [154].

3) DISTRIBUTED CONTROL

In distributed control, there is no central control unit and all LCs communicate among themselves through dedicated DCLs. The distributed control can tolerate some point of communication failure compared to CC. Consensus algorithm has been used in microgrid applications [155], [156]. Basically, the consensus algorithm can work with low bandwidth communication techniques that ensure stable DC bus voltage and enhance output current sharing by proportional-integral (PI) controller [157]. The researchers in [158] proposed a dynamic consensus algorithm, which has DC bus voltage measurement system with noise resiliency, while neighbouring DERs voltage are also observed to calculate local DC set points. In [159], a linear circuit model based distributed control is proposed for droop control strategy of the DC microgrid, while [160] proposed an agent based approach for distributed control of DC microgrid. A unified distributed control is proposed in [161], and it does not require DBS. Energy management and DC bus voltage regulation are obtained by distributed control of ESSs in a DC microgrid. Distributed control can tolerate some point of communication failure and have better information awareness compared to centralized control. However, the stability margin and high complexity on analytical performance are the major shortcomings of distributed control [162]. Table 8 summarizes basic properties of these control schemes.

B. CONTROL TECHNIQUES USED IN DC MICROGRIDS

This subsection critically reviews general control methods employed for individual DERs and storage systems in DC microgrids. As mentioned in the previous section, DC microgrid control architecture consists of LC and coordinated control. The LC of the DERs and the storage systems include voltage, current, and droop control. The proper LC of the individual DERs and the coordinated control between different components in the DC microgrid ensure proper power-sharing and stable operation. Some of these control techniques are presented bellow.

1) DROOP CONTROL

Droop control method is commonly employed in DC microgrids for DC bus voltage regulation and proper power sharing. Droop control methods in DC microgrid are classified into two categories, 1) power-voltage (P-V) droop or voltage droop, 2) current-voltage (I-V) droop or current droop [163], [164]. In current droop the DERs current reference is generated from the measured DC bus voltage, whereas in voltage droop the DERs voltage reference is generated from the load current. For both of these droop control methods, the output

TABLE 8. Comparative analysis of DC microgrid control techniques.

Approach	Distributed control	Decentralized control	Centralized control
Communication	Yes	No	Yes
Communication Link	DCL	Power line communication	DCL
Control decision	Processed locally	Local	global
Functional Reliability	Tolerate some point of failure	Depends on the reliability of the communication protocol	Single point of failure damage total control
Cost effectiveness	Cost effective	Easy to implement	Costly as redundant communication line needed

current/power dispatch of each DER is regulated by the DC bus voltage and the droop characteristics. Improved power sharing performance can be achieved with a large droop gain which can cause poor voltage regulation.

2) INVERSE DROOP

Inverse droop is proposed in [165] for DC-DC converter based parallel operating DERs in DC microgrids. The problem associated with the droop is the DERs output reference voltage decrease with the increase of the loads in the DC microgrids. Since the droop coefficient of the output current feedback is positive (negative for conventional droop), the reverse droop will linearly increase the reference output voltage with the load increase. Although the inverse droop does not use input voltage in the control loop, this droop control method increases the output reference with the increase of the load. This approach can be implemented without the central controller which ensures reliability and flexibility.

3) ADAPTIVE DROOP

Droop control method is commonly employed in DC microgrids for DC bus voltage regulation and proper power sharing. Improved power sharing performance can be achieved with large droop gain which can cause poor voltage regulation. Problems associated with the droop-based control method are the voltage deviations and the current sharing inaccuracy. To solve these problems researchers have proposed adaptive droop, where the gain of the adaptive PI controller is adjusted autonomously to improve current sharing errors and handle the non-linearity of the microgrid dynamics [166]–[168].

4) VIRTUAL IMPEDANCE METHOD

The output impedance mismatch of the interfacing converter and to enhance active damping researcher have proposed [114], [176] virtual impedance method. Constant power loads (CPLs) have introduced negative incremental impedance and hence instability issues that are eliminated by a virtual impedance based method. This control approach is utilized to match the output impedance matching of the interfacing converter at harmonic frequencies and resonance damping. Virtual impedance in DC microgrid is related to active power sharing, while in AC microgrid virtual impedance is related to active and reactive power [174], [181]. Researcher in [182] proposed multi-agents stabilization to eliminate the negative impedance impact of CPL which will improve the fault-tolerant capability of the DC microgrid.

5) MASTER-SLAVE CONTROL

The recent technological advancement in communication technologies (Zigbee, WiFi, etc.) and exchange of information (consensus, gossip, p2p, etc.) have paved the way for distributed control and power management in DC microgrid applications [183], [184]. The fast communication infrastructure based master-slave control for DC microgrid has been proposed in [185], [186], where some DERs operate as a master, and some other DERs operate as a slave. The master DERs regulate the DC bus voltage and acts as VSCs, whereas slave DERs act as current source converters. The reliability of the master-salve control will be challenged if there is a single point of communication infrastructure failure [187]. Key characteristics of the aforementioned control methods are presented in Table 9.

C. STABILITY STUDIES OF DC MICROGRIDS

Stable operation of the DC microgrid is a major challenge where instability may occur due to abnormal weather conditions of intermittent DERs, control and line parameters, and load dynamics. The stability study of the DC microgrid is carried out to test the reliability and quality of the microgrid. Load dynamics influence the stability of the microgrid. Generally, impedance (or passive) loads and active loads (CPLs) are being used in the power system. Passive load introduces positive impedance which improves damping, while CPL loads introduce negative impedance which results in poor damping of the microgrid. Basic stability studies in DC microgrid are summarized in Table 10.

VII. CONTROL TECHNIQUES OF HYBRID AC/DC MICROGRIDS

The AC microgrid is the most commonly used microgrid configuration as the existing power networks are operating at AC, while the DC microgrid is getting the attention due to advantages such as increasing use of DC-based loads and

TABLE 9. Control methods used in DC microgrid.

Approach	Methodology	Result
Local Control	LC is based on voltage control, current control, and droop control. Solar-PV operates on MPPT is a kind of LC. Voltage and current control of converter play an important role in power sharing. PI controllers are commonly used because of its zero steady state error. An adaptive controller such as fuzzy logic is also used for voltage and current control.	Local controller ensures the power quality of DERs. For accurate coordination control, LC should be ensured first [69], [144], [169].
Droop control	Droop gain is adjusted in order to achieve equal power sharing among parallel converters and avoid circulating current.	Droop gain affects system stability. There are proportional relationships between droop gain, system damping and power sharing [162], [170].
	A droop controller for the ESS was designed for power balancing and maintaining constant DC bus voltage [171], [172].	
	Droop control is easy to implement and it does not require any communication link. Due to line resistance in distribution network, a circulating current might flow which causes poor power sharing	Distributed control is proposed to improve power sharing [170].
	Communication based distributed control is employed to improve power sharing. It requires complex communication network, and hence it is expensive.	Modified droop control is proposed to achieve zero circulating current [173].
Virtual impedance	Since virtual impedance is employed to match the impedance of the grid side inverter, active and reactive power can be decoupled effectively.	The damping performance of the DC microgrid with CPL loads can be improved by employing virtual-impedance based stabilizers. Furthermore, it improves resonance damping of the LCL filters. Meanwhile, at a particular frequency, it ensures better harmonic sharing and damping performance [114], [174]–[176].
Master-slave control	In this method of control several DERs act as master DERs and maintain DC bus voltage. On the other hand, some DERs supply a constant amount of power. Master DERs is like a VSC while the slave DERs are current source converter.	All control actions are processed by a central controller, which is complex and costly as well [177], [178].
Adaptive control.	An adaptive control strategy was introduced for exact power management and eliminate the intermittent behaviour of various energy sources. It provides better performance than conventional PI.	It does not require a communication link. It requires a large computational time [179], [180].

TABLE 10. Stability studies in DC microgrids.

Approach	Methodology	Result
Stability with droop control	The voltage stability issues of the droop controlled DC microgrid are investigated considering CPL loads. CPL loads have negative impedance effects which reduce the stability margin.	Droop gain affects stability. Higher the droop gain, higher the power sharing, however; lower the system damping [188], [189].
Frequency dependent VR	In depth stability analysis and damping performance of DC microgrid with droop coefficient, line parameters, and filter are performed.	If the line filter is not properly designed, it introduces poor damping and high frequency oscillations in the microgrid [190].
Stability analysis with CPLs	A small-signal stability analysis of the DC microgrid with CPLs is carried out.	VR is proposed to cancel out negative impedance impact of CPL and therefore, it improves stability [174], [191].
Robust stability with CPLs	The DC microgrid stability analysis with some nominal values of CPLs are presented. Model uncertainty was introduced by considering arbitrary values of CPLs within a certain time interval.	A dynamic simulation is carried out in MATLAB/Simulink with the convex optimization toolbox to identify the stability of all the operationally feasible equilibrium by varying the CPL load from the minimum value to maximum value. This research identifies equilibrium conditions for a given range of CPLs, which ensures the robust stability of the DC microgrids [192].
Stability analysis with storage system	A relationship between voltage and CPL loads are developed to ensure robust stability of DC microgrids. The impact of CPLs as well as ESS on DC microgrid stability studies are analysed.	The stability issues imposed by negative impedance effect with CPL in the DC microgrid is eliminated by the ESS [193], [194].

sources, no synchronization problem, and no reactive power requirements. Therefore, hybrid AC/DC microgrid is the optimal architecture as it combines the advantages of both the DC and the AC microgrids [31], [194]–[196].

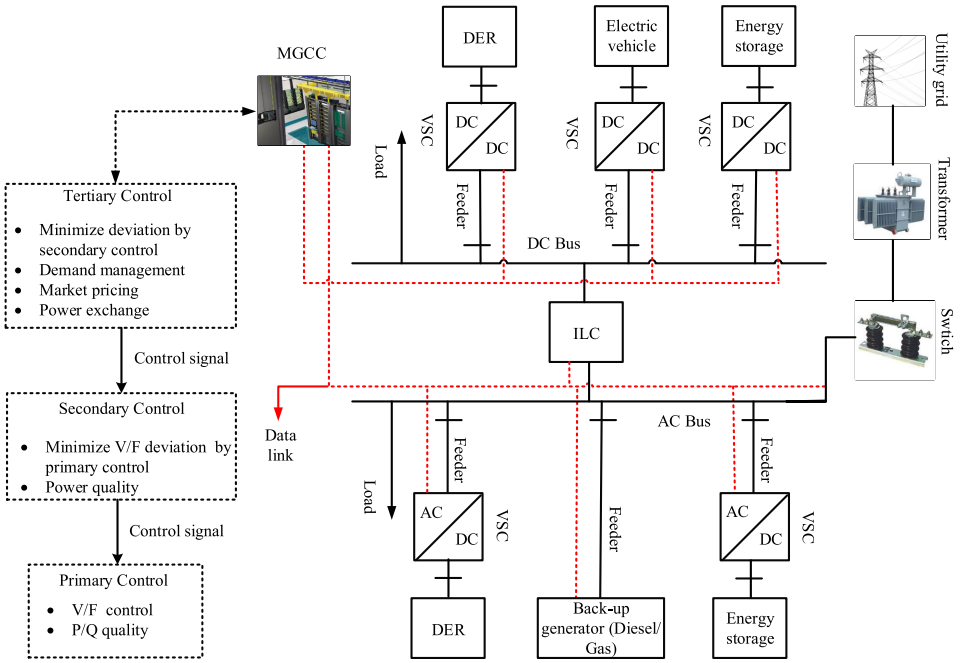

FIGURE 14. A hierarchical control structure of the hybrid AC/DC microgrid.

A. HIERARCHICAL CONTROL SCHEMES

Despite these advantages, the major challenges of the hybrid AC/DC microgrid are energy management and stability. Extensive research and review have been done on stability and control strategies of hybrid AC/DC microgrids [82], [197]. Different control strategies are adopted for optimal energy management of hybrid AC/DC microgrids. The most important control objectives are stability, power balance, synchronization, and protection. To fulfill these objectives complex control architecture is required. Mainly, hierarchical control architecture is employed in hybrid AC/DC microgrids. This control architecture has three level control strategies, 1) primary control, 2) secondary control, and 3) tertiary control. A hierarchical control structure of the hybrid AC/DC microgrid is presented in Fig. 14 and detail descriptions are presented in the subsequent sections.

1) PRIMARY CONTROL

Primary controller controls voltage and current of the DER and ESS interfacing converters. In order to maintain stable voltage and frequency, optimal power management and power-sharing of multiple DERs and ESSs are essential. Existing literature proposed two converter control modes for the primary control, 1) grid following mode, and 2) grid forming mode. In primary control level, the inverter control strategy should be selected based on the mode of operation of the hybrid AC/DC microgrid. In grid following mode, the utility grid maintains stable voltage and frequency at the hybrid AC/DC microgrid, while the DERs and the ESSs are operating in CCVSI for maximum power generation and charging mode respectively. In grid forming mode, the hybrid AC/DC microgrid is disconnected from the utility grid, and multiple DERs and ESSs maintain stable voltage and frequency of both the AC and the DC busbars. Thus, all DERs operate in VCVSI and ESSs operate in discharging mode [67]–[70]. Depending on the number of DERs participating in voltage control, this control method is further subdivided into two categories:

- A single DER interfacing converter operates in grid forming mode and is maintaining stable voltage and frequency while other DERs operate in CCVSI [69], [70].
- More than one DER interfacing converters operate in grid forming mode and are maintaining stable voltage and frequency. Proper synchronization is required for the DERs interfacing converters, which are operating in grid forming mode [67], [68].

2) SECONDARY CONTROL

The secondary control method is employed to compensate the DC bus voltage deviation in the DC sub-grid and voltage and frequency deviations in the AC sub-grid of the hybrid AC/DC microgrid. This controller also maintains black-start and synchronization after mode switching. The secondary control is divided into two categories- (1) centralized control and (2) decentralized control [198]–[200]. In the centralized control method, a global controller known as MGCC performs power management in the hybrid AC/DC microgrid. To maintain the exact power balance, MGCC acquires the active and the reactive power information from DERs, ESS, and critical loads; to take care of the security issues and energy market operation. To do so, it requires communication

infrastructure which introduces control complexity and additional costs [201]. In the decentralized control method, there is no MGCC, and the MGCC control function is implemented into the local controller. Therefore, DERs and ESSs are responsible for power management [84]. As there is no global controller, in case of a fault the microgrid can maintain its operation by disconnecting the faulty part from the rest of the microgrid.

3) TERTIARY CONTROL

This control approach is applied in the grid forming mode. This method controls real and reactive power flows between the hybrid AC/DC microgrid and the utility grid to regulate voltage and frequency. This method can also be implemented either in centralized or in distributed manner. In centralized management, active and reactive power are measured at the PCC, while reference active and reactive power are calculated based on the microgrid power requirements and energy market operations. In this way, power quality, efficiency, and economic operation are ensured. In contrast to the distributed control, the tertiary control level is implemented in the main grid rather than at the microgrid MGCC. However, in [202], [203], a hybrid AC/DC microgrid architecture with the tertiary control approach is proposed with distributed control. In this tertiary control approach, consensus/gossip algorithm help to gather global information and the optimization algorithm is used to find the local optimal decision which compensates power quality issues. The tertiary controller generates a compensation signal for the DERs local controller to improve power quality at the local bus. This control approaches have two communication links, one is dedicated for consensus/gossip-based tertiary control and the second link is dedicated to the primary controller. A concise summary of these three control approaches are presented in Table 11.

TABLE 11. Hybrid AC/DC microgrid control approach.

Primary	Secondary	Tertiary
• Grid forming • Grid following	• Centralized • Decentralized	• Centralized • Distributed
Based on LC	Both the local and the global control	Global control
Can be applicable for autonomous mode and grid-connected mode	Can be applicable for autonomous mode and grid-connected mode	Applicable for only grid forming mode
No communication link is required	It requires communication infrastructure	Two communication links are needed. One link is dedicated to tertiary control while second link is dedicated for primary and secondary control
Can be implemented easily	Complex control	Control is complex and costly

B. POWER MANAGEMENT STRATEGY OF HYBRID AC/DC MICROGRID

The most important aspects of a hybrid AC/DC microgrid operation are the power management and control strategies. Multiple renewable sources and ESSs are connected to both the AC and DC busbars of the hybrid AC/DC microgrid while these buses are connected by a bidirectional ILC. The output power of the DERs and ESSs are determined by the power management strategies which is also used to maintain the stable voltage and frequency on both sub-grids. The detailed control strategies based on the mode of operation are explained in the subsequent sections.

1) GRID-CONNECTED MODE

In grid connected hybrid AC/DC microgrids voltage control and power balance can be achieved either in dispatched output power mode (where high level control approach regulates power flow between the utility grid and the hybrid AC/DC microgrid) or in un-dispatched output power mode (where hybrid AC/DC microgrid is not dispatching power) [204]–[206]. In dispatched output power mode, DERs and ESSs operate in either voltage control or current control modes. In the current control mode, the reference power is tracked by controlling the DERs output current while the voltage and frequency are determined by the utility grid. In the voltage control mode, DERs output power is regulated by controlling its output voltage and DERs operate as synchronous generators [207]. The bi-directional ILC can be operated in AC sub-grid voltage control, DC sub-grid voltage control, and power control modes with the essential coordination between the AC and the DC sub-grid DERs, ESS and ILC. In the grid connected dispatched output power mode, the DC sub-grid voltage and dispatched output power can be controlled by two approaches. In the first approach, the DC sub-grid voltage is regulated by the ILC, while the DERs and the ESSs on both the AC and the DC sub-grids are coordinated to maintain dispatched output power. In the second approach, DC sub-grid DERs and ESSs regulate the DC sub-grid voltage, while DERs, ESSs, and ILC in the AC sub-grid produce dispatched output power [195], [195], [208]. In the un-dispatched mode, all DERs in AC and DC sub-grids operate in current controlled mode which means that the microgrid is injecting power to the utility grid and the ESSs are in charging mode, whereas the ILC regulates DC sub-grid voltage [20], [51]. The power management modes of hybrid AC/DC microgrids are illustrated in Fig. 15.

2) STAND-ALONE MODE

In stand-alone mode, the coordinated control between ILC, DERs, and ESSs either in AC sub-grid or DC sub-grid is essential to regulate the AC sub-grid voltage and frequency, DC sub-grid voltage, and to balance load demand and power generation respectively. Droop control [69], [209], master-slave control [89], [210],

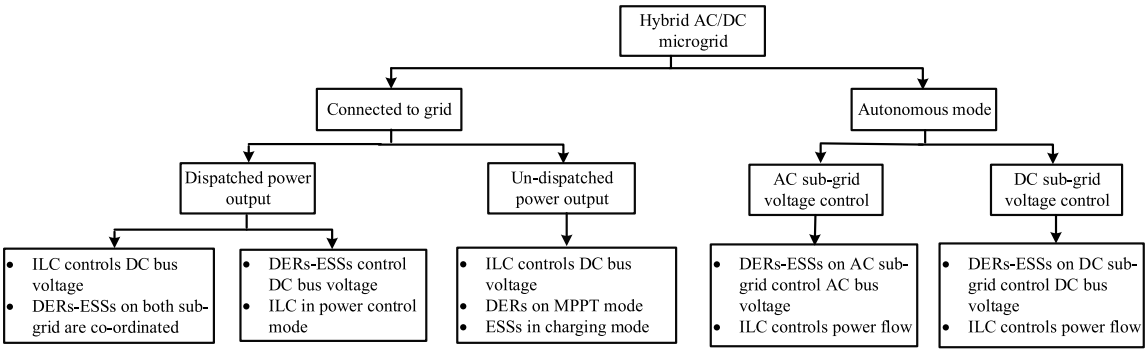

FIGURE 15. Hybrid AC/DC microgrid power management strategies.

etc. are used for power management in AC sub-grid in stand-alone operation mode, while DC bus voltage management in DC sub-grid can be achieved either by DERs-ESSs direct droop control method [195] or by indirect power balancing [51], [211] method. The DC sub-grid voltage control mode, AC sub-grid voltage control mode, and output power control mode are important control aspects of the ILC. In stand-alone mode, DERs and ESSs connected to the AC and DC sub-grids, are used to regulate AC and DC bus voltages respectively, while the ILC manages the power flow between the two sub-grids. However, for parallel operating multiple ILCs in a hybrid AC/DC microgrid, some ILCs can operate in DC sub-grid voltage control mode while other ILCs can operate in AC sub-grid voltage control mode.

3) POWER MANAGEMENT STRATEGY OF HYBRID AC/DC MICROGRID DURING MODE TRANSITION

Previously mentioned power management strategies for hybrid AC/DC microgrid are utilized in the steady-state operation mode. The mode transition between the grid-connected mode and the islanded mode of hybrid AC/DC microgrid should be seamless; however, it may cause voltage spikes, large voltage/frequency deviations, and circulating current in DERs during mode transition. Two transition modes, 1) grid following mode to grid forming mode transition, 2) grid forming mode to the grid following mode transition will be discussed in the subsequent sections.

a: GRID FOLLOWING MODE TO GRID FORMING MODE TRANSITION

Mainly two types of control strategies are used for hybrid AC/DC microgrid mode transition from grid following mode to grid forming mode, 1) changing of the current/power control mode in grid following mode to voltage control mode in the grid forming mode, 2) unified control method on both modes of operation. Usually, DERs in current/power control mode operates on MPPT to supply the maximum power to the utility grid, whereas voltage control mode is utilized to maintain generation and load demand, and to supply continuous power to the critical loads. For a smooth mode transition, in [212], [213], a new seamless mode transition is proposed which reduces DERs line current to zero before mode transition. A faster mode transition without making DERs line current to zero during the mode transition can be achieved by coordinating voltage control in grid forming mode and the current control in grid following mode [214]–[216]. To switch the controller of hybrid AC/DC microgrid from the grid following mode to grid forming mode, various islanding detection algorithms such as active, passive, and communication link based detection approaches are used to select mode transition time [217], [218]. Immediately after isolation, voltage control is activated, and the synchronization unit starts its function at a fixed frequency as an isolator. In the second approach, the control strategy is same as before and after mode transition, and there is no need to modify the control strategy [219]–[222]. It is therefore challenging to develop a robust control method which should work well in grid forming mode, grid following mode, and transient mode. Thus, there is no need for islanding detection. Therefore, in a unified control method in both modes of operation, smaller capacity DERs-ESSs are operated in current control mode, whereas large DERs-ESSs are operated in voltage control mode. However, some modification on the control approach is needed as the same control approach is being used for grid-connected, stand-alone, and transition modes. For instance, conventional droop is modified by combining virtual impedance droop [220], [223], [224] with the PI based droop control.

b: GRID FORMING MODE TO GRID FOLLOWING MODE TRANSITION

Mainly two types of control strategies are used for hybrid AC/DC microgrid mode transition from grid forming mode to grid following mode, 1) switching of voltage control mode in the grid forming mode to current/power control mode in grid following mode, 2) unified control method on both modes of operation. The microgrid voltage should be synchronized with the utility voltage before re-connection, where active and passive synchronization are used. In passive synchronization, microgrid and main grid are connected when they have the same phase angle assuming that both have nearly

equal voltage. This synchronization approach is widely used, and an unequal voltage between microgrid and utility grid may lead to some transients at the time of re-connection. Active synchronization provides a fast synchronization and seamless transition between the microgrid and the utility grid. Active synchronization requires the coordination of multiple DERs and ESSs. In some cases, a separate synchronization unit embedded into the microgrid as an independent entity to provide a synchronization signal to connect microgrid with the main grid; whereas, in others, a synchronization unit is embedded with the control strategies to reconnect the microgrid to the main grid. In the grid forming mode, mainly two control approaches are used, 1) some DERs operating on voltage control mode while others are operating on current control mode, 2) all DERs operating on voltage control mode. Depending on these control modes, the active synchronization is classified into the following two categories, 1) some DERs initiating synchronization while the others are following them, 2) all DERs are participating in the synchronization process. The first approach is used in a microgrid where some DERs are operating on voltage control mode while other DERs are operating on current control mode [225]–[227]. However, the second synchronization approach is used in a microgrid where all the DERs are operating on voltage control mode [225], [228]. Hybrid AC/DC microgrid power management strategies during mode transition are summarized in Fig. 16.

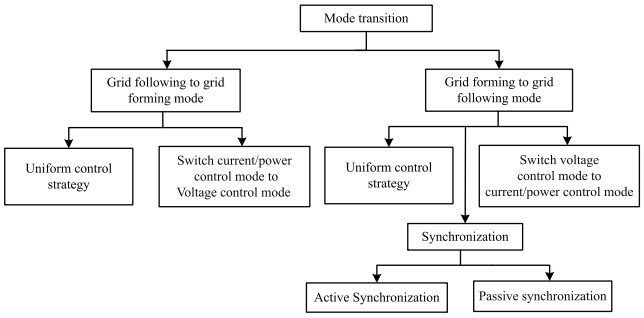

FIGURE 16. Hybrid AC/DC microgrids power management strategies during mode transition.

C. COORDINATED CONTROL OF ILC AND ESS

The ILC connects both AC and DC sub-grids to form hybrid AC/DC microgrid. It behaves like a source to one sub-grid and load to another sub-grid. The main responsibilities of the ILC are bidirectional power transfer between two sub-grids, the DC bus voltage regulation, voltage/frequency regulation of the AC bus, and plug-play operation [229]. When hybrid AC/DC microgrid are connected to the utility grid, utility grid maintains real/reactive power in AC sub-grid, and the ILC regulates the DC bus voltage by providing active power. While in islanded mode, coordinated control among DERs, ESSs and ILC is needed to maintain voltage/frequency of the AC sub-grid and the DC bus voltage of the DC sub-grid. Droop based autonomous control of ILC is proposed in [230], whereas autonomous control operation of ILC with droop utilizing normalized frequency and DC bus voltage are investigated in [231]. The studies have only considered single droop based VSC rather than multiple DERs connected in parallel.

Autonomous control operation of ILC with combined power/frequency and voltage/frequency droop are proposed in [195]. Multiple DERs droop coefficients are difficult to combine properly by dynamic droop characteristics and any DER may shutdown due to maintenance [229]. Conventional DC voltage based droop for the hybrid AC/DC microgrid ILC creates circulating power because of line resistances which overstress the ILC. In order to avoid circulating power between multiple ILCs, frequency based droop is proposed in [232]. Existing hybrid AC/DC microgrid architectures use two separate storage system for the AC sub-grid and the DC sub-grid. Because of significant amount of power exchange and multiple interconnections between the AC and the DC sub-grids, multiple ILCs are proposed in [233]. Important ILC control approaches are presented in the subsequent sections.

1) UNIFIED CONTROL OF ILC

Unified control of the ILC is proposed in [233], and the control block diagram is illustrated in Fig. 17 which consists of an outer power control loop and an inner voltage/frequency control loop. The DERs and the ESS on both the AC and the DC sub-grids are categorized into two types, 1) power terminals, 2) slack terminals. The DERs-ESSs on the AC and DC sub-grids which are used to control frequency and AC and DC sub-grid voltages are known as slack terminals (or power balancing unit) while the DERs-ESSs on the AC and the DC sub-grids which are working in MPPT mode (dispatched output power mode) are known as power terminals. Lets consider that the total real power output of the AC and the DC sub-grid power terminals are P_{ac} and P_{dc} respectively, and the droop characteristics of the slack terminals take the following forms;

$$\begin{aligned} V_{dc} &= V^*_{dc} + (P^*_{dc} - P_{dc})/K_{dc} \\ \omega_{ac} &= \omega^*_{ac} + (P^*_{ac} - P_{ac})/K_{ac} \end{aligned} \tag{21}$$

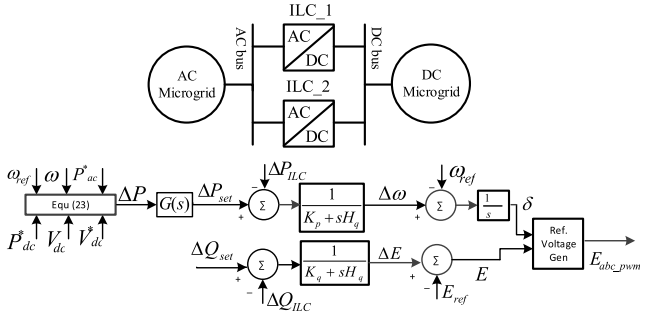

FIGURE 17. Unified control structure for ILC.

Here, V_{dc}, V^*_{dc}, K_{dc}, P^*_{dc}, and P_{dc} are DC sub-grid slack terminal voltage, reference DC bus voltage, DC droop gain,

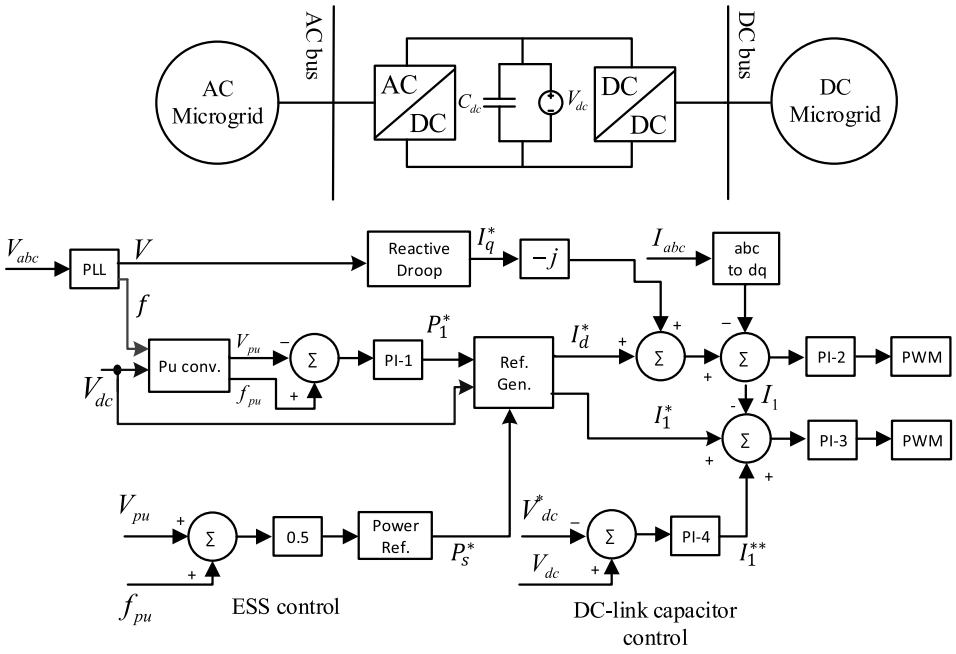

FIGURE 18. Control structure of the ILC with ESS.

reference real power, and actual real power, respectively whereas ω_{ac}, ω_{ac}^*, P_{ac}^*, P_{ac}, and K_{ac} are AC sub-grid slack terminal voltage, actual frequency, reference frequency, reference real power, actual real power, and AC droop gain, respectively. The actual active power output of the PCC of the AC sub-grid and the DC sub-grid is maintained based on the capacity (K) in normal condition. The power error (ΔP) at the PCC of the AC sub-grid and DC sub-grid takes the following form;

$$\Delta P = P_{ac} - K * P_{dc} \tag{22}$$

After applying the droop characteristics from (21) into (22)

$$\Delta P = [P_{ac}^* + K_{ac}(\omega_{ac}^* - \omega_{ac})] - K[P_{dc}^* + K_{dc}(V_{dc}^* - V_{dc})] \tag{23}$$

In Fig. 17 the output power reference can be measured by applying the (23), and after that, the active power reference set-point can be calculated from the regulator transfer function $G(s)$. For inner control loop, the amplitude reference (E) and phase reference (δ) are calculated based on the reactive power/voltage droop ($Q-v$) and real power/frequency droop (P-f), respectively [234]–[236]. Therefore, instantaneous AC voltage control is utilized and the proportional resonant controller is used for the AC voltage tracking which reduces steady-state error and improves dynamic stability.

2) ENERGY STORAGE WITH INTERLINKING CONVERTER

A new structure of the hybrid AC/DC microgrid which includes ESS within the ILC is presented in [195]. The capacitor or battery system at the DC-link of the ILC can be used for energy storage purposes. The ILC storage system is connected to the DC sub-grid through a DC-DC boost converter and to AC sub-grid through a DC-AC converter. The control structure of the ILC with the storage system is illustrated in Fig. 18. AC sub-grid voltage (V_{abc}) is converted to voltage (V) and frequency (f) through PLL and, these two quantities are then converted to per-unit values. The control error is caused by the different droop gains due to the line and system parameters, and it is eliminated by converting system parameters to per-unit quantities. The per-unit quantity of frequency (f_{pu}) and voltage (V_{pu}) can be formulated as;

$$\begin{aligned} f_{pu} &= \frac{f - \frac{1}{2}(f_{max} + f_{min})}{\frac{1}{2}(f_{max} - f_{min})} \\ V_{pu} &= \frac{V - \frac{1}{2}(V_{max} - V_{min})}{\frac{1}{2}(V_{max} - V_{min})} \end{aligned} \tag{24}$$

The error of the per-unit voltage and frequency is passed through the PI-1 controller which generates an active power reference signal (P_1^*). The active power reference signal determines the active power transfer between the AC and the DC sub-grid. After that, the active current reference (I_d^*) and the DC current reference (I_1^*) are calculated from P_1^* using the following equations;

$$\begin{aligned} I_d^* &= 2 * P_1^*/3V \\ I_1^* &= -P_1^*/V_{dc} \end{aligned} \tag{25}$$

where, V_{dc} is the DC terminal voltage of the ILC. The reactive component of the current (I_q^*) is calculated from the reactive power droop by the following equations;

$$\begin{aligned} Q_1^* &= \frac{V - V_{max}}{Q} \\ I_q^* &= -2Q_1^*/3V \end{aligned} \tag{26}$$

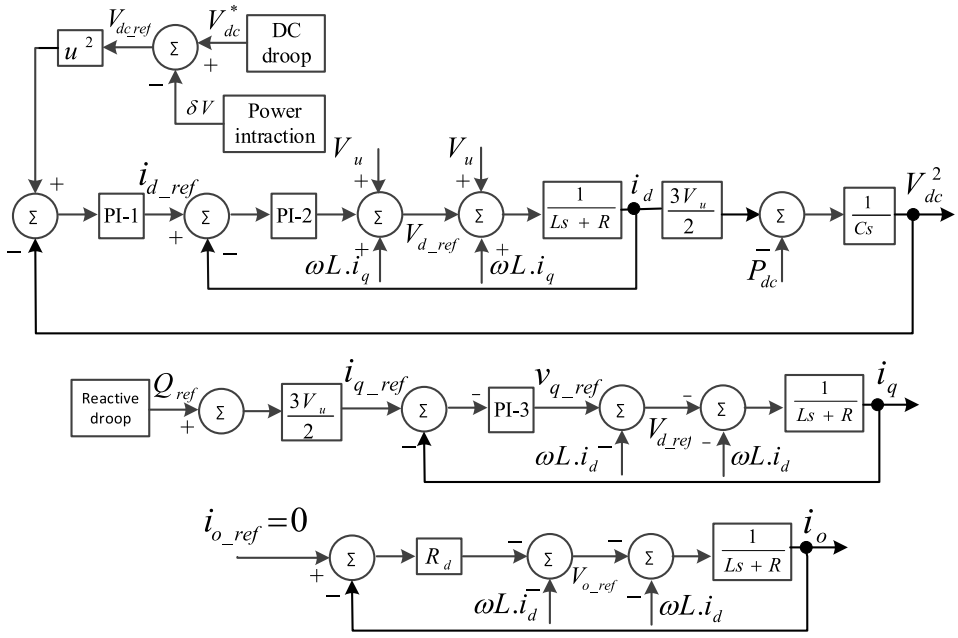

FIGURE 19. Bi-directional ILCs control structure for the *d*-axis, *q*-axis, and 0-axis.

Here, Q is the reactive power droop co-efficient. AC side current ($I_d^* + jI_q^*$) and DC side current (I_1^*) of the ILC are tracked by the PI-2 and PI-3 respectively. The DC-link capacitor voltage is kept constant by using PI-4 controller. This PI-4 controller produces small active current signal (I_1^{**}) which is added to the active DC current reference (I_1^*) signal. A storage system, instead of a DC-link capacitor can be added to the ILC. The charging and discharging of the storage system is fixed based on the two basic criterion, 1) the storage should be charged when the generation is greater than the demand, 2) the storage should be discharged when generation is less than the demand. These two criterion require sensing of generation and demand which are done by measuring DC terminal voltage and frequency. The mean value, $V_1 = \frac{f_{pu}+V_{pu}}{2}$ is passed through the charging-discharging reference power generator (P_s^*) which incorporates with the active power reference signal (P_1^*), and modifies the AC and DC current references.

3) CONTROL OF MULTIPLE BI-DIRECTIONAL ILCs

A distributed coordination control of multiple parallel bi-directional ILCs in a hybrid AC/DC microgrid is proposed in [52], where AC and DC sub-grids are connected through multiple ILCs, and the ESS is attached to the AC sub-grid. The significant difference of the existing control methods presented in [69], [243]–[245] with this approach [52] is three-axis $d-q-o$ control in inner current control loop of the bi-directional multiple ILCs and the feedback linearization technique. Furthermore, normalized (per-unit) frequency/DC voltage droop is adopted to realize power interaction. As highlighted in many literature, multiple parallel ILCs can create a circulating current which is suppressed by the $d-q-o$ inner current controller while the square of the DC sub-grid voltage based feedback linearization technique is used as a decoupling controller [246], [247]. The detailed control architecture of the multiple ILCs with three axis $d-q-o$ inner current loop is illustrated in Fig. 19. These two combined control strategies greatly enhance ILCs inner current control performance, active power sharing (outer loop DC droop) between ILCs, and reduce ESS stress by producing reactive power. The power management which includes power interaction between AC and DC sub-grids, and DC current sharing is mainly achieved by the outer control loop. DC droop is utilized to achieve DC current sharing. The power interaction can be derived as follows;

$$V_{dc,ref} = V_{dc}^* - \delta V - R_K(i_{dc} - i_{dc}^*) \tag{27}$$

where, i_{dc}^*, i_{dc}, $V_{dc,ref}$, V_{dc}^*, δV, and R_K are rated output DC current, output DC current, DC-link voltage reference, rated DC-link voltage of inner loop, output of power interaction control, and droop co-efficient respectively. The δV can be obtained by $\delta V = K(f_{ref} - f)$. where, f_{ref}, K and f are reference frequency, droop coefficient, and actual frequency respectively. The reactive droop used to generate reactive power can be expressed as;

$$Q_{ref} = Q - N_K(V_u - V_u^*) \tag{28}$$

where, V_u, Q_{ref}^*, N_K, and Q are actual AC sub-grid voltage, reactive power reference, reactive droop co-efficient, and rated reactive power output respectively. The outer control loop generates reactive current reference (i_{q_ref}) for the inner control loop. As mentioned earlier that the inner control loop is based on three axis $d-q-o$ control and feedback linearization based on V_{dc}^2 is adopted to avoid non-linear coupling

TABLE 12. Coordinated control between ILC and ESS of a hybrid AC/DC microgrid.

Approach	Pros	Cons
Unified control of ILC	Unified control comprises two control layers, 1) outer power control, 2) the inner voltage and frequency control. These two control loops ensure autonomous mode of operation and seamless mode transition. Moreover, it can be easily implemented without a communication link.	It proposed multiple ILCs between the AC and the DC sub-grids. However, the co-ordination control between multiple ILCs and ESS are missing [235].
ILC with Energy storage	ILC is equipped either with DC-link capacitor or energy storage. The ILC seems like storage system is connected to DC sub-grid through a DC-DC boost converter and storage system is connected to AC sub-grid through DC-AC converter.	A single ILC is incapable of large amount of power transfer because of practical inverter size constraint. In autonomous mode, if the storage system SoC is less than 20% and AC sub-grid or DC sub-grid generation is less than demand, then AC and DC sub-grids will lose its synchronism [196].
Three co-ordinate control of multiple ILCs	AC and DC sub-grids are connected through multiple ILCs, and ESS is attached in the AC sub-grid. The significant difference of the existing control methods in literature with this approach is three axes $d-q-o$ control in the inner current loop of the bi-directional multiple ILCs. Multiple parallel converters can create a circulating current which is suppressed by the inner current controller and square of the DC-link voltage is used in feedback linearization method as a decoupling controller.	As three axis $d-q-o$ controller increase the system order and also its a coupled system, therefore the stability analysis is a very complicated task [52].
Modified droop based control of ILC as a key segment	Modified droop based control strategy for ILC in hybrid AC/DC microgrids is proposed as a key segment and exchange required amount of energy between two sub-grids. The significant difference of this approach with the literature [196], [225], [239], [240] is ILC is operated in voltage control mode and no need for frequency measurement. The voltage control mode ensures voltage quality in AC sub-grid, and $P-f$ droop slope can be chosen small, leading to small frequency variation.	None of the AC sub-grid and DC sub-grid have a storage system and the coordinated control between ILC and ESS is missing [241].
Superimposed frequency based droop control of multiple ILCs	The AC and the DC sub-grids are interconnected through multiple ILCs, and power-sharing between them is controlled by introducing a superimposed frequency based droop in DC sub-grid. As the AC voltage is proportional to the output power, the DC converter superimposes an AC voltage signal to the DC voltage signal. Since the superimposed frequency signal is the same for all the converters, ILCs can share loads corresponding to the droop gain. Hence, power sharing is not affected by the line resistance.	There is no storage system and the coordinated control between ILC and ESS is missing [242].
The improved virtual impedance control method of ILCs	An improved virtual impedance control is proposed for ILC to accurately share power and circulating current reduction, in which current sharing deviation and circulating current are used as feedback to the controller. The two main drawbacks of virtual impedance, 1) large virtual impedance limits power transfer capability, 2) small virtual impedance degrade current sharing accuracy [243], [244] are solved by this approach.	This approach is suitable for a specific hybrid microgrid configuration, which has a specific bus that is used to connect the bi-directional converters to AC bus to AC loads and the main grid [245].

of active current (i_d) and reactive current (i_q). The inner d-axis controller has two control loops, 1) voltage control loop, 2) current control loop. The voltage control loop is slower than the current control loop. The d-axis voltage controller is a PI based controller which produces i_{d_ref} for the current controller and PI based d-axis current controller generates i_d current. Similarly, PI controller based q-axis current controller generates i_q current. A damping resistance (R_d) is used in the o-axis controller to suppress the circulating current. Furthermore, i_d and i_q decoupling through the corresponding compensations are also implemented here to improve the system performance. Table 12 summarizes existing coordinated control approaches of multiple ILCs and ESS.

VIII. FAULT RIDE-THROUGH OF MICROGRIDS

The voltage restoration technique to support the grid voltage during a fault is known as the low voltage ride through (LVRT). The microgrid inverters should have the voltage support capability under grid faults scenarios. Many research studies have been carried out on the LVRT capability of inverter dominated DERs during grid faults considering inverter maximum current constraints [250]–[253]. The inverters essentially supply allowable reactive power during a grid fault and boost up the PCC voltage. The LVRT requirements and reactive power capability standards for the microgrids are illustrated in Figs. 20 (a) and (b) respectively [248], [249]. In Fig. 20 (a), grid fault occurs at $t = 1.0$ s, if the PCC voltage drops bellow 0.3 pu, the microgrid should be disconnected from the main power grid. On the other hand, if PCC voltage gradually recovers, microgrid should remain connected to the main power grid. The corresponding reactive power requirements due to PCC voltage sag can be calculated from Fig. 20 (b). For example, if the PCC voltage drops by 0.2 pu, the reactive power should be increased by m, where m is reactive power slope constant. If the PCC

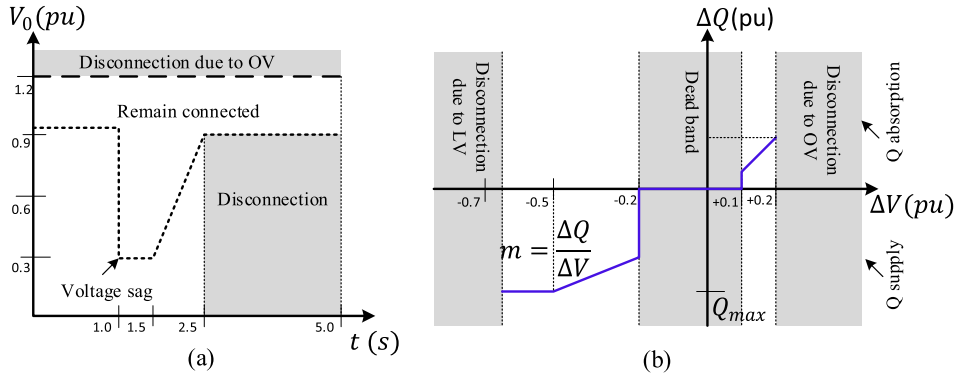

FIGURE 20. LVRT capability curves, (a) LVRT requirements, (b) reactive power capability [248], [249].

voltage is higher than 1.2 pu, the microgrid should be disconnected due to over-voltage and the microgrid's inverter should supply maximum reactive power (Q_{max}) if the PCC voltage drops bellow 0.5 pu. The LVRT capability of the hybrid AC/DC microgrid will be discussed in the subsequent sections.

A. LVRT CAPABILITY OF AC MICROGRIDS

As the penetration level of grid-connected microgrids is increasing, AC microgrids should have LVRT capability against faults either in the utility grid or within the microgrids itself. A hierarchical control strategy for improving the LVRT capability of AC microgrids is proposed in [254] where four distinct control levels are employed, 1) primary fault current limits, 2) secondary fault current limits, 3) tertiary fault current limits, and 4) quartus fault current limits. During a fault, the fault current of the VSC can be controlled by controlling either amplitude or phase angle. Since fault ride-through voltage magnitude is constant, the phase angle is adjusted to limit the fault current. Therefore, the phase angle of the positive/negative sequence fault current of the VSC should be shifted to eliminate the effects of fault current. In summary, the hierarchical control strategy work sequence is as follows: first, the reactive current injection is determined by the grid code requirements; then, the VSC phase angle shift is determined and updated. After that, the active current injection is formulated to justify the phase angle requirements and finally, the VSC generates the output current. A superconducting fault current limiter based on flux coupling is proposed in [255] to limit fault current and improve the LVRT capability of the AC microgrid. This control approach can work well for both grid-connected and islanded modes of operation of AC microgrids which is integrated into the VSC. Once a fault has occurred, it detects the fault condition and initiates control actions to suppress the fault current immediately.

The LVRT capability of a VSC is improved by an additional voltage controller which can be implemented into the VSC controller without any modification into the control architecture [256]. The auxiliary controller identifies faults using fault identification algorithms and determines the active and reactive power dispatch of the VSC according to the grid code requirements. The LVRT capability of the inverter interfaced AC microgrid is proposed in [257], where current and voltage limiters are implemented into the output of the voltage and current controllers of the VSC which limits the current reference during over-current due to the faults.

B. LVRT OF DC MICROGRIDS

The LVRT capability of a hybrid ESS in DC microgrids is briefly analyzed in [258]. Since current drawn during a fault is increased without any control, it will damage equipment and switches. This research proposed a controllable switch in series with hybrid storage systems to limit fault current and hence improved the LVRT capability. A resistive superconducting fault current limiter for DC microgrid is proposed in [259]. The benefits of this control approach are as follows: 1) limiting the DC fault current; 2) compensating DC bus voltage drop to ensure LVRT capability improvement; 3) enhancing the power transfer capability during a fault. A superconducting magnetic ESS embedded with fault current limiting functionality can be utilized to improve LVRT capability in DFIG dominated DC microgrids [260]. In this control method, two DC choppers are connected with the superconducting magnetic coil. In nominal operation, superconducting magnetic ESS acts as the storage system and minimizes power fluctuations of DFIG, whereas during a fault, the superconducting coil detects the fault and initiates control actions to limit severe fault currents. A resistive fault current limiter can be utilized to improve LVRT capability in permanent magnet synchronous generator (PMSG) dominated DC microgrids [261]. The significant advantage of the resistive fault current limiter compared to the inductive limiter is that the PMSG operation is not affected by the resistive device. Moreover, additional resistance together with PMSG inertia will limit the rate of rising of fault current. This research has evaluated the effect of resistance on fault current reduction and identified a possible range of resistor values for LVRT capability improvement of PMSG dominated DC microgrids.

C. LVRT CAPABILITY OF HYBRID AC/DC MICROGRIDS

The hybrid AC/DC microgrid either in grid-connected mode or islanded mode should have LVRT capability against faults both inside the microgrid and in the utility grid. The LVRT capability is ensured by the microgrid energy management system and the DERs remain connected during and after faults. Authors in [262] proposed a control strategy for a DFIG based individual DER to improve the LVRT capability, whereas authors in [263] proposed an ESS integrated into the back-to-back converter for a PMSG based individual DER. The ESS maintains stable DC-link voltage and supplies more reactive power during grid faults and hence improve LVRT capability; however, additional ESS needs more capital investment. Authors in [264] have investigated the LVRT capability of a hybrid AC/DC microgrid only with the AC sub-grid faults. Authors have maintained the same generation capacity and load demand for both the AC and the DC sub-grids for a fair comparison of the LVRT capability. It is identified that the individual DER with LVRT capability enhanced the DC sub-grid LVRT capability and insignificant improvement noticed in the AC sub-grid due to the lack of coordination between the ILC and the AC and DC sub-grids. Authors in [265] have investigated the LVRT capability of a hybrid AC/DC microgrid with the both AC and DC sub-grids faults where the individual DERs have embedded with LVRT control strategy and ILC is operated on power transfer mode. It is identified that DC sub-grid has more LVRT capability compared to the AC sub-grid for both the DC and the AC network faults. It happens because the ILC tracks the pre-fault power reference and helps to quickly restore the DC sub-grid voltage. Different LVRT techniques are presented in the subsequent sections.

1) SECONDARY CONTROL FOR LVRT

An AC microgrid secondary control of DERs for LVRT capability improvement is proposed in [248]. The hierarchical control architecture of the DER is illustrated in Fig. 21 where the primary control is responsible for power-sharing, while the secondary control is responsible for LVRT voltage restoration. The consensus algorithm is used for the secondary control loop and communication infrastructure is used to measure average ac voltage and current (E_{avg} and I_{avg}) which are then used to adjust the reactive power and restore the PCC voltage during grid faults.

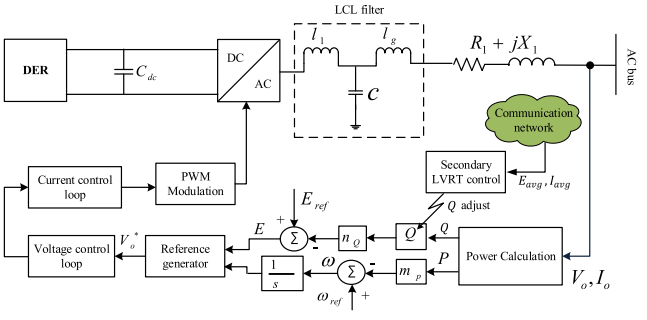

FIGURE 21. Secondary control scheme for LVRT.

2) LVRT WITH DISTRIBUTION STATIC SYNCHRONOUS COMPENSATOR

Using distribution static synchronous compensator (DSTATCOM) at various points of the microgrids is proposed in [266] to improve the LVRT capability of microgrids, which is investigated in grid connected mode by the following two approaches, 1) A DSTATCOM is connected to the low voltage side of the distribution transformer to improve microgrids PCC voltage restoration capability, 2) The external grid voltage and reactive power support are provided by using aggregated reactive power capability of the DERs within the microgrid. In the second approach, the DSTATCOM is connected to the DER terminal and there is no additional voltage support for the low voltage distribution transformer. It was evident that the DSTATCOM improves LVRT capability of the microgrid in both the autonomous and grid connected modes.

3) LVRT CAPABILITY IMPROVEMENT OF WIND TURBINE GENERATOR DOMINATED MICROGRID WITH SUPER-CAPACITOR ESS

The super-capacitor ESS is attracting considerable interest as an effective equipment to improve the LVRT capability of wind turbine generator based microgrids. Authors in [267] have investigated the LVRT capability of super-capacitors for a DFIG based microgrid under main grid faults. The super-capacitor ESS provides additional reactive power due to the voltage imbalance during the main grid fault to keep the microgrid connected by maintaining the LVRT requirements. A super-capacitor with DSTATCOM is utilized to enhanced the LVRT capability of the DFIG where the super-capacitor responds to the active power requirements, while the DSTATCOM responds to the reactive power requirements during main grid faults [268]. In [269], a super-capacitor ESS is incorporated into the DC-link of the PMSG based wind generator to improve the LVRT capability during grid faults. The super-capacitor operates in two modes, 1) Buck converter mode, 2) Boost converter mode i.e., supplying energy to the DC-link capacitor. The DC-link voltage and the super-capacitor voltage control the operating modes. This control approach minimizes short duration power fluctuation and maintains smooth power during the steady-state operation mode. In addition, it improves the LVRT capability of PMSG wind generator by supplying stored energy during grid fault and remaining connected to the power grid.

IX. HYBRID AC/DC MICROGRID PERFORMANCE UNDER DIFFERENT CONTROL STRATEGIES-A CASE STUDY

The hybrid AC/DC microgrids dynamic performance under various control strategies is investigated by developing a hybrid AC/DC microgrid in MATLAB/SIMULINK as shown in Fig. 22 [270], [271]. The AC sub-grid of the hybrid

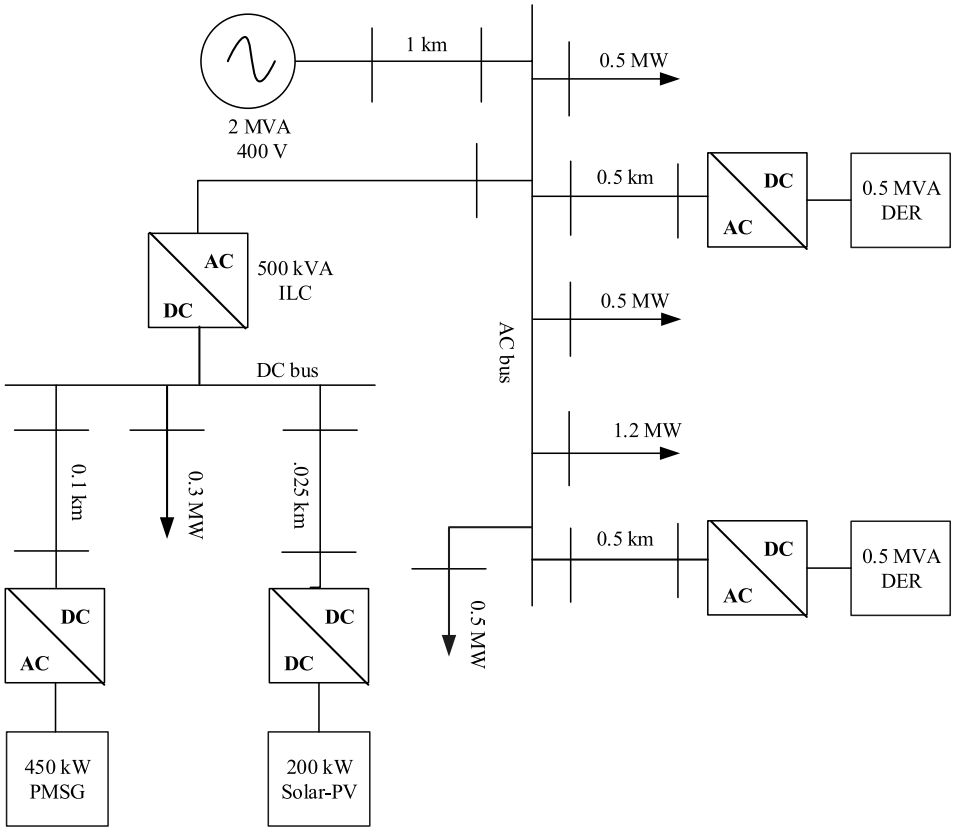

FIGURE 22. Test model of hybrid AC/DC microgrid.

AC/DC microgrid consists of two 0.5 MVA DERs connected to the AC sub-grid PCC via a standard overhead distribution feeders as shown in the single-line diagram. A 1 km distribution feeder connects a 2 MVA, 400 V synchronous generator to the AC sub-grid. The distribution feeder will be considered either resistive or inductive. Therefore, R and X of the resistive distribution feeder are 0.2 Ω and 0.02 Ω respectively, while in the inductive distribution feeder R and X are 0.002 Ω and 0.02 Ω respectively. A 200 kW solar-PV system with a DC-DC boost converter, and a 450 kW PMSG is connected to the DC sub-grid, and the DC bus voltage is maintained at 650 V. A 300 kW constant impedance load is connected to the DC bus of the hybrid AC/DC microgrid. The dynamic performance of the hybrid AC/DC microgrid under different control strategies and different distribution feeder parameters have been carried out considering the following scenarios;

- Dynamic performance under $P-f$ and $Q-v$ droops, and different X/R ratios.
- Dynamic performance with $P-v$ and $Q-f$ droops, and different X/R ratios.
- Dynamic performance with VI in $P-f$ and $Q-v$ droops, and different X/R ratios.
- Dynamic performance with $P-\delta$ and $P-f$ droops, and different X/R ratios.
- Dynamic performance with $P-f$ and $Q-v$ droops, and dynamic loads.

A. DYNAMIC PERFORMANCE UNDER $P-f$ AND $Q-v$ DROOPS AND, DIFFERENT X/R RATIOS

In this scenario, $P-f$ and $Q-v$ droops are applied to the VSC by assuming that the distribution feeder X/R ratio is 10, making it mainly inductive and 0.1 (resistive). A contingency in the hybrid AC/DC microgrid is created by connecting and disconnecting a 300 kW load in the AC sub-grid at $t=1.5$ s and $t=2.5$ s respectively. Figs. 23 (a) and (b) illustrate the AC sub-grid PCC voltage and system frequency respectively, whereas Figs. 23 (c) and (d) illustrate the DC sub-grid voltage and the injected power to the AC sub-grid from the DC sub-grid through ILC respectively. It can be seen from the AC sub-grid PCC voltage and frequency plot that $P-f$ and $Q-v$ droops work well in inductive distribution feeder and its performance deteriorates when distribution feeder becomes resistive causing large voltage and frequency deviations. The AC sub-grid dynamics eventually propagates to the DC sub-grid through the ILC which injects more active power from the DC sub-grid to the AC sub-grid to boost up the PCC voltage which results in DC bus voltage deviation.

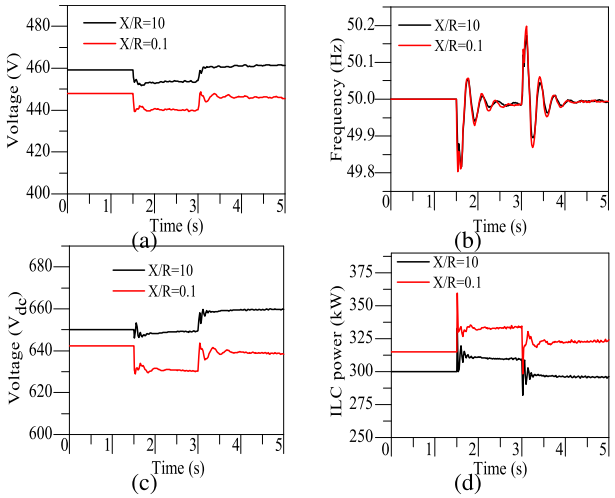

FIGURE 23. Hybrid AC/DC microgrid characteristics with $P-f$ and $Q-v$ droop, (a) PCC voltage, (b) frequency, (c) DC bus voltage, (d) ILC power.

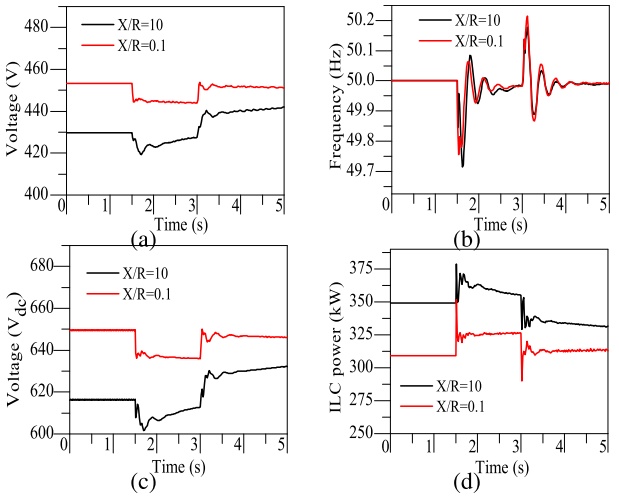

FIGURE 24. Hybrid AC/DC microgrid characteristics with $P-v$ and $Q-f$ droop, (a) PCC voltage, (b) frequency, (c) DC bus voltage, (d) ILC power.

B. DYNAMIC PERFORMANCE WITH $P-v$ AND $Q-f$ DROOPS AND, DIFFERENT X/R RATIOS

According to (5), for a resistive distribution feeder, active power is related to voltage, and reactive power is related to frequency. Therefore, $P-v$ and $Q-f$ droops known as reverse droop will be applied on the VSC, and X/R is maintained at 0.1. The dynamic performance of the reverse droop with $X/R = 0.1$ and $X/R = 10$ are presented here. AC sub-grid PCC voltage and system frequency are illustrated in Figs. 24 (a) and (b) respectively, whereas DC sub-grid voltage and injected power to the AC sub-grid from DC sub-grid through ILC are illustrated in Figs. 24 (c) and (d) respectively. By examining the hybrid AC/DC microgrid characteristics parameters such as AC sub-grid PCC voltage, frequency, and DC bus voltage it is observed that the reverse droop performance is greatly influenced by the distribution feeder X/R. The reason behind the poor performance of the reverse droop when X/R changes from 0.1 to 10, is that it actually changes the basic assumptions of the reverse droop relationship when the feeder becomes inductive.

C. DYNAMIC PERFORMANCE WITH VI IN $P-f$ AND $Q-v$ DROOPS, AND DIFFERENT X/R RATIOS

In this scenario, steady-state and transient performance of the hybrid AC/DC microgrid with VI loop is analyzed briefly. A load disturbance is created by adding a 300 kW load at the AC sub-grid PCC at $t = 1.5$ s, and subsequently, it is removed at $t = 2.5$ s. It is important to note that the VI loop is incorporated into the reference voltage generator loop of the VSC to adjust output impedance of the VSC and the distribution feeder is assumed to be inductive. Figs. 25 (a) and (b) illustrate AC sub-grid PCC voltage and system frequency, whereas Figs. 25 (c) and (d) illustrate DC bus voltage and ILC output power transfer from the DC sub-grid to AC sub-grid respectively. It is clearly seen from the AC sub-grid PCC voltage and system frequency plot that VI loop helps to maintain proper voltage and frequency compared with no

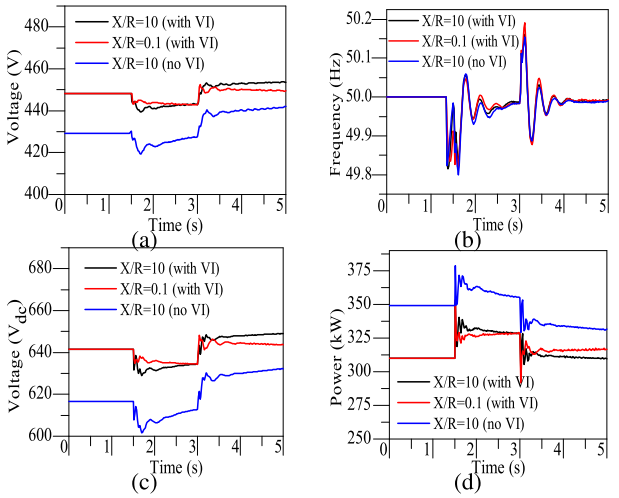

FIGURE 25. Hybrid AC/DC microgrid characteristics with VI, (a) PCC voltage, (b) frequency, (c) DC bus voltage, (d) ILC power.

VI loop in the VSC. Furthermore, AC sub-grid PCC voltage and system frequency plot with the VI loop for $X/R = 0.1$ and $X/R = 10$ shows that the VI loop effectively decouple active and reactive power sharing relationships. However, there are small deviations in the PCC voltage and system frequency. The transient condition in the AC sub-grid eventually propagates to the DC sub-grid through the ILC and affects the DC sub-grid dynamic performance. For instance, ILC injects more power to the AC sub-grid (in case of $X/R = 10$ and without VI loop) as the AC sub-grid PCC voltage deviation is larger and as a results, DC sub-grid voltage deviates from the nominal value.

D. DYNAMIC PERFORMANCE WITH $P-\delta$ AND $P-f$ DROOPS, AND DIFFERENT X/R RATIOS

A comparative analysis is conducted between the $P-\delta$ and $P-f$ droops. A similar contingency like the scenarios of A, B, and C, is applied in the AC sub-grid of the hybrid

AC/DC microgrid. Figs. 26 (a) and (b) illustrate the AC sub-grid PCC voltage and system frequency with angle and frequency droop, whereas DC bus voltage and ILC output power with angle and frequency droop are illustrated in Figs. 26 (c) and (d) respectively. The AC sub-grid PCC voltage (Fig. 26 (a)) and frequency (Fig. 26 (b)) with angle and frequency droop under load disturbances is almost same for $X/R = 10$. However, the PCC voltage and frequency deviate from the nominal values for the $X/R = 0.1$. It indicates that with the microgrid feeder $X/R = 10$, it follows an active power-frequency droop relationship. Therefore, $P-\delta$ droop and $P-f$ droop dynamic performance is similar for inductive microgrid feeder. Although the dynamic performance of $P-\delta$ droop and $P-f$ droop is complementary for inductive microgrid feeder, their performances deteriorate when microgrid feeder becomes resistive i.e., $X/R = 0.1$. The AC sub-grid transients eventually pass through the ILC and correspondingly affected the DC sub-grid. For instance, the poor performance of the $P-\delta$ droop and $P-f$ droop under resistive microgrid feeder ($X/R = 0.1$) caused large DC bus voltage deviation and ILC power transfer imbalance.

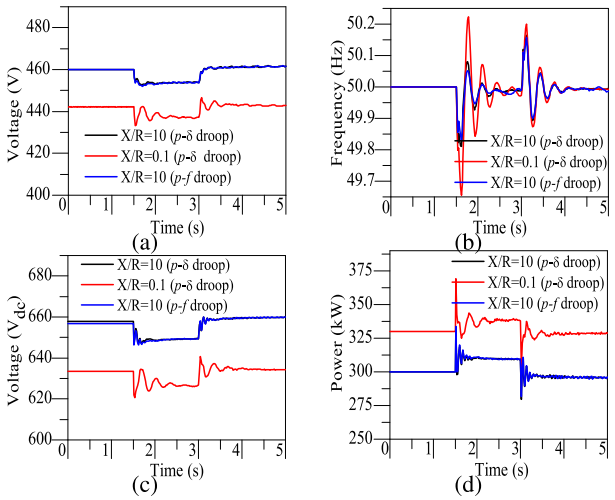

FIGURE 26. Hybrid AC/DC microgrid characteristics with $P-\delta$ and $P-f$ droop, (a) PCC voltage, (b) frequency, (c) DC bus voltage, (d) ILC power.

E. DYNAMIC PERFORMANCE WITH $P-f$ AND $Q-v$ DROOP SCHEMES, AND DYNAMIC LOADS

This simulation sub-section evaluated the hybrid AC/DC microgrid dynamic performance with the presence of dynamic loads, such as IMs. In power system, IMs constitute a large portion of the electric loads from residential to large industrial consumers. The non-linear dynamics of IMs introduce low-frequency oscillations (LFOs) in the system, which can adversely affect the damping of low frequency modes. In this scenario, $P-f$ and $Q-v$ droops are applied to the VSC by assuming that the distribution feeder X/R ratio is 10. The 400 kW load in the AC sub-grid of the hybrid AC/DC microgrid is replaced by, 1) two 200-hp IMs, and 2) one 200-hp IM and forty 5-hp IM. A disturbance in the hybrid AC/DC microgrid is created by connecting and disconnecting a 300 kW load in the AC sub-grid at t = 1.5 s and t = 3.0 s respectively. The rotor speed of the IM and system frequency are illustrated in Figs. 27 (a) and (b) respectively, whereas AC sub-grid voltage and injected power to the AC sub-grid from the DC sub-grid through ILC are illustrated in Figs. 27 (c) and (d) respectively.

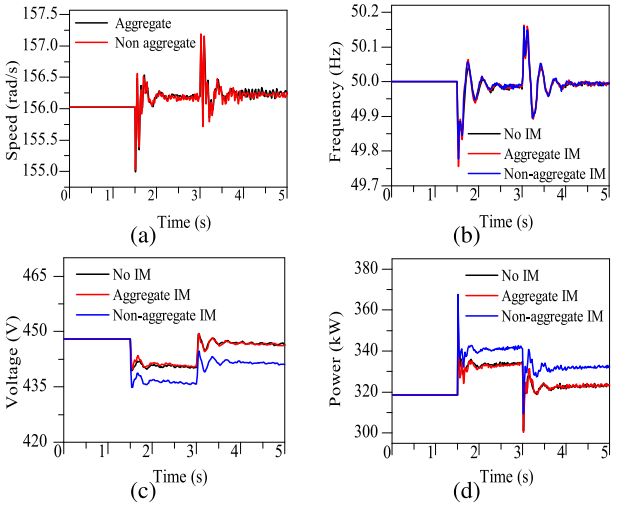

FIGURE 27. Hybrid AC/DC microgrid characteristics with $P-f$ and $Q-v$ droops and dynamic loads, (a) IM rotor speed, (b) frequency, (c) AC bus voltage, (d) ILC power.

The load disturbance at the AC sub-grid causes IM rotor speed oscillations. In steady-state, the IM electro-mechanical torque should be equal to the mechanical load torque. When a large load disturbance occurs, there is a large voltage disturbance at the IM terminal, and hence electro-mechanical torque unbalance occur at the IM. This electro-mechanical torque unbalance leads to rotor speed oscillations which is directly coupled with the system frequency. It is clearly seen from the rotor speed (Fig. 27 (a)) that the speed deviation is larger for the case with one 200-hp IM & forty 5-hp IMs compared to the case with two 200-hp IMs. Even though the total IM load is same, the rotor speed oscillation and frequency deviation are large for multiple parallel operating IMs.

In power system dynamic stability studies, the aggregated model of IMs has been considered, which does not reflect the true dynamics of IMs. Authors previous work investigated the LFO characteristics of the multiple parallel operating small IMs and a large IM of equivalent power rating [132], [271]. It was found that the multiple parallel operating IMs have multiple dominant oscillation frequencies which introduces more non-linearity into system dynamics. Similarly, the voltage deviation at the AC sub-grid and the power injection of the ILC from the DC to AC sub-grid due to the load disturbance are large for the cases with IM loads.

X. CONCLUSION

A comprehensive literature review of the stability, control and power management aspects of AC, DC, and hybrid AC/DC microgrids are presented in this paper. According to the

review, AC and DC microgrids are widely being used, while hybrid AC/DC microgrid is becoming popular due to lower conversion losses, reliability, and efficiency. The microgrids follow hierarchical control architecture including primary, secondary, and tertiary controllers. The primary control (or LC) is embedded in the DER to ensure reliable operation by maintaining stable voltage/frequency and power regulation. Secondary control manages microgrid communication protocols to reduce steady-state voltage/frequency errors caused by the primary control; hence, optimizing the power quality. The tertiary control manages the power-flow between the microgrid and the main grid to ensure economic operation.

The power management and control of hybrid AC/DC microgrids are more complex compared to the individual AC and DC microgrids. The bidirectional ILC coordinates the AC and DC microgrids; hence, the stability of the hybrid AC/DC microgrid depends on the reliability of the bi-directional ILCs. Moreover, the bi-directional ILC will either control the DC microgrid voltage or the AC microgrid voltage/frequency depending on whether the hybrid AC/DC microgrid is operating on the grid-connected or autonomous mode. Furthermore, multiple ILCs can increase the power transfer capacity between the AC and DC microgrids, but can lead to further stability and the reliability issues in the system. A case study on the dynamic performance of a hybrid AC/DC microgrid under different control strategies are investigated in this paper and the following conclusions can be drawn from the simulation results and the literature review;

- After recognizing the benefits of both AC and DC microgrids, they have been combined to form hybrid AC/DC microgrids, which intends to improve the reliability, efficiency and economic operation of the system. However, the network structure of the hybrid AC/DC microgrids is complex compared to individual AC and DC microgrids, which requires further research studies on coordinated control strategies for individual AC and DC microgrids, intermittency of DERs, reactive power compensation, etc.
- Because of the significant amount of power exchange between the AC and DC sub-grids, multiple ILCs are utilized between the AC and the DC sub-grids. However, having multiple ILCs would increase the overall cost and creates circulating power because of line impedance mismatch which can overstress the ILCs.
- The distributed ESSs are connected to both the AC and the DC sub-grids. The main problem of the distributed ESSs with different SoC levels are the charging and discharging control. Some research studies focused on equalizing the different SoC levels of distributed ESSs, while some other research studies utilized the master-slave control scheme for distributed ESSs of different SoC levels.
- The control strategy of multiple parallel operating ILCs between two sub-grids is more critical with the presence of distributed ESSs in both the AC and DC sub-grids. Therefore, further studies are required for a coordinated control strategy between multiple parallel operating ILCs and distributed ESSs.
- The $P-f$ and $Q-v$ droop control schemes are applied to the VSC by assuming that the microgrid feeder is inductive and a contingency in the hybrid AC/DC microgrid is created by load switching in the AC sub-grid of the hybrid AC/DC microgrid. It is identified that the $P-f$ and $Q-v$ droop are performing well when the microgrid feeder is inductive and the performance deteriorates when the microgrid feeder become more resistive.
- Similar results are observed when the $P-v$ and $Q-f$ droop are applied to the VSC by assuming that the microgrid feeder is resistive and the performance deteriorates when the microgrid feeder becomes more inductive.
- The VI control is utilized to eliminate the microgrid feeder X/R ratio effect and hence improve the dynamic performance of the hybrid AC/DC microgrid. However, the performance of the VI control deteriorates when it is designed for a particular X/R ratio of the microgrid feeder and the X/R ratio of the microgrid feeder is changed from the pre-designed value. Therefore, a universal control strategy is required for the VSC which will work for any X/R ratio of the microgrid feeder.
- Similar results are observed between the $P-\delta$ and the $P-f$ droop. The dynamic performance of these two droops depend on the X/R ratio of the microgrid feeder.
- The entire microgrid will go into complete shutdown if the central controller fails due to the failure of the communication infrastructure. However, in distributed control techniques there is no central controller and the LCs of the individual DERs exchange information with each other, hence they are capable of improving microgrid's reliability.
- Hybrid AC/DC microgrid dynamic stability is significantly affected by the dynamic loads, such as IMs. Moreover, the stability impact of multiple parallel operating IMs of equivalent power rating is more severe compared to the aggregated model of IMs.
- Some research studies proposed a power oscillation damping controller for the ESS controller to damp LFOs generating from the dynamic loads such as IMs. Therefore, further research studies are required to damp the high-frequency oscillations in the hybrid AC/DC microgrids by the ESS.
- In future more and more microgrids will be interconnected with each other and eventually, they will form microgrid clusters resulting in complex dynamics between them.

This review will pave the way for policymakers, power industry, and academic researchers to understand the stability, control and power management aspects of various microgrid architectures and ultimately assist to improve the stability and reliability of future microgrids.

REFERENCES

[1] F. Ktiraei, R. Iravani, N. Hatziargyriou, and A. Dimeas, "Microgrids management-controls and operation aspects of microgrids," *IEEE Power Energy*, vol. 6, no. 3, pp. 54–65, May 2008.

[2] R. H. Lasseter and P. Piagi, "Microgrid: A conceptual solution," in *Proc. IEEE Power Electron. Specialists Conf.*, Aachen, Germany, Jun. 2004, pp. 4285–4291.

[3] H. Nikkhajoei and R. H. Lasseter, "Distributed generation interface to the CERTS microgrid," *IEEE Trans. Power Del.*, vol. 24, no. 3, pp. 1598–1608, Jul. 2009.
[4] N. Hatziargyriou, *Microgrids: Architectures Control*. Hoboken, NJ, USA: Wiley, Mar. 2014.
[5] M. Farrokhabadi *et al.*, "Microgrid stability definitions, analysis, and examples," *IEEE Trans. Power Syst.*, vol. 35, no. 1, pp. 13–29, Jan. 2020.
[6] M. E. Baran and N. R. Mahajan, "DC distribution for industrial systems: Opportunities and challenges," *IEEE Trans. Ind. Appl.*, vol. 39, no. 6, pp. 1596–1601, Nov. 2003.
[7] N. Eghtedarpour and E. Farjah, "Control strategy for distributed integration of photovoltaic and energy storage systems in DC micro-grids," *Renew. Energy*, vol. 45, pp. 96–110, Sep. 2012.
[8] L. Xu and D. Chen, "Control and operation of a DC microgrid with variable generation and energy storage," *IEEE Trans. Power Del.*, vol. 26, no. 4, pp. 2513–2522, Oct. 2011.
[9] N. Eghtedarpour and E. Farjah, "Distributed charge/discharge control of energy storages in a renewable-energy-based DC micro-grid," *IET Renew. Power Gener.*, vol. 8, no. 1, pp. 45–57, Jan. 2014.
[10] B. Dong, Y. Li, Z. Zheng, and L. Xu, "Control strategies of microgrid with hybrid DC and AC buses," in *Proc. IEEE 14th Eur. Conf. Power Electron. Appl.*, Birmingham, U.K., Aug. 2011, pp. 1–8.
[11] A. Karabiber, C. Keles, A. Kaygusuz, and B. B. Alagoz, "An approach for the integration of renewable distributed generation in hybrid DC/AC microgrids," *Renew. Energy*, vol. 52, pp. 251–259, Apr. 2013.
[12] K. Kurohane, T. Senjyu, A. Uehara, A. Yona, T. Funabashi, and C.-H. Kim, "A hybrid smart AC/DC power system," in *Proc. IEEE 5th Conf. Ind. Electron. Appl.*, Jul. 2010, pp. 764–769.
[13] J. Hu, Y. Shan, Y. Xu, and J. M. Guerrero, "A coordinated control of hybrid AC/DC microgrids with PV-wind-battery under variable generation and load conditions," *Int. J. Electr. Power Energy Syst.*, vol. 104, pp. 583–592, Jan. 2019.
[14] D. E. Olivares, A. Mehrizi-Sani, A. H. Etemadi, C. A. Cañizares, R. Iravani, M. Kazerani, A. H. Hajimiragha, O. Gomis-Bellmunt, M. Saeedifard, R. Palma-Behnke, G. A. Jiménez-Estévez, and N. D. Hatziargyriou, "Trends in microgrid control," *IEEE Trans. Smart Grid*, vol. 5, no. 4, pp. 1905–1919, Jul. 2014.
[15] A. Mohammed, S. S. Refaat, S. Bayhan, and H. Abu-Rub, "AC microgrid control and management strategies: Evaluation and review," *IEEE Power Electron. Mag.*, vol. 6, no. 2, pp. 18–31, Jun. 2019.
[16] S. Parhizi, H. Lotfi, A. Khodaei, and S. Bahramirad, "State of the art in research on microgrids: A review," *IEEE Access*, vol. 3, pp. 890–925, Jun. 2015.
[17] F. Nejabatkhah, Y. W. Li, and H. Tian, "Power quality control of smart hybrid AC/DC microgrids: An overview," *IEEE Access*, vol. 7, pp. 52295–52318, Apr. 2019.
[18] E. Hossain, E. Kabalci, R. Bayindir, and R. Perez, "Microgrid testbeds around the world: State of art," *Energy Convers. Manage.*, vol. 86, pp. 132–153, Oct. 2014.
[19] D. J. Hammerstrom, "AC versus DC distribution SystemsDid we get it right?" in *Proc. IEEE Power Eng. Soc. Gen. Meeting*, Tampa, FL, USA, Jun. 2007, pp. 1–5.
[20] Z. Jiang and X. Yu, "Hybrid DC-and AC-linked microgrids: Towards integration of distributed energy resources," in *Proc. IEEE Energy Conf.*, Atlanta, GA, USA, Feb. 2008, pp. 1–8.
[21] C. Marnay, "Introduction to microgrids," in *Proc. Introduction Consortium Electr. Rel. Technol. 981 Solutions Berkeley Symp. Microgrids*, 2005.
[22] Y. Tan, L. Meegahapola, and K. M. Muttaqi, "A review of technical challenges in planning and operation of remote area power supply systems," *Renew. Sustain. Energy Rev.*, vol. 38, pp. 876–889, Oct. 2014.
[23] A. Arulampalam, M. Barnes, A. Engler, A. Goodwin, and N. Jenkins, "Control of power electronic interfaces in distributed generation microgrids," *Int. J. Electron.*, vol. 91, no. 9, pp. 503–523, Sep. 2004.
[24] E. Unamuno and J. A. Barrena, "Hybrid AC/DC microgrids—Part I: Review and classification of topologies," *Renew. Sustain. Energy Rev.*, vol. 52, pp. 1251–1259, Dec. 2015.
[25] A. Zayegh, A. Kalam, and A. M. Oo, "Wide area power system monitoring, protection and control," *AMSE lectures Model. Simul.*, vol. 6, no. 1, p. 137, Jul. 2005.
[26] M. H. Rashid, *Power Electronics Handbook: Devices, Circuits and Applications*. New York, NY, USA: Academic, 2010.
[27] G. F. Reed, "DC technologies: Solutions to electric power system advancements [guest editorial]," *IEEE Power Energy Mag.*, vol. 10, no. 6, pp. 10–17, Nov. 2012.
[28] G. W. Arnold, "Challenges and opportunities in smart grid: A position article," *Proc. IEEE*, vol. 99, no. 6, pp. 922–927, Jun. 2011.
[29] A. Battaglini, J. Lilliestam, A. Haas, and A. Patt, "Development of SuperSmart grids for a more efficient utilisation of electricity from renewable sources," *J. Cleaner Prod.*, vol. 17, no. 10, pp. 911–918, Jul. 2009.
[30] P. Wang, L. Goel, X. Liu, and F. Hoong Choo, "Harmonizing AC and DC: A hybrid AC/DC future grid solution," *IEEE Power Energy Mag.*, vol. 11, no. 3, pp. 76–83, May 2013.
[31] I. Patrao, E. Figueres, G. Garcerá, and R. González-Medina, "Microgrid architectures for low voltage distributed generation," *Renew. Sustain. Energy Rev.*, vol. 43, pp. 415–424, Mar. 2015.
[32] D. Fregosi, S. Ravula, D. Brhlik, J. Saussele, S. Frank, E. Bonnema, J. Scheib, and E. Wilson, "A comparative study of DC and AC microgrids in commercial buildings ACross different climates and operating profiles," in *Proc. IEEE 1st Int. Conf. DC Microgrids (ICDCM)*, Atlanta, GA, USA, Jun. 2015, pp. 159–164.
[33] U. Manandhar, A. Ukil, and T. K. K. Jonathan, "Efficiency comparison of DC and AC microgrid," in *Innov. Smart Grid Technol.-Asia (ISGT ASIA)*, Sep. 2015, pp. 1–6.
[34] A. Moreno-Muñoz, J. De La Rosa, M. Lopez, and A. G. de Castro, "Distributed energy resources interconnection: The Spanish normative," in *Proc. 35th Annu. Conf. IEEE Ind. Electron.*, Capri, Italy, Jun. 2009, pp. 408–412.
[35] D. L. Brooks and M. Patel, "Panel: Standards & interconnection requirements for wind and solar generation NERC integrating variable generation task force," in *Proc. PES T&D*, Jul. 2012, pp. 1–3.
[36] *Standard for Interconnecting Distributed Resources With Electric Power Systems*, IEEE Standard 1547-2003, Jul. 2003.
[37] D. G. Photovoltaics and E. Storage, *IEEE Standard for Interconnection and Interoperability of Distributed Energy Resources With Associated Electric Power Systems Interfaces*, IEEE Standard 1547-2018, Apr. 2018.
[38] *IEEE Guide for Design, Operation, and Integration of Distributed Resource Island Systems With Electric Power Systems*, IEEE Standards Association 1547.4-2011, New York, NY, USA, Jul. 2011.
[39] V. F. Martins and C. L. T. Borges, "Active distribution network integrated planning incorporating distributed generation and load response uncertainties," *IEEE Trans. Power Syst.*, vol. 26, no. 4, pp. 2164–2172, Nov. 2011.
[40] S. Mazumder, A. Ghosh, and F. Zare, "Improving power quality in low-voltage networks containing distributed energy resources," *Int. J. Emerg. Electr. Power Syst.*, vol. 14, no. 1, pp. 67–78, May 2013.
[41] J. Li, R. Xiong, Q. Yang, F. Liang, M. Zhang, and W. Yuan, "Design/test of a hybrid energy storage system for primary frequency control using a dynamic droop method in an isolated microgrid power system," *Appl. Energy*, vol. 201, pp. 257–269, Sep. 2017.
[42] F. Diaz-Gonzalez, F. D. Bianchi, A. Sumper, and O. Gomis-Bellmunt, "Control of a flywheel energy storage system for power smoothing in wind power plants," *IEEE Trans. Energy Convers.*, vol. 29, no. 1, pp. 204–214, Mar. 2014.
[43] A. Zeng, Q. Xu, M. Ding, K. Yukita, and K. Ichiyanagi, "A classification control strategy for energy storage system in microgrid," *IEEJ Trans. Electr. Electron. Eng.*, vol. 10, no. 4, pp. 396–403, Mar. 2015.
[44] T. Hosseinimehr, A. Ghosh, and F. Shahnia, "Cooperative control of battery energy storage systems in microgrids," *Int. J. Electr. Power Energy Syst.*, vol. 87, pp. 109–120, May 2017.
[45] M. Faisal, M. A. Hannan, P. J. Ker, A. Hussain, M. B. Mansor, and F. Blaabjerg, "Review of energy storage system technologies in microgrid applications: Issues and challenges," *IEEE Access*, vol. 6, pp. 35143–35164, May 2018.
[46] D. Sandoval, P. Goffin, and H. Leibundgut, "How low exergy buildings and distributed electricity storage can contribute to flexibility within the demand side," *Appl. Energy*, vol. 187, pp. 116–127, Feb. 2017.
[47] M. Shahidehpour, "Role of smart microgrid in a perfect power system," in *Proc. IEEE Power Eng. Soc. Gen. Meeting*, Providence, RI, USA, Sep. 2010, pp. 1–6.
[48] M. T. L. Gayatri, A. M. Parimi, and A. V. Pavan Kumar, "A review of reactive power compensation techniques in microgrids," *Renew. Sustain. Energy Rev.*, vol. 81, pp. 1030–1036, Jan. 2018.
[49] S. Bolognani and S. Zampieri, "A distributed control strategy for reactive power compensation in smart microgrids," *IEEE Trans. Autom. Control*, vol. 58, no. 11, pp. 2818–2833, Nov. 2013.

[50] M. N. I. Sarkar, L. G. Meegahapola, and M. Datta, "Reactive power management in renewable rich power grids: A review of grid-codes, renewable generators, support devices, control strategies and optimization algorithms," *IEEE Access*, vol. 6, pp. 41458–41489, May 2018.

[51] X. Liu, P. Wang, and P. C. Loh, "A hybrid AC/DC microgrid and its coordination control," *IEEE Trans. Smart Grid*, vol. 2, no. 2, pp. 278–286, Jun. 2011.

[52] Y. Xia, Y. Peng, P. Yang, M. Yu, and W. Wei, "Distributed coordination control for multiple bidirectional power converters in a hybrid AC/DC microgrid," *IEEE Trans. Power Electron.*, vol. 32, no. 6, pp. 4949–4959, Jun. 2017.

[53] S. S. Thale, R. G. Wandhare, and V. Agarwal, "A novel reconfigurable microgrid architecture with renewable energy sources and storage," *IEEE Trans. Ind. Appl.*, vol. 51, no. 2, pp. 1805–1816, Mar. 2015.

[54] S. M. Malik, X. Ai, Y. Sun, C. Zhengqi, and Z. Shupeng, "Voltage and frequency control strategies of hybrid AC/DC microgrid: A review," *IET Gener., Transmiss. Distrib.*, vol. 11, no. 2, pp. 303–313, Jan. 2017.

[55] P. Lin, P. Wang, C. Jin, J. Xiao, X. Li, F. Guo, and C. Zhang, "A distributed power management strategy for multi-paralleled bidirectional interlinking converters in hybrid AC/DC microgrids," *IEEE Trans. Smart Grid*, vol. 10, no. 5, pp. 5696–5711, Sep. 2019.

[56] P. Yang, Y. Xia, M. Yu, W. Wei, and Y. Peng, "A decentralized coordination control method for parallel bidirectional power converters in a hybrid AC–DC microgrid," *IEEE Trans. Ind. Electron.*, vol. 65, no. 8, pp. 6217–6228, Aug. 2018.

[57] A. Reznik, M. G. Simões, A. Al-Durra, and S. Muyeen, "*LCL* filter design and performance analysis for grid-interconnected systems," *IEEE Trans. Ind. Appl.*, vol. 50, no. 2, pp. 1225–1232, Jul. 2014.

[58] M. Liserre, F. Blaabjerg, and S. Hansen, "Design and control of an LCL-filter-based three-phase ACtive rectifier," *IEEE Trans. Ind. Appl.*, vol. 41, no. 5, pp. 1281–1291, Sep. 2005.

[59] M. Said-Romdhane, M. Naouar, I. Belkhodja, and E. Monmasson, "An improved LCL filter design in order to ensure stability without damping and despite large grid impedance variations," *Energies*, vol. 10, no. 3, p. 336, Mar. 2017.

[60] A. Micallef, M. Apap, C. Spiteri-Staines, and J. M. Guerrero, "Mitigation of harmonics in grid-connected and islanded microgrids via virtual admittances and impedances," *IEEE Trans. Smart Grid*, vol. 8, no. 2, pp. 651–661, Mar. 2017.

[61] S. G. Parker, B. P. McGrath, and D. G. Holmes, "Regions of ACtive damping control for LCL filters," *IEEE Trans. Ind. Appl.*, vol. 50, no. 1, pp. 424–432, Jan. 2014.

[62] H. Nikkhajoei and R. H. Lasseter, "Microgrid protection," in *Proc. IEEE Power Eng. Soc. Gen. Meeting*, Jun. 2007, pp. 1–6.

[63] S. M. Brahma and A. A. Girgis, "Development of adaptive protection scheme for distribution systems with high penetration of distributed generation," *IEEE Trans. Power Del.*, vol. 19, no. 1, pp. 56–63, Jan. 2004.

[64] M. R. Islam and H. A. Gabbar, "Analysis of microgrid protection strategies," in *Proc. Int. Conf. Smart Grid (SGE)*, Aug. 2012, pp. 1–6.

[65] M. Monadi, M. A. Zamani, J. I. Candela, A. Luna, and P. Rodriguez, "Protection of AC and DC distribution systems embedding distributed energy resources: A comparative review and analysis," *Renew. Sustain. Energy Rev.*, vol. 51, pp. 1578–1593, Nov. 2015.

[66] J. Shiles, E. Wong, S. Rao, C. Sanden, M. A. Zamani, M. Davari, and F. Katiraei, "Microgrid protection: An overview of protection strategies in north American microgrid projects," in *Proc. IEEE Power Energy Soc. Gen. Meeting*, Chicago, IL, USA, Jul. 2017, pp. 1–5.

[67] A. Bidram, V. Nasirian, A. Davoudi, and F. L. Lewis, "Control and modeling of microgrids," in *Cooperative Synchronization in Distributed Microgrid Control*. Cham, Switzerland: Springer, Feb. 2017, pp. 7–43.

[68] J. A. P. Lopes, C. L. Moreira, and A. G. Madureira, "Defining control strategies for MicroGrids islanded operation," *IEEE Trans. Power Syst.*, vol. 21, no. 2, pp. 916–924, May 2006.

[69] J. M. Guerrero, J. C. Vasquez, J. Matas, L. G. De Vicuña, and M. Castilla, "Hierarchical control of droop-controlled AC and DC microgrids—A general approach toward standardization," *IEEE Trans. Ind. Electron.*, vol. 58, no. 1, pp. 158–172, Aug. 2011.

[70] F. Katiraei and M. R. Iravani, "Power management strategies for a microgrid with multiple distributed generation units," *IEEE Trans. Power Syst.*, vol. 21, no. 4, pp. 1821–1831, Nov. 2006.

[71] A. Bidram and A. Davoudi, "Hierarchical structure of microgrids control system," *IEEE Trans. Smart Grid*, vol. 3, no. 4, pp. 1963–1976, Dec. 2012.

[72] M. Savaghebi, A. Jalilian, J. C. Vasquez, and J. M. Guerrero, "Secondary control scheme for voltage unbalance compensation in an islanded droop-controlled microgrid," *IEEE Trans. Smart Grid*, vol. 3, no. 2, pp. 797–807, Jun. 2012.

[73] E. Barklund, N. Pogaku, M. Prodanovic, C. Hernandez-Aramburo, and T. C. Green, "Energy management in autonomous microgrid using stability-constrained droop control of inverters," *IEEE Trans. Power Electron.*, vol. 23, no. 5, pp. 2346–2352, Sep. 2008.

[74] A. Pantoja and N. Quijano, "A population dynamics approach for the dispatch of distributed generators," *IEEE Trans. Ind. Electron.*, vol. 58, no. 10, pp. 4559–4567, Oct. 2011.

[75] T. L. Vandoorn, J. D. M. De Kooning, B. Meersman, and L. Vandevelde, "Review of primary control strategies for islanded microgrids with power-electronic interfaces," *Renew. Sustain. Energy Rev.*, vol. 19, pp. 613–628, Mar. 2013.

[76] E. Rokrok, M. Shafie-Khah, and J. P. S. Catalão, "Review of primary voltage and frequency control methods for inverter-based islanded microgrids with distributed generation," *Renew. Sustain. Energy Rev.*, vol. 82, pp. 3225–3235, Feb. 2018.

[77] D. Shanxu, M. Yu, X. Jian, K. Yong, and C. Jian, "Parallel operation control technique of voltage source inverters in ups," in *Proc. IEEE Int. Conf. Power Electron. Drive Syst. (PEDS)*, vol. 2, Hong Kong, Mar. 1999, pp. 883–887.

[78] M. Rasheduzzaman, S. N. Bhaskara, and B. H. Chowdhury, "Implementation of a microgrid central controller in a laboratory microgrid network," in *Proc. North Amer. Power Symp. (NAPS)*, Champaign, IL, USA, Sep. 2012, pp. 1–6.

[79] T. F. Wu, K. Siri, and J. Banda, "The central-limit control and impact of cable resistance in current distribution for parallel-connected DC-DC converters," in *Proc. Power Electron. Specialist Conf. (PESC)*, vol. 1, Taipei, Taiwan, 1994, pp. 694–702.

[80] J. Banda and K. Siri, "Improved central-limit control for parallel-operation of DC-DC power converters," in *Proc. IEEE Power Electron. Specialist Conf. (PESC)*, vol. 2, Atlanta, GA, USA, Aug. 1995, pp. 1104–1110.

[81] M. M. A. Abdelaziz, M. F. Shaaban, H. E. Farag, and E. F. El-Saadany, "A multistage centralized control scheme for islanded microgrids with PEVs," *IEEE Trans. Sustain. Energy*, vol. 5, no. 3, pp. 927–937, Jul. 2014.

[82] H. Han, X. Hou, J. Yang, J. Wu, M. Su, and J. M. Guerrero, "Review of power sharing control strategies for islanding operation of AC microgrids," *IEEE Trans. Smart Grid*, vol. 7, no. 1, pp. 200–215, Jan. 2016.

[83] X. Sun, Y.-S. Lee, and D. Xu, "Modeling, analysis, and implementation of parallel multi-inverter systems with instantaneous average-current-sharing scheme," *IEEE Trans. Power Electron.*, vol. 18, no. 3, pp. 844–856, May 2003.

[84] Q. Shafiee, J. M. Guerrero, and J. C. Vasquez, "Distributed secondary control for islanded microgrids—A novel approach," *IEEE Trans. Power Electron.*, vol. 29, no. 2, pp. 1018–1031, Apr. 2014.

[85] A. Bidram, A. Davoudi, and F. L. Lewis, "A multiobjective distributed control framework for islanded AC microgrids," *IEEE Trans. Ind. Informat.*, vol. 10, no. 3, pp. 1785–1798, Aug. 2014.

[86] H. Xin, L. Zhang, Z. Wang, D. Gan, and K. P. Wong, "Control of island AC microgrids using a fully distributed approach," *IEEE Trans. Smart Grid*, vol. 6, no. 2, pp. 943–945, Mar. 2015.

[87] M. A. Mahmud, M. J. Hossain, H. R. Pota, and A. M. T. Oo, "Robust nonlinear distributed controller design for ACtive and reactive power sharing in islanded microgrids," *IEEE Trans. Energy Convers.*, vol. 29, no. 4, pp. 893–903, Dec. 2014.

[88] T. Caldognetto and P. Tenti, "Microgrids operation based on master–slave cooperative control," *IEEE J. Emerg. Sel. Topics Power Electron.*, vol. 2, no. 4, pp. 1081–1088, Dec. 2014.

[89] Y. Pei, G. Jiang, X. Yang, and Z. Wang, "Auto-master-slave control technique of parallel inverters in distributed AC power systems and ups," in *Proc. IEEE 35th Annu. Power Electron. Specialists Conf.*, vol. 3, Aachen, Germany, Jun. 2004, pp. 2050–2053.

[90] J. Tan, H. Lin, J. Zhang, and J. Ying, "A novel load sharing control technique for paralleled inverters," in *Proc. IEEE 34th Annu. Conf. Power Electron. Specialist (PESC)*, vol. 3, Acapulco, Mexico, Aug. 2003, pp. 1432–1437.

[91] F. Petruzziello, P. D. Ziogas, and G. Joos, "A novel approach to paralleling of power converter units with true redundancy," in *Proc. 21st Annu. IEEE Conf. Power Electron. Specialists (PESC)*, San Antonio, TX, USA, Aug. 1990, pp. 808–813.

[92] A. Bergen, *Power System Analysis*. Upper Saddle River, NJ, USA: Prentice-Hall, 1986.
[93] T. Kawabata and S. Higashino, "Parallel operation of voltage source inverters," *IEEE Trans. Ind. Appl.*, vol. 24, no. 2, pp. 281–287, Mar. 1988.
[94] M. C. Chandorkar, D. M. Divan, and R. Adapa, "Control of parallel connected inverters in standalone AC supply systems," *IEEE Trans. Ind. Appl.*, vol. 29, no. 1, pp. 136–143, Jan. 1993.
[95] N. Pogaku, M. Prodanovic, and T. C. Green, "Modeling, analysis and testing of autonomous operation of an inverter-based microgrid," *IEEE Trans. Power Electron.*, vol. 22, no. 2, pp. 613–625, Mar. 2007.
[96] G. Diaz, C. Gonzalez-Moran, J. Gomez-Aleixandre, and A. Diez, "Scheduling of droop coefficients for frequency and voltage regulation in isolated microgrids," *IEEE Trans. Power Syst.*, vol. 25, no. 1, pp. 489–496, Feb. 2010.
[97] E. Rokrok and M. E. H. Golshan, "Adaptive voltage droop scheme for voltage source converters in an islanded multibus microgrid," *IET Gener., Transmiss. Distrib.*, vol. 4, no. 5, pp. 562–578, May 2010.
[98] A. Bidram, V. Nasirian, A. Davoudi, and F. L. Lewis, *Cooperative Synchronization in Distributed Microgrid Control*. New York, NY, USA: Springer, 2017.
[99] U. Borup, F. Blaabjerg, and P. N. Enjeti, "Sharing of nonlinear load in parallel-connected three-phase converters," *IEEE Trans. Ind. Appl.*, vol. 37, no. 6, pp. 1817–1823, Nov. 2001.
[100] Q.-C. Zhong, "Harmonic droop controller to reduce the voltage harmonics of inverters," *IEEE Trans. Ind. Electron.*, vol. 60, no. 3, pp. 936–945, Mar. 2013.
[101] J. M. Guerrero, J. Matas, L. Garcia de Vicuna, M. Castilla, and J. Miret, "Decentralized control for parallel operation of distributed generation inverters using resistive output impedance," *IEEE Trans. Ind. Electron.*, vol. 54, no. 2, pp. 994–1004, Apr. 2007.
[102] R. Majumder, A. Ghosh, G. Ledwich, and F. Zare, "Angle droop versus frequency droop in a voltage source converter based autonomous microgrid," in *Proc. IEEE Power Energy Soc. Gen. Meeting*, Calgary, AB, Canada, Jul. 2009, pp. 1–8.
[103] R. Majumder, B. Chaudhuri, A. Ghosh, R. Majumder, G. Ledwich, and F. Zare, "Improvement of stability and load sharing in an autonomous microgrid using supplementary droop control loop," *IEEE Trans. Power Syst.*, vol. 25, no. 2, pp. 796–808, May 2010.
[104] R. Majumder, G. Ledwich, A. Ghosh, S. Chakrabarti, and F. Zare, "Droop control of converter-interfaced microsources in rural distributed generation," *IEEE Trans. Power Del.*, vol. 25, no. 4, pp. 2768–2778, Oct. 2010.
[105] O. Palizban and K. Kauhaniemi, "Hierarchical control structure in microgrids with distributed generation: Island and grid-connected mode," *Renew. Sustain. Energy Rev.*, vol. 44, pp. 797–813, Apr. 2015.
[106] Y. Sun, X. Hou, J. Yang, H. Han, M. Su, and J. M. Guerrero, "New perspectives on droop control in AC microgrid," *IEEE Trans. Ind. Electron.*, vol. 64, no. 7, pp. 5741–5745, Jul. 2017.
[107] Y. Li and Y. W. Li, "Power management of inverter interfaced autonomous microgrid based on virtual frequency-voltage frame," *IEEE Trans. Smart Grid*, vol. 2, no. 1, pp. 30–40, Mar. 2011.
[108] T. Wu, Z. Liu, J. Liu, S. Wang, and Z. You, "A unified virtual power decoupling method for droop-controlled parallel inverters in microgrids," *IEEE Trans. Power Electron.*, vol. 31, no. 8, pp. 5587–5603, Aug. 2016.
[109] Y. Li and Y. W. Li, "Virtual frequency-voltage frame control of inverter based low voltage microgrid," in *Proc. IEEE Electr. Power Energy Conf. (EPEC)*, Montreal, QC, Canada, Oct. 2009, pp. 1–6.
[110] Y. Li and Y. Wei Li, "Decoupled power control for an inverter based low voltage microgrid in autonomous operation," in *Proc. IEEE 6th Int. Power Electron. Motion Control Conf.*, Wuhan, China, May 2009, pp. 2490–2496.
[111] J. M. Guerrero, J. Matas, L. G. de Vicuña, N. Berbel, and J. Sosa, "Wireless-control strategy for parallel operation of distributed generation inverters," in *Proc. IEEE Int. Symp. Ind. Electron. (ISIE)*, vol. 2, Dubrovnik, Croatia, Nov. 2005, pp. 845–850.
[112] W. Yao, M. Chen, J. Matas, J. M. Guerrero, and Z.-M. Qian, "Design and analysis of the droop control method for parallel inverters considering the impact of the complex impedance on the power sharing," *IEEE Trans. Ind. Electron.*, vol. 58, no. 2, pp. 576–588, Feb. 2011.
[113] K. De Brabandere, B. Bolsens, J. Van den Keybus, A. Woyte, J. Driesen, R. Belmans, and K. U. Leuven, "A voltage and frequency droop control method for parallel inverters," in *Proc. IEEE 35th Annu. Power Electron. Specialists Conf.*, vol. 22, no. 4, Jul. 2007, pp. 1107–1115.
[114] J. M. Guerrero, L. GarciadeVicuna, J. Matas, M. Castilla, and J. Miret, "Output impedance design of parallel-connected UPS inverters with wireless load-sharing control," *IEEE Trans. Ind. Electron.*, vol. 52, no. 4, pp. 1126–1135, Aug. 2005.
[115] C. K. Sao and P. W. Lehn, "Autonomous load sharing of voltage source converters," *IEEE Trans. Power Del.*, vol. 20, no. 2, pp. 1009–1016, Apr. 2005.
[116] P. E. S. N. Raju and T. Jain, "Small signal modelling and stability analysis of an islanded AC microgrid with inverter interfaced DGs," in *Proc. Int. Conf. Smart Electr. Grid (ISEG)*, Guntur, India, Sep. 2014, pp. 1–8.
[117] K. Yu, Q. Ai, S. Wang, J. Ni, and T. Lv, "Analysis and optimization of droop controller for microgrid system based on small-signal dynamic model," *IEEE Trans. Smart Grid*, vol. 7, no. 2, pp. 695–705, Mar. 2016.
[118] H. Shi, F. Zhuo, L. Hou, X. Yue, and D. Zhang, "Small-signal stability analysis of a microgrid operating in droop control mode," in *Proc. IEEE ECCE Asia Downunder (ECCE Asia)*, Jun. 2013, pp. 882–887.
[119] A. Krismanto, N. Mithulananthan, and K. Y. Lee, "Comprehensive modelling and small signal stability analysis of RES-based microgrid," *IFAC-PapersOnLine*, vol. 48, no. 30, pp. 282–287, 2015.
[120] W. Al-Saedi, S. W. Lachowicz, D. Habibi, and O. Bass, "Stability analysis of an autonomous microgrid operation based on particle swarm optimization," in *Proc. IEEE Int. Conf. Power Syst. Technol. (POWERCON)*, Auckland, New Zealand, Oct. 2012, pp. 1–6.
[121] D. K. Dheer, N. Soni, and S. Doolla, "Improvement of small signal stability margin and transient response in inverter-dominated microgrids," *Sustain. Energy, Grids Netw.*, vol. 5, pp. 135–147, Mar. 2016.
[122] P. H. Divshali, S. H. Hosseinian, M. Abedi, and A. Alimardani, "Small-signal stability and load-sharing improvement of autonomous microgrids using auxiliary loop," *Electr. Power Compon. Syst.*, vol. 40, no. 6, pp. 648–671, Mar. 2012.
[123] P. A. Mendoza-Araya and G. Venkataramanan, "Stability analysis of AC microgrids using incremental phasor impedance matching," *Electr. Power Compon. Syst.*, vol. 43, no. 4, pp. 473–484, Feb. 2015.
[124] P. A. Mendoza-Araya and G. Venkataramanan, "Dynamic phasor models for AC microgrids stability studies," in *Proc. IEEE Energy Convers. Congr. Expo. (ECCE)*, Pittsburgh, PA, USA, Sep. 2014, pp. 3363–3370.
[125] S. M. Amelian and R. Hooshmand, "Small signal stability analysis of microgrids considering comprehensive load models—A sensitivity based approach," in *Proc. Smart Grid Conf. (SGC)*, Tehran, Iran, Dec. 2013, pp. 143–149.
[126] A. Kahrobaeian and Y. A.-R.-I. Mohamed, "Analysis and mitigation of low-frequency instabilities in autonomous medium-voltage converter-based microgrids with dynamic loads," *IEEE Trans. Ind. Electron.*, vol. 61, no. 4, pp. 1643–1658, Apr. 2014.
[127] D. K. Dheer, S. Doolla, and A. K. Rathore, "Small signal modeling and stability analysis of a droop based hybrid AC/DC microgrid," in *Proc. IEEE 42nd Annu. Conf. Ind. Electron. Soc. (IECON)*, Florence, Italy, Dec. 2016, pp. 3775–3780.
[128] M. Ahmed, A. Vahidnia, L. Meegahapola, and M. Datta, "Small signal stability analysis of a hybrid AC/DC microgrid with static and dynamic loads," in *Proc. Australas. Universities Power Eng. Conf. (AUPEC)*, Melbourne, VIC, Australia, Nov. 2017, pp. 1–6.
[129] Z. Li and M. Shahidehpour, "Small-signal modeling and stability analysis of hybrid AC/DC microgrids," *IEEE Trans. Smart Grid*, vol. 10, no. 2, pp. 2080–2095, Mar. 2019.
[130] M. Ahmed, L. Meegahapola, A. Vahidnia, and M. Datta, "Analyzing the effect of X/R ratio on dynamic performance of microgrids," in *Proc. IEEE PES Innov. Smart Grid Technol. Eur. (ISGT-Eur.)*, Bucharest, Romania, Sep. 2019, pp. 1–5.
[131] M. Ahmed, L. Meegahapola, A. Vahidnia, and M. Datta, "Influence of feeder characteristics on hybrid AC/DC microgrids stability," in *Proc. 9th Int. Conf. Power Energy Syst. (ICPES)*, Perth, WA, Australia, Dec. 2019, pp. 1–6.
[132] M. Ahmed, A. Vahidnia, M. Datta, and L. Meegahapola, "An adaptive power oscillation damping controller for a hybrid AC/DC microgrid," *IEEE Access*, vol. 6, pp. 41458–41489, May 2020.
[133] Y. Yan, D. Shi, D. Bian, B. Huang, Z. Yi, and Z. Wang, "Small-signal stability analysis and performance evaluation of microgrids under distributed control," *IEEE Trans. Smart Grid*, vol. 10, no. 5, pp. 4848–4858, Sep. 2019.
[134] Z. Lu, Z. Wang, H. Xin, and K. Wong, "Small signal stability analysis of a synchronized control-based microgrid under multiple operating conditions," *J. Mod. Power Syst. Clean Energy*, vol. 2, no. 3, pp. 244–255, Sep. 2014.
[135] K. Sun, L. Zhang, Y. Xing, and J. M. Guerrero, "A distributed control strategy based on DC bus signaling for modular photovoltaic generation systems with battery energy storage," *IEEE Trans. Power Electron.*, vol. 26, no. 10, pp. 3032–3045, Oct. 2011.

[136] J. Schonbergerschonberger, R. Duke, and S. D. Round, "DC-bus signaling: A distributed control strategy for a hybrid renewable nanogrid," *IEEE Trans. Ind. Electron.*, vol. 53, no. 5, pp. 1453–1460, Oct. 2006.

[137] D. Boroyevich, I. Cvetković, D. Dong, R. Burgos, F. Wang, and F. Lee, "Future electronic power distribution systems a contemplative view," in *Proc. IEEE 12th Int. Conf. Optim. Electr. Electron. Equip.*, Basov, Romania, Jul. 2010, pp. 1369–1380.

[138] C. Gavriluta, J. I. Candela, C. Citro, J. Rocabert, A. Luna, and P. Rodríguez, "Decentralized primary control of MTDC networks with energy storage and distributed generation," *IEEE Trans. Ind. Appl.*, vol. 50, no. 6, pp. 4122–4131, Nov. 2014.

[139] Y. Gu, W. Li, and X. He, "Frequency-coordinating virtual impedance for autonomous power management of DC microgrid," *IEEE Trans. Power Electron.*, vol. 30, no. 4, pp. 2328–2337, Apr. 2015.

[140] X. Lu, K. Sun, J. M. Guerrero, J. C. Vasquez, and L. Huang, "State-of-Charge balance using adaptive droop control for distributed energy storage systems in DC microgrid applications," *IEEE Trans. Ind. Electron.*, vol. 61, no. 6, pp. 2804–2815, Jun. 2014.

[141] T. Dragičević, J. M. Guerrero, J. C. Vasquez, and D. Škrlec, "Supervisory control of an adaptive-droop regulated DC microgrid with battery management capability," *IEEE Trans. Power Electron.*, vol. 29, no. 2, pp. 695–706, Feb. 2014.

[142] X. Lu, K. Sun, J. M. Guerrero, J. C. Vasquez, and L. Huang, "Double-quadrant state-of-charge-based droop control method for distributed energy storage systems in autonomous DC microgrids," *IEEE Trans. Smart Grid*, vol. 6, no. 1, pp. 147–157, Jan. 2015.

[143] H. Kakigano, Y. Miura, and T. Ise, "Distribution voltage control for DC microgrids using fuzzy control and gain-scheduling technique," *IEEE Trans. Power Electron.*, vol. 28, no. 5, pp. 2246–2258, May 2013.

[144] N. L. Diaz, T. Dragičević, J. C. Vasquez, and J. M. Guerrero, "Intelligent distributed generation and storage units for DC microgrids—A new concept on cooperative control without communications beyond droop control," *IEEE Trans. Smart Grid*, vol. 5, no. 5, pp. 2476–2485, Aug. 2014.

[145] A. Gkountaras, S. Dieckerhoff, and T. Sezi, "Performance analysis of hybrid microgrids applying SoC-adaptive droop control," in *Proc. 16th Eur. Conf. Power Electron. Appl.*, Lappeenranta, Finland, Aug. 2014, pp. 1–10.

[146] E. Liegmann and R. Majumder, "An efficient method of multiple storage control in microgrids," *IEEE Trans. Power Syst.*, vol. 30, no. 6, pp. 3437–3444, Nov. 2015.

[147] T. Dragičević, J. M. Guerrero, and J. C. Vasquez, "A distributed control strategy for coordination of an autonomous LVDC microgrid based on power-line signaling," *IEEE Trans. Ind. Electron.*, vol. 61, no. 7, pp. 3313–3326, Jul. 2014.

[148] W. Stefanutti, S. Saggini, P. Mattavelli, and M. Ghioni, "Power line communication in digitally controlled DC–DC converters using switching frequency modulation," *IEEE Trans. Ind. Electron.*, vol. 55, no. 4, pp. 1509–1518, Apr. 2008.

[149] F. Valenciaga and P. F. Puleston, "Supervisor control for a stand-alone hybrid generation system using wind and photovoltaic energy," *IEEE Trans. Energy Convers.*, vol. 20, no. 2, pp. 398–405, Jun. 2005.

[150] F. Valenciaga and P. F. Puleston, "High-order sliding control for a wind energy conversion system based on a permanent magnet synchronous generator," *IEEE Trans. Energy Convers.*, vol. 23, no. 3, pp. 860–867, Sep. 2008.

[151] L. Che and M. Shahidehpour, "DC microgrids: Economic operation and enhancement of resilience by hierarchical control," *IEEE Trans. Smart Grid*, vol. 5, no. 5, pp. 2517–2526, Sep. 2014.

[152] C. Jin, P. Wang, J. Xiao, Y. Tang, and F. H. Choo, "Implementation of hierarchical control in DC microgrids," *IEEE Trans. Ind. Electron.*, vol. 61, no. 8, pp. 4032–4042, Aug. 2014.

[153] B. Wang, M. Sechilariu, and F. Locment, "Intelligent DC microgrid with smart grid communications: Control strategy consideration and design," *IEEE Trans. Smart Grid*, vol. 3, no. 4, pp. 2148–2156, Dec. 2012.

[154] X. Lu, J. M. Guerrero, K. Sun, J. C. Vasquez, R. Teodorescu, and L. Huang, "Hierarchical control of parallel AC-DC converter interfaces for hybrid microgrids," *IEEE Trans. Smart Grid*, vol. 5, no. 2, pp. 683–692, Mar. 2014.

[155] A. Bidram, F. L. Lewis, Z. Qu, and A. Davoudi, "Secondary control of microgrids based on distributed cooperative control of multi-agent systems," *IET Gener., Transmiss. Distrib.*, vol. 7, no. 8, pp. 822–831, Aug. 2013.

[156] L. Meng, T. Dragicevic, J. M. Guerrero, and J. C. Vasquez, "Dynamic consensus algorithm based distributed global efficiency optimization of a droop controlled DC microgrid," in *Proc. IEEE Int. Energy Conf. (ENERGYCON)*, Cavtat, Croatia, May 2014, pp. 1276–1283.

[157] X. Lu, J. M. Guerrero, K. Sun, and J. C. Vasquez, "An improved droop control method for DC microgrids based on low bandwidth communication with DC bus voltage restoration and enhanced current sharing ACcuracy," *IEEE Trans. Power Electron.*, vol. 29, no. 4, pp. 1800–1812, Apr. 2014.

[158] V. Nasirian, S. Moayedi, A. Davoudi, and F. L. Lewis, "Distributed cooperative control of DC microgrids," *IEEE Trans. Power Electron.*, vol. 30, no. 4, pp. 2288–2303, Apr. 2015.

[159] J. Zhao and F. Dörfler, "Distributed control and optimization in DC microgrids," *Automatica*, vol. 61, pp. 18–26, Nov. 2015.

[160] M. Nasri, M. R. Hossain, H. L. Ginn, and M. Moallem, "Distributed control of converters in a DC microgrid using agent technology," in *Proc. IEEE Power Systems Conf. (PSC)*, Mar. 2016, pp. 1–6.

[161] T. Morstyn, B. Hredzak, G. D. Demetriades, and V. G. Agelidis, "Unified distributed control for DC microgrid operating modes," *IEEE Trans. Power Syst.*, vol. 31, no. 1, pp. 802–812, Jan. 2016.

[162] T. Dragičević, X. Lu, J. C. Vasquez, and J. M. Guerrero, "Dc microgrids—Part I: A review of control strategies and stabilization techniques," *IEEE Trans. Power Electron.*, vol. 31, no. 7, pp. 4876–4891, Sep. 2015.

[163] F. Gao, S. Bozhko, A. Costabeber, C. Patel, P. Wheeler, C. I. Hill, and G. Asher, "Comparative stability analysis of droop control approaches in voltage-source-converter-based DC microgrids," *IEEE Trans. Power Electron.*, vol. 32, no. 3, pp. 2395–2415, Mar. 2017.

[164] K. Rouzbehi, A. Miranian, A. Luna, and P. Rodriguez, "DC voltage control and power sharing in multiterminal DC grids based on optimal DC power flow and voltage-droop strategy," *IEEE J. Emerg. Sel. Topics Power Electron.*, vol. 2, no. 4, pp. 1171–1180, Dec. 2014.

[165] G. Xu, D. Sha, and X. Liao, "Decentralized inverse-droop control for input-series–output-parallel DC–DC converters," *IEEE Trans. Power Electron.*, vol. 30, no. 9, pp. 4621–4625, Sep. 2015.

[166] V. Nasirian, A. Davoudi, F. L. Lewis, and J. M. Guerrero, "Distributed adaptive droop control for DC distribution systems," *IEEE Trans. Energy Convers.*, vol. 29, no. 4, pp. 944–956, Dec. 2014.

[167] M. Mokhtar, M. I. Marei, and A. A. El-Sattar, "An adaptive droop control scheme for DC microgrids integrating sliding mode voltage and current controlled boost converters," *IEEE Trans. Smart Grid*, vol. 10, no. 2, pp. 1685–1693, Mar. 2019.

[168] T. V. Vu, D. Perkins, F. Diaz, D. Gonsoulin, C. S. Edrington, and T. El-Mezyani, "Robust adaptive droop control for DC microgrids," *Electr. Power Syst. Res.*, vol. 146, pp. 95–106, May 2017.

[169] L. Guo, J. Y. Hung, and R. M. Nelms, "Evaluation of DSP-based PID and fuzzy controllers for DC–DC converters," *IEEE Trans. Ind. Electron.*, vol. 56, no. 6, pp. 2237–2248, Jun. 2009.

[170] S. Anand, B. G. Fernandes, and J. Guerrero, "Distributed control to ensure proportional load sharing and improve voltage regulation in low-voltage DC microgrids," *IEEE Trans. Power Electron.*, vol. 28, no. 4, pp. 1900–1913, Apr. 2013.

[171] X. Lu, K. Sun, J. M. Guerrero, J. C. Vasquez, L. Huang, and R. Teodorescu, "Soc-based droop method for distributed energy storage in DC microgrid applications," in *Proc. IEEE Int. Symp. Ind. Electron. (ISIE)*, Jul. 2012, pp. 1640–1645.

[172] W. W. Weaver, R. D. Robinett, G. G. Parker, and D. G. Wilson, "Energy storage requirements of DC microgrids with high penetration renewables under droop control," *Int. J. Electr. Power Energy Syst.*, vol. 68, pp. 203–209, Jun. 2015.

[173] S. Anand and B. G. Fernandes, "Modified droop controller for paralleling of DC–DC converters in standalone DC system," *IET Power Electron.*, vol. 5, no. 6, pp. 782–789, Jul. 2012.

[174] X. Lu, K. Sun, J. M. Guerrero, J. C. Vasquez, L. Huang, and J. Wang, "Stability enhancement based on virtual impedance for DC microgrids with constant power loads," *IEEE Trans. Smart Grid*, vol. 6, no. 6, pp. 2770–2783, Nov. 2015.

[175] J. He, Y. W. Li, and M. S. Munir, "A flexible harmonic control approach through voltage-controlled DG–grid interfacing converters," *IEEE Trans. Ind. Electron.*, vol. 59, no. 1, pp. 444–455, Jan. 2012.

[176] A. A. Rockhill, M. Liserre, R. Teodorescu, and P. Rodriguez, "Grid-filter design for a multimegawatt medium-voltage voltage-source inverter," *IEEE Trans. Ind. Electron.*, vol. 58, no. 4, pp. 1205–1217, Apr. 2011.

[177] W. Lu and B.-T. Ooi, "DC overvoltage control during loss of converter in multiterminal voltage-source converter-based HVDC (M-VSC-HVDC)," *IEEE Trans. Power Del.*, vol. 18, no. 3, pp. 915–920, Jul. 2003.
[178] A. A. A. Radwan and Y. A.-R.-I. Mohamed, "Linear ACtive stabilization of converter-dominated DC microgrids," *IEEE Trans. Smart Grid*, vol. 3, no. 1, pp. 203–216, Mar. 2012.
[179] J. Umuhoza, Y. Zhang, S. Zhao, and H. A. Mantooth, "An adaptive control strategy for power balance and the intermittency mitigation in battery-PV energy system at residential DC microgrid level," in *Proc. IEEE Appl. Power Electron. Conf. Expo. (APEC)*, Tampa, FL, USA, Mar. 2017, pp. 1341–1345.
[180] S. Sahoo and S. Mishra, "A multi-objective adaptive control framework in autonomous DC microgrid," *IEEE Trans. Smart Grid*, vol. 9, no. 5, pp. 4918–4929, Sep. 2018.
[181] C. Li, S. K. Chaudhary, M. Savaghebi, J. C. Vasquez, and J. M. Guerrero, "Power flow analysis for low-voltage AC and DC microgrids considering droop control and virtual impedance," *IEEE Trans. Smart Grid*, vol. 8, no. 6, pp. 2754–2764, Nov. 2017.
[182] P. Magne, B. Nahid-Mobarakeh, and S. Pierfederici, "Dynamic consideration of DC microgrids with constant power loads and ACtive damping system—A design method for fault-tolerant stabilizing system," *IEEE J. Emerg. Sel. Topics Power Electron.*, vol. 2, no. 3, pp. 562–570, Feb. 2014.
[183] S. D. McArthur, E. M. Davidson, V. M. Catterson, A. L. Dimeas, N. D. Hatziargyriou, F. Ponci, and T. Funabashi, "Multi-agent systems for power engineering applications—Part I: Concepts, approaches, and technical challenges," *IEEE Trans. Power Syst.*, vol. 22, no. 4, pp. 1743–1752, Oct. 2007.
[184] R. C. Qiu, Z. Hu, Z. Chen, N. Guo, R. Ranganathan, S. Hou, and G. Zheng, "Cognitive radio network for the smart grid: Experimental system architecture, control algorithms, security, and microgrid testbed," *IEEE Trans. Smart Grid*, vol. 2, no. 4, pp. 724–740, Dec. 2011.
[185] S. K. Mazumder, M. Tahir, and K. Acharya, "Master–slave current-sharing control of a parallel DC–DC converter system over an RF communication interface," *IEEE Trans. Ind. Electron.*, vol. 55, no. 1, pp. 59–66, Jan. 2008.
[186] J. Rajagopalan, K. Xing, Y. Guo, F. C. Lee, and B. Manners, "Modeling and dynamic analysis of paralleled DC/DC converters with master-slave current sharing control," in *Proc. Appl. Power Electron. Conf. (APEC)*, vol. 2, San Jose, CA, USA, 1996, pp. 678–684.
[187] Y. Xia, W. Wei, Y. Peng, P. Yang, and M. Yu, "Decentralized coordination control for parallel bidirectional power converters in a grid-connected DC microgrid," *IEEE Trans. Smart Grid*, vol. 9, no. 6, pp. 6850–6861, Nov. 2018.
[188] L. Herrera, W. Zhang, and J. Wang, "Stability analysis and controller design of DC microgrids with constant power loads," *IEEE Trans. Smart Grid*, vol. 8, no. 2, pp. 881–888, Mar. 2017.
[189] A. P. N. Tahim, D. J. Pagano, E. Lenz, and V. Stramosk, "Modeling and stability analysis of islanded DC microgrids under droop control," *IEEE Trans. Power Electron.*, vol. 30, no. 8, pp. 4597–4607, Aug. 2015.
[190] L. Guo, S. Zhang, X. Li, Y. W. Li, C. Wang, and Y. Feng, "Stability analysis and damping enhancement based on frequency-dependent virtual impedance for DC microgrids," *IEEE J. Emerg. Sel. Topics Power Electron.*, vol. 5, no. 1, pp. 338–350, Mar. 2017.
[191] Z. Liu, M. Su, Y. Sun, W. Yuan, and H. Han, "On existence and stability of equilibria of DC microgrid with constant power loads," Jun. 2017, *arXiv:1711.06993*. [Online]. Available: http://arxiv.org/abs/1711.06993
[192] J. Liu, W. Zhang, and G. Rizzoni, "Robust stability analysis of DC microgrids with constant power loads," *IEEE Trans. Power Syst.*, vol. 33, no. 1, pp. 851–860, Jan. 2018.
[193] X. Liu and Y. Bian, "Large signal stability analysis of the DC microgrid with the storage system," in *Proc. 20th Int. Conf. Electr. Mach. Syst. (ICEMS)*, Sydney, NSW, Australia, Aug. 2017, pp. 1–5.
[194] E. Planas, J. Andreu, J. I. Gárate, I. M. de Alegría, and E. Ibarra, "AC and DC technology in microgrids: A review," *Renew. Sustain. Energy Rev.*, vol. 43, pp. 726–749, Mar. 2015.
[195] P. C. Loh, D. Li, Y. K. Chai, and F. Blaabjerg, "Autonomous operation of hybrid microgrid with AC and DC subgrids," *IEEE Trans. Power Electron.*, vol. 28, no. 5, pp. 2214–2223, May 2013.
[196] N. Eghtedarpour and E. Farjah, "Power control and management in a hybrid AC/DC microgrid," *IEEE Trans. Smart Grid*, vol. 5, no. 3, pp. 1494–1505, May 2014.
[197] M. S. Rahman, M. J. Hossain, and J. Lu, "Coordinated control of three-phase AC and DC type EV–ESSs for efficient hybrid microgrid operations," *Energy Convers. Manage.*, vol. 122, pp. 488–503, Aug. 2016.
[198] A. Dimeas, A. Tsikalakis, G. Kariniotakis, and G. Korres, "Microgrids control issues," in *Microgrids: Architectures and Control*. Chichester, U.K.: Wiley, doi: 10.1002/9781118720677.ch02.
[199] C. Yuen, A. Oudalov, and A. Timbus, "The provision of frequency control reserves from multiple microgrids," *IEEE Trans. Ind. Electron.*, vol. 58, no. 1, pp. 173–183, Jan. 2011.
[200] F. Katiraei, R. Iravani, N. Hatziargyriou, and A. Dimeas, "Microgrids management," *IEEE Power Energy Mag.*, vol. 6, no. 3, pp. 54–65, May/Jun. 2008.
[201] E. Planas, A. Gil-de-Muro, J. Andreu, I. Kortabarria, and I. M. de Alegría, "General aspects, hierarchical controls and droop methods in microgrids: A review," *Renew. Sustain. Energy Rev.*, vol. 17, pp. 147–159, Jan. 2013.
[202] P. Piagi and R. H. Lasseter, "Autonomous control of microgrids," in *Proc. IEEE Power Eng. Soc. Gen. Meeting*, Montreal, QC, Canada, Oct. 2006, p. 8.
[203] L. Meng, T. Dragicevic, J. Guerrero, J. Vasquez, M. Savaghebi, and F. Tang, "Agent-based distributed unbalance compensation for optimal power quality in islanded microgrids," in *Proc. IEEE 23rd Int. Symp. Ind. Electron. (ISIE)*, Istanbul, Turkey, Jun. 2014, pp. 2535–2540.
[204] F. Nejabatkhah and Y. W. Li, "Overview of power management strategies of hybrid AC/DC microgrid," *IEEE Trans. Power Electron.*, vol. 30, no. 12, pp. 7072–7089, Dec. 2015.
[205] T. Zhou and B. François, "Energy management and power control of a hybrid active wind generator for distributed power generation and grid integration," *IEEE Trans. Ind. Electron.*, vol. 58, no. 1, pp. 95–104, Jan. 2011.
[206] F. Blaabjerg, R. Teodorescu, M. Liserre, and A. V. Timbus, "Overview of control and grid synchronization for distributed power generation systems," *IEEE Trans. Ind. Electron.*, vol. 53, no. 5, pp. 1398–1409, Oct. 2006.
[207] Y. Li, D. M. Vilathgamuwa, and P. C. Loh, "Design, analysis, and real-time testing of a controller for multibus microgrid system," *IEEE Trans. Power Electron.*, vol. 19, no. 5, pp. 1195–1204, Sep. 2004.
[208] H. Louie and K. Strunz, "Superconducting magnetic energy storage (SMES) for energy cache control in modular distributed hydrogen-electric energy systems," *IEEE Trans. Appl. Supercond.*, vol. 17, no. 2, pp. 2361–2364, Jul. 2007.
[209] J. Rocabert, A. Luna, F. Blaabjerg, and P. Rodríguez, "Control of power converters in AC microgrids," *IEEE Trans. Power Electron.*, vol. 27, no. 11, pp. 4734–4749, Nov. 2012.
[210] J.-F. Chen and C.-L. Chu, "Combination voltage-controlled and current-controlled PWM inverters for UPS parallel operation," *IEEE Trans. Power Electron.*, vol. 10, no. 5, pp. 547–558, Sep. 1995.
[211] H. Zhou, T. Bhattacharya, D. Tran, T. S. T. Siew, and A. M. Khambadkone, "Composite energy storage system involving battery and ultracapacitor with dynamic energy management in microgrid applications," *IEEE Trans. Power Electron.*, vol. 26, no. 3, pp. 923–930, Mar. 2011.
[212] Z. Yao, L. Xiao, and Y. Yan, "Seamless transfer of single-phase grid-interactive inverters between grid-connected and stand-alone modes," *IEEE Trans. Power Electron.*, vol. 25, no. 6, pp. 1597–1603, Jun. 2010.
[213] R.-J. Wai, C.-Y. Lin, Y.-C. Huang, and Y.-R. Chang, "Design of high-performance stand-alone and grid-connected inverter for distributed generation applications," *IEEE Trans. Ind. Electron.*, vol. 60, no. 4, pp. 1542–1555, Apr. 2013.
[214] I. J. Balaguer, Q. Lei, S. Yang, U. Supatti, and F. Z. Peng, "Control for grid-connected and intentional islanding operations of distributed power generation," *IEEE Trans. Ind. Electron.*, vol. 58, no. 1, pp. 147–157, Jan. 2011.
[215] H. Karimi, A. Yazdani, and R. Iravani, "Negative-sequence current injection for fast islanding detection of a distributed resource unit," *IEEE Trans. Power Electron.*, vol. 23, no. 1, pp. 298–307, Jan. 2008.
[216] M. Karimi-Ghartemani, "Universal integrated synchronization and control for single-phase DC/AC converters," *IEEE Trans. Power Electron.*, vol. 30, no. 3, pp. 1544–1557, Mar. 2015.
[217] G. Hernandez-Gonzalez and R. Iravani, "Current injection for ACtive islanding detection of electronically-interfaced distributed resources," *IEEE Trans. Power Del.*, vol. 21, no. 3, pp. 1698–1705, Jul. 2006.
[218] L. A. C. Lopes and Y. Zhang, "Islanding detection assessment of multi-inverter systems with ACtive frequency drifting methods," *IEEE Trans. Power Del.*, vol. 23, no. 1, pp. 480–486, Jan. 2008.
[219] Y. A.-R.-I. Mohamed and A. A. Radwan, "Hierarchical control system for robust microgrid operation and seamless mode transfer in ACtive distribution systems," *IEEE Trans. Smart Grid*, vol. 2, no. 2, pp. 352–362, Jun. 2011.

[220] J. Kim, J. M. Guerrero, P. Rodriguez, R. Teodorescu, and K. Nam, "Mode adaptive droop control with virtual output impedances for an inverter-based flexible AC microgrid," *IEEE Trans. Power Electron.*, vol. 26, no. 3, pp. 689–701, Mar. 2011.

[221] J. Matas, M. Castilla, L. G. D. Vicuña, J. Miret, and J. C. Vasquez, "Virtual impedance loop for droop-controlled single-phase parallel inverters using a second-order general-integrator scheme," *IEEE Trans. Power Electron.*, vol. 25, no. 12, pp. 2993–3002, Dec. 2010.

[222] J. M. Guerrero, J. C. Vasquez, J. Matas, M. Castilla, and L. G. de Vicuna, "Control strategy for flexible microgrid based on parallel line-interactive UPS systems," *IEEE Trans. Ind. Electron.*, vol. 56, no. 3, pp. 726–736, Mar. 2009.

[223] J. He and Y. W. Li, "Hybrid voltage and current control approach for DG-grid interfacing converters with *LCL* filters," *IEEE Trans. Ind. Electron.*, vol. 60, no. 5, pp. 1797–1809, May 2013.

[224] F. Gao and M. R. Iravani, "A control strategy for a distributed generation unit in grid-connected and autonomous modes of operation," *IEEE Trans. Power Del.*, vol. 23, no. 2, pp. 850–859, Apr. 2008.

[225] C. Cho, J.-H. Jeon, J.-Y. Kim, S. Kwon, K. Park, and S. Kim, "Active synchronizing control of a microgrid," *IEEE Trans. Power Electron.*, vol. 26, no. 12, pp. 3707–3719, Dec. 2011.

[226] H. Xu, X. Zhang, F. Liu, D. Zhu, R. Shi, H. Ni, and W. Cao, "Synchronization strategy of microgrid from islanded to grid-connected mode seamless transfer," in *Proc. IEEE Int. Conf. IEEE Region (TENCON)*, Xi'an, China, Oct. 2013, pp. 1–4.

[227] T. L. Vandoorn, B. Meersman, D. Kooning, and L. Vandevelde, "Transition from islanded to grid-connected mode of microgrids with voltage-based droop control," *IEEE Trans. Power Syst.*, vol. 28, no. 3, pp. 2545–2553, Aug. 2013.

[228] Y. Jia, D. Liu, and J. Liu, "A novel seamless transfer method for a microgrid based on droop characteristic adjustment," in *Proc. 7th Int. Power Electron. Motion Control Conf.*, vol. 1, Harbin, China, Jun. 2012, pp. 362–367.

[229] A. A. A. Radwan and Y. A.-R. I. Mohamed, "Bidirectional power management in hybrid AC-DC islanded microgrid system," in *Proc. PES Gen. Meeting Conf. Expo.*, National Harbor, MD, USA, Jul. 2014, pp. 1–5.

[230] P. J. Hart, R. H. Lasseter, and T. M. Jahns, "Symmetric droop control for improved hybrid AC/DC microgrid transient performance," in *Proc. IEEE Energy Convers. Congr. Expo. (ECCE)*, Milwaukee, WI, USA, Sep. 2016, pp. 1–8.

[231] J. M. Guerrero, M. Chandorkar, T.-L. Lee, and P. C. Loh, "Advanced control architectures for intelligent microgrids—Part I: Decentralized and hierarchical control," *IEEE Trans. Ind. Electron.*, vol. 60, no. 4, pp. 1254–1262, Apr. 2013.

[232] S. Peyghami, H. Mokhtari, and F. Blaabjerg, "Autonomous operation of a hybrid AC/DC microgrid with multiple interlinking converters," *IEEE Trans. Smart Grid*, vol. 9, no. 6, pp. 6480–6488, Nov. 2018.

[233] X. Li, L. Guo, Y. Li, Z. Guo, C. Hong, Y. Zhang, and C. Wang, "A unified control for the DC–AC interlinking converters in hybrid AC/DC microgrids," *IEEE Trans. Smart Grid*, vol. 9, no. 6, pp. 6540–6553, Nov. 2018.

[234] J. Liu, Y. Miura, and T. Ise, "Comparison of dynamic characteristics between virtual synchronous generator and droop control in inverter-based distributed generators," *IEEE Trans. Power Electron.*, vol. 31, no. 5, pp. 3600–3611, May 2016.

[235] J. Liu, Y. Miura, H. Bevrani, and T. Ise, "Enhanced virtual synchronous generator control for parallel inverters in microgrids," *IEEE Trans. Smart Grid*, vol. 8, no. 5, pp. 2268–2277, Sep. 2017.

[236] H. Wu, X. Ruan, D. Yang, X. Chen, W. Zhao, Z. Lv, and Q.-C. Zhong, "Small-signal modeling and parameters design for virtual synchronous generators," *IEEE Trans. Ind. Electron.*, vol. 63, no. 7, pp. 4292–4303, Jul. 2016.

[237] F. Shahnia, A. Ghosh, S. Rajakaruna, and R. P. S. Chandrasena, "Primary control level of parallel distributed energy resources converters in system of multiple interconnected autonomous microgrids within self-healing networks," *IET Gener., Transmiss. Distrib.*, vol. 8, no. 2, pp. 203–222, Feb. 2014.

[238] C. Jin, P. C. Loh, P. Wang, Y. Mi, and F. Blaabjerg, "Autonomous operation of hybrid AC-DC microgrids," in *Proc. IEEE Int. Conf. Sustain. Energy Technol. (ICSET)*, Dec. 2010, pp. 1–7.

[239] M. Baharizadeh, H. R. Karshenas, and J. M. Guerrero, "Control strategy of interlinking converters as the key segment of hybrid AC–DC microgrids," *IET Gener., Transmiss. Distrib.*, vol. 10, no. 7, pp. 1671–1681, May 2016.

[240] J. He and Y. W. Li, "Analysis, design, and implementation of virtual impedance for power electronics interfaced distributed generation," *IEEE Trans. Ind. Appl.*, vol. 47, no. 6, pp. 2525–2538, Nov. 2011.

[241] Y. Wei Li and C.-N. Kao, "An ACcurate power control strategy for power-electronics-interfaced distributed generation units operating in a low-voltage multibus microgrid," *IEEE Trans. Power Electron.*, vol. 24, no. 12, pp. 2977–2988, Dec. 2009.

[242] H. Xiao, A. Luo, Z. Shuai, G. Jin, and Y. Huang, "An improved control method for multiple bidirectional power converters in hybrid AC/DC microgrid," *IEEE Trans. Smart Grid*, vol. 7, no. 1, pp. 340–347, Jan. 2016.

[243] K. De Brabandere, B. Bolsens, J. Van den Keybus, A. Woyte, J. Driesen, and R. Belmans, "A voltage and frequency droop control method for parallel inverters," *IEEE Trans. Power Electron.*, vol. 22, no. 4, pp. 1107–1115, Jul. 2007.

[244] Q.-C. Zhong, "Robust droop controller for ACcurate proportional load sharing among inverters operated in parallel," *IEEE Trans. Ind. Electron.*, vol. 60, no. 4, pp. 1281–1290, Apr. 2013.

[245] A. Bidram, A. Davoudi, F. L. Lewis, and J. M. Guerrero, "Distributed cooperative secondary control of microgrids using feedback linearization," *IEEE Trans. Power Syst.*, vol. 28, no. 3, pp. 3462–3470, Aug. 2013.

[246] V. Blasko and V. Kaura, "A novel control to ACtively damp resonance in input LC filter of a three-phase voltage source converter," *IEEE Trans. Ind. Appl.*, vol. 33, no. 2, pp. 542–550, Mar. 1997.

[247] J. R. Espinoza and G. Joos, "State variable decoupling and power flow control in PWM current-source rectifiers," *IEEE Trans. Ind. Electron.*, vol. 45, no. 1, pp. 78–87, Feb. 1998.

[248] W.-G. Lee, T.-T. Nguyen, H.-J. Yoo, and H.-M. Kim, "Low-voltage ride-through operation of grid-connected microgrid using consensus-based distributed control," *Energies*, vol. 11, no. 11, p. 2867, Oct. 2018.

[249] X. Liu, Z. Xu, and K. P. Wong, "Recent advancement on technical requirements for grid integration of wind power," *J. Modern Power Syst. Clean Energy*, vol. 1, no. 3, pp. 216–222, Dec. 2013.

[250] A. Moawwad, M. S. El Moursi, and W. Xiao, "A novel transient control strategy for VSC-HVDC connecting offshore wind power plant," *IEEE Trans. Sustain. Energy*, vol. 5, no. 4, pp. 1056–1069, Oct. 2014.

[251] J. Matas, M. Castilla, J. M. Guerrero, L. G. de Vicuña, and J. Miret, "Feedback linearization of direct-drive synchronous wind-turbines via a sliding mode approach," *IEEE Trans. Power Electron.*, vol. 23, no. 3, pp. 1093–1103, May 2008.

[252] K.-H. Kim, Y.-C. Jeung, D.-C. Lee, and H.-G. Kim, "LVRT scheme of PMSG wind power systems based on feedback linearization," *IEEE Trans. Power Electron.*, vol. 27, no. 5, pp. 2376–2384, May 2012.

[253] C.-T. Lee, C.-W. Hsu, and P.-T. Cheng, "A low-voltage ride-through technique for grid-connected converters of distributed energy resources," *IEEE Trans. Ind. Appl.*, vol. 47, no. 4, pp. 1821–1832, Jul. 2011.

[254] X. Liu, C. Li, M. Shahidehpour, Y. Gao, B. Zhou, Y. Zhang, J. Yi, and Y. Cao, "Fault current hierarchical limitation strategy for fault ride-through scheme of microgrid," *IEEE Trans. Smart Grid*, vol. 10, no. 6, pp. 6566–6579, Nov. 2019.

[255] H. He, L. Chen, T. Yin, Z. Cao, J. Yang, X. Tu, and L. Ren, "Application of a SFCL for fault ride-through capability enhancement of DG in a microgrid system and relay protection coordination," *IEEE Trans. Appl. Supercond.*, vol. 26, no. 7, pp. 1–8, Oct. 2016.

[256] P. Piya, M. Ebrahimi, M. Karimi-Ghartemani, and S. A. Khajehoddin, "Fault ride-through capability of voltage-controlled inverters," *IEEE Trans. Ind. Electron.*, vol. 65, no. 10, pp. 7933–7943, Oct. 2018.

[257] I. Sadeghkhani, M. E. H. Golshan, J. M. Guerrero, and A. Mehrizi-Sani, "A current limiting strategy to improve fault ride-through of inverter interfaced autonomous microgrids," *IEEE Trans. Smart Grid*, vol. 8, no. 5, pp. 2138–2148, Sep. 2017.

[258] R. Georgious, J. García, P. García, and M. Sumner, "Analysis of hybrid energy storage systems with DC link fault ride-through capability," in *Proc. IEEE Energy Convers. Congr. Expo. (ECCE)*, Milwaukee, WI, USA, Sep. 2016, pp. 1–8.

[259] L. Chen, X. Zhang, Y. Qin, H. Chen, Q. Shen, Y. Xu, L. Ren, and Y. Tang, "Application and design of a resistive-type superconducting fault current limiter for efficient protection of a DC microgrid," *IEEE Trans. Appl. Supercond.*, vol. 29, no. 2, pp. 1–7, Mar. 2019.

[260] I. Ngamroo and T. Karaipoom, "Improving low-voltage ride-through performance and alleviating power fluctuation of DFIG wind turbine in DC microgrid by optimal SMES with fault current limiting function," *IEEE Trans. Appl. Supercond.*, vol. 24, no. 5, pp. 1–5, Oct. 2014.

[261] D. M. Yehia, D.-E.-A. Mansour, and W. Yuan, "Fault ride-through enhancement of PMSG wind turbines with DC microgrids using resistive-type SFCL," *IEEE Trans. Appl. Supercond.*, vol. 28, no. 4, pp. 1–5, Jun. 2018.
[262] D. Xiang, L. Ran, P. J. Tavner, and S. Yang, "Control of a doubly fed induction generator in a wind turbine during grid fault ride-through," *IEEE Trans. Energy Convers.*, vol. 21, no. 3, pp. 652–662, Sep. 2006.
[263] T. H. Nguyen and D.-C. Lee, "Advanced fault ride-through technique for PMSG wind turbine systems using line-side converter as STATCOM," *IEEE Trans. Ind. Electron.*, vol. 60, no. 7, pp. 2842–2850, Jul. 2013.
[264] L. Meegahapola, I. U. Nutkani, and B. McGrath, "Investigation of fault ride-through capability of AC/DC hybrid microgrids during AC network faults," in *Proc. IEEE Power Eng. Soc. Gen. Meeting*, Chicago, IL, USA, Jul. 2017, pp. 1–5.
[265] L. Meegahapola, I. U. Nutkani, B. McGrath, and D. G. Holmes, "Fault ride-through capability of hybrid AC/DC microgrids during AC and DC network faults," in *Proc. IEEE Energy Convers. Congr. Expo. (ECCE)*, Oct. 2017, pp. 44–51.
[266] A. Jayawardena, L. G. Meegahapola, D. A. Robinson, and S. Perera, "Low-voltage ride-through characteristics of microgrids with distribution static synchronous compensator (DSTATCOM)," in *Proc. 2015 IEEE Australas. Universities Power Eng. Conf. (AUPEC)*, Wollongong, NSW, Australia, Sep. 2015, pp. 1–6.
[267] S. I. Gkavanoudis, K. O. Oureilidis, and C. S. Demoulias, "Fault ride-through capability of a microgrid with WTGS and supercapacitor storage during balanced and unbalanced utility voltage sags," in *Proc. IEEE Int. Conf. Renew. Energy Res. Appl. (ICRERA)*, Madrid, Spain, Oct. 2013, pp. 231–236.
[268] A. Rahim and E. Nowicki, "Supercapacitor energy storage system for fault ride-through of a dfig wind generation system," *Energy Convers. Manage.*, vol. 59, pp. 96–102, Jul. 2012.
[269] M. Y. Worku and M. A. Abido, "Fault ride-through and power smoothing control of PMSG-based wind generation using supercapacitor energy storage system," *Arabian J. Sci. Eng.*, vol. 44, no. 3, pp. 2067–2078, Mar. 2019.
[270] M. Ahmed, L. Meegahapola, A. Vahidnia, and M. Datta, "Analysis and mitigation of low-frequency oscillations in hybrid AC/DC microgrids with dynamic loads," *IET Gener., Transmiss. Distrib.*, vol. 13, no. 9, pp. 1477–1488, May 2019.
[271] M. Ahmed, A. Vahidnia, L. Meegahapola, and M. Datta, "Impact of multiple motor loads on dynamic performance and stability of microgrids," in *Proc. IEEE Int. Conf. Ind. Tech. (ICIT)*, Melbourne, VIC, Australia, Feb. 2019, pp. 1704–1709.

MOUDUD AHMED (Member, IEEE) received the B.Sc. degree (Hons.) in electrical engineering from the Chittagonj University of Engineering and Technology, Bangladesh, in 2012, and the M.Sc. degree in electrical and electronic engineering from the Khulna University of Engineering and Technology, Bangladesh, in 2016. He is currently pursuing the Ph.D. degree with the Royal Melbourne Institute of Technology (RMIT) University, Melbourne, VIC, Australia. His current research interests include hybrid AC/DC microgrid stability and power system control. He is a member of the IEEE Power and Energy Society (PES).

LASANTHA MEEGAHAPOLA (Senior Member, IEEE) received the B.Sc. Eng. degree (Hons.) in electrical engineering from the University of Moratuwa, Sri Lanka, in 2006, and the Ph.D. degree from the Queen's University of Belfast, U.K., in 2010. He was a Visiting Researcher with the Electricity Research Centre, University College Dublin, Ireland, from 2009 to 2010. From 2011 to 2014, he was employed as a Lecturer at the University of Wollongong (UOW) and continues as an Honorary Fellow at UOW. He is currently employed as a Senior Lecturer with the Royal Melbourne Institute of Technology (RMIT) University. His doctoral study was based on the investigation of power system stability issues with high wind penetration, and research was conducted in collaboration with EirGrid (Republic of Ireland-TSO). He has over ten years research experience in power system dynamics and stability with renewable power generation and has published more than 80 journal and conference papers. He has also conducted research studies on microgrid dynamics & stability, and coordinated reactive power dispatch during steady-state and dynamic/transient conditions for networks with high wind penetration. He is a member of the IEEE Power and Energy Society (PES).

ARASH VAHIDNIA (Senior Member, IEEE) received the Ph.D. degree in power engineering from the Queensland University of Technology (QUT). He was a Research Fellow with the Power Engineering Group, QUT, before joining RMIT. He also has several years of industry experience working at power consultancy and utility firms. He is currently a Lecturer with the School of Engineering, RMIT University. His research interests include power system stability, reliability, microgrids, renewable energies, and system planning and control.

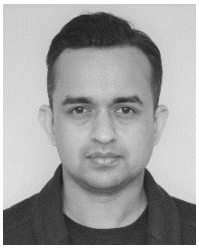

MANOJ DATTA (Senior Member, IEEE) received the doctor of engineering degree in interdisciplinary intelligent systems engineering from Japan, in 2011. From 2011 to 2012, he was a JSPS Postdoctoral Research Fellow with the Faculty of Engineering, University of the Ryukyus, Japan. From 2012 to 2013, he was an Assistant Professor with the Department of Human and Information Systems, Gifu University, Japan. Since late 2013, he has been with the School of Electrical and Computer Engineering, RMIT University, Melbourne, VIC, Australia. His research interests include motor drives, distributed generation forecasting, microgrid modeling, grid integration of DGs, and intelligent ancillary services in the smart grid. He is a member of the Institute of Electrical Engineers, Japan, and IEEE, USA. He was a recipient of the University of the Ryukyus President's Honorary Award for an outstanding Ph.D. thesis.